ARMY RESEARCH LABORATORY

Preliminary High Spectral-Resolution PFNDAT

by Alan Wetmore, David Ligon, and Ramaz Kvavilashvili

ARL-TR-3194 May 2004

NOTICES

Disclaimers

The findings in this report are not to be construed as an official Department of the Army position, unless so designated by other authorized documents.

Citation of manufacturers' or trade names does not constitute an official endorsement or approval of the use thereof.

DESTRUCTION NOTICE—Destroy this report when it is no longer needed. Do not return it to the originator.

Army Research Laboratory
Adelphi, MD 20783-1145

ARL-TR-3194 **May 2004**

Preliminary High Spectral-Resolution PFNDAT

Alan Wetmore, David Ligon, and Ramaz Kvavilashvili
Computational and Information Sciences Directorate, ARL

REPORT DOCUMENTATION PAGE

Form Approved OMB No. 0704-0188

1. REPORT DATE (DD-MM-YYW)	2. REPORT TYPE	3. DATES COVERED (From - To)
May 2004	Final	

4. TITLE AND SUBTITLE	5a. CONTRACT NUMBER
Preliminary High Spectral-ResolutionPFNDAT	5b. GRANT NUMBER
	5c. PROGRAM ELEMENT NUMBER

6. AUTHOR(S)	5d. PROJECT NUMBER
Alan Wetmore, David Ligon, and Ramaz Kvavilashvili	5e. TASK NUMBER
	5f. WORK UNIT NUMBER

7. PERFORMING ORGANIZATION NAME(S) AND ADDRESS(ES)	8. PERFORMING ORGANIZATION REPORT NUMBER
U.S. Army Research Laboratory Computational and Information Sciences Directorate (ATTN: AMSRL-CI-EE) awetmore@arl.army.mil Adelphi, MD 20783-1145	ARL-TR-3194

9. SPONSORING/MONITORING AGENCY NAME(S) AND ADDRESS(ES)	10. SPONSOR/MONITOR'S ACRONYM(S)
U.S. Army Research Laboratory 2800 Powder Mill Road Adelphi, MD 20783-1145	11. SPONSOR/MONITOR'S REPORT NUMBER(S)

12. DISTRIBUTION/AVAILABILITY STATEMENT

Approved for public release: distribution unlimited.

13. SUPPLEMENTARY NOTES

14. ABSTRACT

The High Resolution Phase Function Database (HRPFNDAT) is a component of the Weather and Atmospheric Visualization Effects for Simulation (WAVES) suite. It is also usable with models such as the Electro-Optical Systems Atmospheric Effects Library (EOSAEL) and MODTRAN. The interim version of HRPFNDAT consists of a series of phase functions and extinction and scattering coefficient data for the rural, urban, and maritime haze models, water fog models, and fog oil smoke model for the wavelength region 0.35–40.0 μm at 1 cm^{-1} resolution. The resolution of HRPFNDAT is comparable to the ~1 cm^{-1} resolution available from MODTRAN.

15. SUBJECT TERMS Aerosols, scattering, phase function, transmission, haze, smoke

16. SECURITY CLASSIFICATION OF:			17. LIMITATION OF ABSTRACT	18. NUMBER OF PAGES	19a. NAME OF RESPONSIBLE PERSON
a. REPORT	b. ABSTRACT	c. THIS PAGE			Alan Wetmore
UNCLASSIFIED	UNCLASSIFIED	UNCLASSIFIED	SAR	109	19b. TELEPHONE NUMBER (Include area code) (301) 394-2499

Standard Form 298 (Rev. 8/98)

Contents

List of Figures

List of Tables

Chapter 1

Introduction

An important element for the modeling and simulation of electromagnetic (EM) radiation propagation in the atmosphere are the characterization of the scattering and absorption features of both natural and man-made particulate matter suspended in air (aerosols). In fact, aerosols are the dominant mechanism for scattering of EM radiation in the boundary layer atmosphere. The boundary layer represents that portion of the atmosphere contained in the first two kilometers above ground level. The Army conducts most of its military operations, armor, infantry, helicopter, within the boundary layer; making an understanding of the portion of the atmosphere very important.. There have been a considerable number of models developed for characterizing natural and man-made aerosols[4, 5, 6, 9, 10]. For the natural hazes and fogs, the standard models are those of Shettle and Fenn[14]. The Shettle and Fenn haze models, hereafter referred as the standard models, have had the broadest use within the atmospheric modeling community. The standard haze models were based upon review of data on the nature of the aerosols, including sizes, distribution, and variability. They do not represent any exact aerosol type but instead represent a generalized description of atmospheric aerosol types. Shettle and Fenn's models for rural, urban, and maritime hazes have become the standard within other large environmental and atmospheric simulations and libraries (including: MODTRAN, LOWTRAN, EOSAEL,WAVES)[8, 3, 12].

The aerosol Phase Function Database (PFNDAT) is the primary aerosol scattering property database within the Electro Optical Systems Atmospheric Effects Library (EOSAEL)[15]. The PFNDAT database characterizes many of the battlefield and natural aerosols found in the boundary-layer atmosphere. The natural haze models in PFNDAT closely follow the haze models of Shettle and Fenn. The spectral resolution of the database is fairly coarse, with aerosol properties computed for two sets of wavelengths. The first set, which comprises the natural hazes, fogs, and some of the smokes, is computed at 32 wavelengths between 0.35μm and 40μm. The second set, which comprises some of the smoke and dust models, are computed at 22 wavelengths between 0.55μm and 14μm. This High Spectral-Resolution Phase Function Database (HSPFN-

DAT) contains all of the haze and fog natural aerosol models of PFNDAT and one obscurant (Fog Oil) calculated at 33,000 wavelengths between $0.35\mu m$ and $40\mu m$. For spectral signature modeling of plumes or atmospheric contaminants, it is necessary to model both target and background aerosols, as well as atmospheric molecular transmission at the finest resolution available. The resolution of HSPFNDAT matches that currently available from the U.S. Air Force's MODTRAN. MODTRAN is classified as a moderate resolution model in that it does not resolve individual atomic or molecular lines (like the model FASCODE does). We do not expect any line-shapes comparable to atomic or molecular transitions within typical atmospheric aerosol distributions. For this reason, matching the optical properties computed for aerosol models to the moderate resolution available from MODTRAN seems sufficient for a complete characterization of atmospheric aerosol optical properties.

Currently, WAVES incorporates the EOSAEL module PFNDAT which models 55 separate natural and man made aerosols at low resolutions. The motivation for developing HSPFNDAT is because of the necessity for modeling and simulation of the electro-optic properties of natural and man-made aerosol clouds as well as natural hazes and obscurants in high spectral resolution.

Future versions of HSPFNDAT will incorporate a complete set of the aerosols present in PFNDAT with scattering properties calculated at $1\ cm^{-1}$ resolution. In addition, the restriction for homogeneous, spherical particles will be lifted

for those aerosols such as ice crystals in which particle morphology can play an important role in scattering properties. We also hope to provide optical properties for aerosol "Basis Functions" that may be used to build representations of particular aerosol distributions.

1.1 Overview

As with PFNDAT, all of the aerosol models used to represent the natural and man-made aerosols in HSPFNDAT are assumed to be ensembles of homogeneous dielectric spheres characterized by a size distribution. For the fog models, this can be considered to be a very good assumption. However, application of this assumption to background hazes may not be as accurate. For the standard haze models, an effective refractive index is assumed which is an average of several different materials. Also, assuming a smooth, spherical morphology is likely to be an inaccurate. However, we can make the case that for the wavelength region between $2.5\mu m$ and $40\mu m$ the effect of ensemble averaging over a distribution of particle sizes effectively renders the arguments of non-sphericity and inhomogeneity moot. In addition, to the extent that non-spherical particles are randomly oriented in the atmosphere, an averaging effect will take place, making the measured optical properties more like those of spherical aerosol properties.

It is important to remember that the aerosol modelswe are using are designed to provide a small number of models that can represent the extinction and scattering effectsof the vastly more complex inhomogenious aerosols found in nature and on the battlefield. As such, we expect to never find an actual

aerosol that cehemically and morphologically matches these models. The models do however serve as suitable approximations for the wavelength dependent extinction, scattering, and absorption processes need in various atmospheric radiative transport models.

Within HSPFNDAT, we have used a Mie model, adapted from the model of Bohren and Huffman[1], to represent the single-particle scattering characteristics of the individual, homogeneous spheres comprising the aerosol.

There are two methods of calculating aerosol optical properties at high spectral resolution. The first is to calculate the properties using Mie theory at several wavelengths and interpolate the resulting optical properties. The second is to interpolate the complex index of refraction data and perform the Mie scattering calculation at each wavelength. In this work we used the second method, partially because we have high resolution index of refraction data for at least the liquid water found in fogs and all hygroscopic aerosols. In order to accurately calculate the scattering properties at spectral resolution of 1 cm^{-1} the complex refractive index is needed with the same spectral resolution. Our calculations for the maritime, rural, and urban aerosol models used the refractive index database given by Shettle and Fenn (1979)[14]. A linear interpolation routine was used to calculate the refractive index at the finer spectral resolution for use by the Mie scattering code. For the water fogs, the subroutine REFWAT, described in section 1.1.1 was used to determine the refractive index for water at 20°C. For non-zero relative humidities the data from REFWAT were also used as part of the calculation of the index of refraction for the haze aerosols .

As stated above, all of the aerosol models used in HSPFNDAT were represented by homogeneous spheres. The ensemble averaged aerosol extinction, scattering and absorption coefficients are calculated from the single particle cross sections, $Q(r, \mathrm{A}; \mathrm{m})$, and the particle size distribution, $n(r)$, using the Fredholm integral of Type I,

$$c(\lambda) = \int n(r)\pi r^2 Q(r, \lambda; m(\lambda))\,\mathrm{dr}, \tag{1.1}$$

where $c(\lambda)$ is either the volume extinction, scattering or absorption coefficient as a function of wavelength A, and $Q(r, \mathrm{A}; \mathrm{m})$ is the respective single particle extinction, scattering, or absorption efficiency calculated from Mie theory. Explicitly, the efficiency Q is dependent on the particle radius r, wavelength λ and the complex refractive index, $\mathrm{m} = \mathrm{n} + ik$, at wavelength A. The phase function is similarly calculated

$$\Phi(\lambda, \cos\theta) = \frac{1}{c_{\mathrm{scatter}}(\lambda)} \int n(r) \frac{d\sigma_{\mathrm{scatter}}}{d\Omega}(r, \lambda; m(\lambda))\,dr \quad , \tag{1.2}$$

where $n(r)$ is the particle size distribution, $d\sigma_{\mathrm{scatter}}/d\Omega$ is the differential scattering cross section. Additional properties can be calculated from these basic quantities such as the radar backscatter coefficient given by

$$\beta_\pi = 4\pi\Phi(\mathrm{A}, \cos\pi) \quad , \tag{1.3}$$

and the asymmetry parameter g given by

$$g = \langle \cos\theta \rangle = \int_{-1}^{1} (\cos 0) \cdot \Phi(\lambda, \cos 0)\, d(\cos\theta) \quad . \tag{1.4}$$

The asymmetry parameter is often used as a single descriptor for aerosol scattering properties. It only provides a rough estimate of the actual directional scattering properties, but can allow much faster calculations than using a full scattering phase function. We include the asymmetry parameter in our tabulations for use by such models.

The aerosol models in HSPFNDAT are described by only two types of size distributions. For the background hazes, the size distributions are modeled as log-normal distributions. For the natural fog aerosols, the size distributions are modeled as modified gamma size distributions. Following the notation of Kerker[7], the log-normal (LN) size distribution is given by

$$n(r) = \frac{dN}{dr} = \left[\frac{N}{r\sqrt{2\pi}\ln(\sigma_g)}\right] \exp\left\{-\frac{[\ln(r) - \ln(r_g)]^2}{2\ln(\sigma_g)^2}\right\} \quad , \tag{1.5}$$

where N is the number concentration of the aerosol, r_g is the geometric mean radius (or modal radius), and σ_g is the mode width[1]. Following the formalism of last version of PFNDAT[15] the Modified Gamma (MG) distribution is given by

$$n(r) = \frac{dN}{dr} = A'\left(\frac{r}{r_c}\right)^{\alpha} \exp\left[\frac{-\alpha}{\gamma}\left(\frac{r}{r_c}\right)^{\gamma}\right] \quad , \tag{1.6}$$

$$A' = \frac{N}{r_c} \frac{\gamma\left(\frac{\alpha}{\gamma}\right)^{\theta}}{\Gamma(\theta)} \quad , \tag{1.7}$$

$$\theta = \frac{\alpha + 1}{\gamma} \quad . \tag{1.8}$$

where, r_c, is the modal radius and 0, a, and y are fitting parameters.

As the relative humidity increases, the atmospheric haze aerosols will tend to increase in size due to absorption of water. Within HSPFNDAT, we treat this change of composition by changing the modal radius, r,, as well as the effective refractive index using a volume-weighted average of the dry material and water. This results in a change in the optical scattering properties of the aerosol.

1.1.1 REFWAT

REFWAT was developed by P. Flateau, principally based on the work of Ray[11]. REFWAT operates from a compilation of index of refraction datadases[13, 16, 11]. The routine REFWAT provides the complex refractive index given a wavelength and temperature. The REFWAT routine operates in four modes depending upon wavelength region.

[1]It is important to mention that the form of the log-normal size distribution given above is slightly different than that used by Shettle and Fenn and in PFNDAT.

1. For wavelengths less then 10.0 microns: tabular interpolation assuming real index and log(imaginary index) linear in log(wavelength),

2. for wavelengths between 10.0 microns and 20.0 microns: weighted data correction using Ray's model[11] to account for temperature dependence,

3. for wavelengths between 20.0 microns and 1.0 x 10^7 microns: data correction using Ray's model[11] to account for temperature dependence,

4. for wavelengths greater than 1.0×10^7 microns: Ray's analytic fits[11] based on some theories of Debye.

Chapter 2

Aerosol Models

2.1 Boundary Layer Hazes—Rural, Urban, and Maritime Aerosol Models

The maritime, urban, and rural aerosol models used in HSPFNDAT are those found in Shettle and Fenn (1979)[14] and are identical to the models of PFNDAT. They are characterized as bimodal, lognormal distributions with the mode radii varying as a function of humidity. The refractive indices for each of these aerosols were assumed to be a simple admixture, by volume, of the refractive indices of the component aerosol with water. Following the formulation of Shettle and Fenn, the complex refractive indices, m, of the hydrated aerosols were calculated by simply considering the hydrated aerosol's refractive index as being the volume averaged refractive index of the dry fraction, f_{dry}, and water fraction, f_{water}, of the hydrated aerosol. The volume of the dry or wet particle is in each instance calculated from the appropriate modal radius, r_g, as a function of relative humidity (RH).

$$f_{\text{dry}}(\%\text{RH}) = \frac{r_g^3(\%\text{RH}=0)}{r_g^3(\%\text{RH})} \quad , \tag{2.1}$$

$$f_{\text{water}}(\%\text{RH}) = 1 - f_{\text{dry}}(\%\text{RH}) \quad , \tag{2.2}$$

$$m(\%\text{RH}) = m_{\text{dry}} f_{\text{dry}}(\%\text{RH}) + m_{\text{water}} f_{\text{water}}(\%\text{RH}) \quad . \tag{2.3}$$

Plots of the refractive indices as a function of wavenumber for the haze models for several values of the relative humidity can be found in appendix A. The particle concentrations for the haze models were adjusted so that the default meteorological visibility (at 0.55 μm) was 5 km. Tables 2.1, 2.2, and 2.3 summarize the parameters for the bimodal distributions as a function of humidity.

Table 2.1: Effective mode radii, spread, and number densities as a function of relative humidity for the small (S) and large (L) modes of the AFGL Maritime haze model.

	Relative Humidity							
	0	50	70	80	90	95	98	99
Small Mode								
$N(\mathrm{S})$	38251	35129	27757	13902	9697	6976	4360	2948
$r_g(\mathrm{S})$	0.02700	0.02748	0.02846	0.03274	0.03884	0.04238	0.04751	0.05215
$\sigma_g(\mathrm{S})$	2.239	2.239	2.239	2.239	2.239	2.239	2.239	2.239
Large Mode								
$N(\mathrm{L})$	386.4	354.8	280.4	140.4	98.0	70.5	44.0	29.8
$r_g(\mathrm{L})$	0.1600	0.1711	0.2041	0.3180	0.3803	0.4606	0.6024	0.7505
$\sigma_g(\mathrm{L})$	2.512	2.512	2.512	2.512	2.512	2.512	2.512	2.512

Table 2.2: Effective mode radii, spread, and number densities as a function of relative humidity for the small (S) and large (L) modes of the AFGL urban haze model.

	Relative Humidity							
	0	50	70	80	90	95	98	99
Small Mode								
$N(\mathrm{S})$	87204	83354	64829	42776	27693	18217	10516	7286
$r_g(\mathrm{S})$	0.02500	0.02563	0.02911	0.03514	0.04187	0.04904	0.05996	0.06847
$\sigma_g(\mathrm{S})$	2.239	2.239	2.239	2.239	2.239	2.239	2.239	2.239
Large Mode								
$N(\mathrm{L})$	10.9	10.4	8.1	5.4	3.5	2.3	1.3	0.9
$r_g(\mathrm{L})$	0.4000	0.4113	0.4777	0.5805	0.7601	0.8634	1.1690	1.4850
$\sigma_g(\mathrm{S})$	2.512	2.512	2.512	2.512	2.512	2.512	2.512	2.512

Table 2.3: Effective mode radii, spread, and number densities as a function of relative humidity for the small (S) and large (L) modes of the AFGL rural haze model.

	Relative Humidity							
	0	50	70	80	90	95	98	99
Small Mode								
$N(\mathrm{S})$	79076	76305	70804	51674	33895	27052	19290	14761
$r_{\mathrm{g}}(\mathrm{S})$	0.02700	0.02748	0.02846	0.03274	0.03884	0.04238	0.04751	0.05215
$\sigma_g(\mathrm{S})$	2.239	2.239	2.239	2.239	2.239	2.239	2.239	2.239
Large Mode								
$N(L)$	9.9	9.5	8.9	6.4	4.2	3.4	2.4	1.9
$r_{\mathrm{g}}(\mathrm{L})$	0.4300	0.4377	0.4571	0.5477	0.6462	0.7078	0.9728	1.1760
$\sigma_{\mathrm{g}}(\mathrm{L})$	2.512	2.512	2.512	2.512	2.512	2.512	2.512	2.512

2.2 Fog models

The fog models used in HSPFNDAT correspond to the heavy advection and moderate radiation fog models described in Shettle and Fenn[14]. These fogs form when the air becomes saturated either by mixing of different air masses (advection fog) or by cooling until the air temperature approaches the dew point temperature (radiation fog). These models use the Modified Gamma (MG) distribution to describe the size distribution. Although we know that the fog aerosols are composed of both water and the condensation nuclei, we assume the refractive index to be that of pure water as calculated by REFWAT. The effect of this assumption for the calculated optical properties is likely to be very small. The heavy advection fog model uses a mode radius of 10 μm, particle concentration of 20 particles/cm^3 and the MG parameters $\mathbf{a} = 3$, and $\gamma = 1$. The moderate radiation fog is characterized by a mode radius of 2 pm, particle density of 200 particles/cm^3, and MG parameters $\mathbf{a} = 6$ and y = 1.

2.3 Aerosol Smoke Model

In this interim HSPFNDAT, only the fog-oil model has been computed. This model scales the scattering parameters for a mass concentration of 1 gm/cm^3. The aerosol size distribution is described by a log-normal size distribution with a geometric mean $r_g = 0.19\mu$m, and a width $a, = 1.45$. These parameters were found to be appropriate for the current military generators designed to produce particles for obscuration at visible wavelengths[2]. This model does not incorporate any hygroscopic growth due to ambient humidity. For this model, the tabulated refractive index from PFNDAT92[15] was interpolated for the high spectral resolution of HSPFNDAT.

Chapter 3

Database Guide

3.1 Aerosol Identification Indices

In the interim version of the high resolution PFNDAT, the phase function database is structured similar to PFNDAT92[15]. This database is comprised of a series of ASCII text files, one for each of the aerosols listed in table 3.1.

Table 3.1: Aerosols in HRPFNDAT

Aerosol Index	Aerosol Name	Relative Humidity
1	Maritime	0
2	Maritime	50
3	Maritime	70
4	Maritime	80
5	Maritime	90
6	Maritime	95
7	Maritime	98
8	Maritime	99
9	Urban	0
10	Urban	50
11	Urban	70
12	Urban	80
13	Urban	90
14	Urban	95
15	Urban	98
16	Urban	99
17	Rural	0
18	Rural	50
19	Rural	70
20	Rural	80
21	Rural	90
22	Rural	95
23	Rural	98
24	Rural	99
25	Fog (Heavy Advection)	NA
26	Fog (Moderate Radiation)	NA
56	Fog Oil	50

3.2 Structure of the Databases

As with the phase function database PFNDAT, the files are called PFNDAT.nnn, where nnn identifies the particular aerosol index from table 3.1. Each file begins with a list of the 126 discrete angles between 0 and 180 degrees. The remainder of the file contains sets of a preamble and phase function results at each wavelength. The one-line preamble records the number of angular data items, the aerosol identifier, wavelength λ (in μm), the spectral single scattering albedo at λ, and the extinction and scattering coefficients (in km^{-1}). After this the values of the phase function at each angle is listed.

Table 3.2: Structure for an individual HRPFNDAT file PFNDAT.nnn

θ_1	θ_2		...		θ_{11}
θ_{56}	...			θ_{126}	999.99
NANG	*nnn*	λ_1	ϖ_0	Pex	β_s
$P(\theta_1, \lambda_1$	$P(\theta_2, \lambda_1)$		...		$P(\theta_6, \lambda_1$
$P(\theta_{61}, \lambda_1)$	$P(\theta_{62}, \lambda_1)$		...		$P(\theta_{126}, \lambda_1)$
NANG	*nnn*	λ_{max}	ϖ_0	Pex	β_s
$P(\theta_1, \lambda_{max})$	$P(\theta_2, \lambda_{max})$		...		$P(\theta_6, \lambda_{max})$
$P(\theta_{61}, \lambda_{max})$	$P(\theta_{62}, \lambda_{max})$		...		$P(\theta_{126}, \lambda_{max})$

θ_i = discrete angles (degrees)
NANG = number of discrete angles
nnn = phase function identifier
λ_l = l^{th} wavelength (μm)
ϖ_0 = single scattering albedo
β_{ex} = Extinction coefficient (km^{-1})
β_s = Scattering coefficient (km^{-1})
$P(\theta_i, \lambda_l)$ = value of phase function at angle ***i***, wavelength 1

In addition to the phase function data files, the high resolution PFNDAT has an additional file, called SCAT.nnn, containing only the extinction, scattering and radar backscatter coefficients as a function of wavelength.

Table **3.3:** Structure for an individual HRPFNDAT file SCAT.nnn

k_1	$\beta_{\text{ext}}(k_1)$	$\beta_{\text{scat}}(k_1)$	$\beta_\pi(k_1)$
⋮	⋮	⋮	⋮
k_n	$\beta_{\text{ext}}(k_n)$	$\beta_{\text{scat}}(k_n)$	$\beta_\pi(k_n)$

$k_l = l^{th}$ wavenumber (cm^{-1})

β_{ext} = Extinction coefficient (km^{-1})

β_{scat} = Scattering coefficient (km^{-1})

β_π = Backscattering coefficient (km^{-1})

Chapter 4

Conclusion

We have presented some interim results for a high resolution **PFNDAT** database of optical properties. Although this preliminary database contains only the natural haze, fogs, and fog-oil smoke models, we will be adding the rest of the smoke and dust models found in PFNDAT92. We will also be including new models that will characterize several biological aerosols as well as new models characterizing natural clouds. A more formal data model is being developed for the final version of **HSPFNDAT.**

Appendix A

Indices of Refraction

In this chapter we have collected graphs of the real and imaginary indices of refraction. These are plots of the data used in the Mie scattering calculations to produce the plots in appendix B. In many cases the index of refraction data are interpolated between a few measurements. In some wavelength regions the structure is well described, in others, the location and shape of the features is poorly resolved. We propose that revisiting the measurements of the indices of refraction should be undertaken to provide the level of detail necessary for accurate processing of hyperspectral atmospheric data or for use with tunable lasers.

A.1 Indices of Refraction of Maritime Aerosols

Figure A.1: Real Index Aerosol 01, Maritime Haze 0% relative humidity

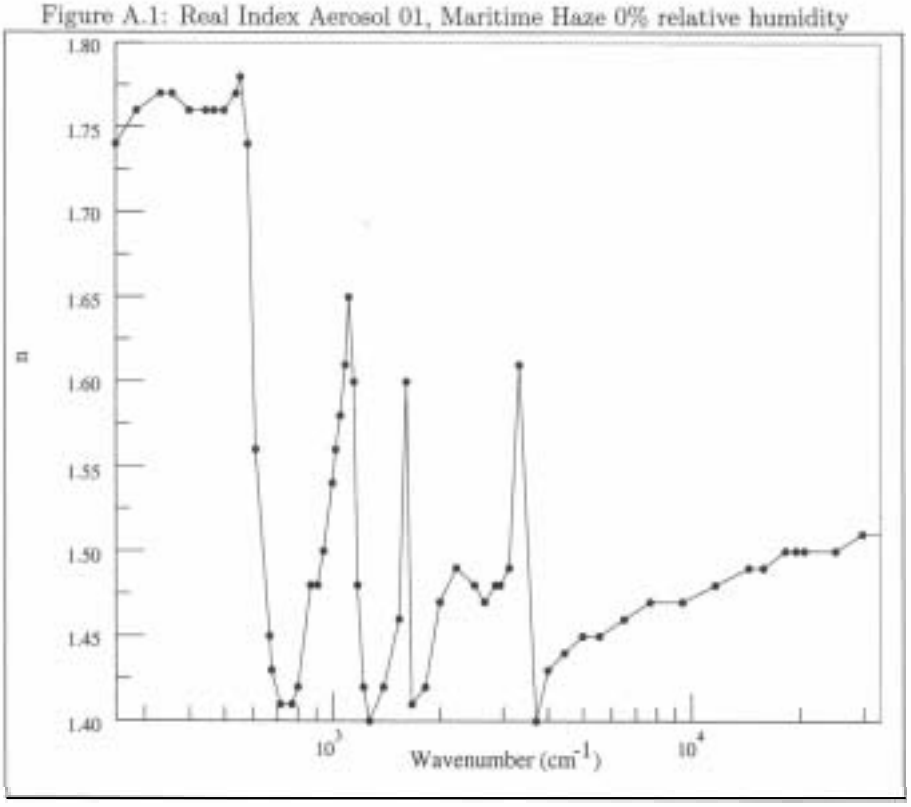

Figure A.2: Imaginary Index Aerosol 01, Maritime Haze 0% relative humidity

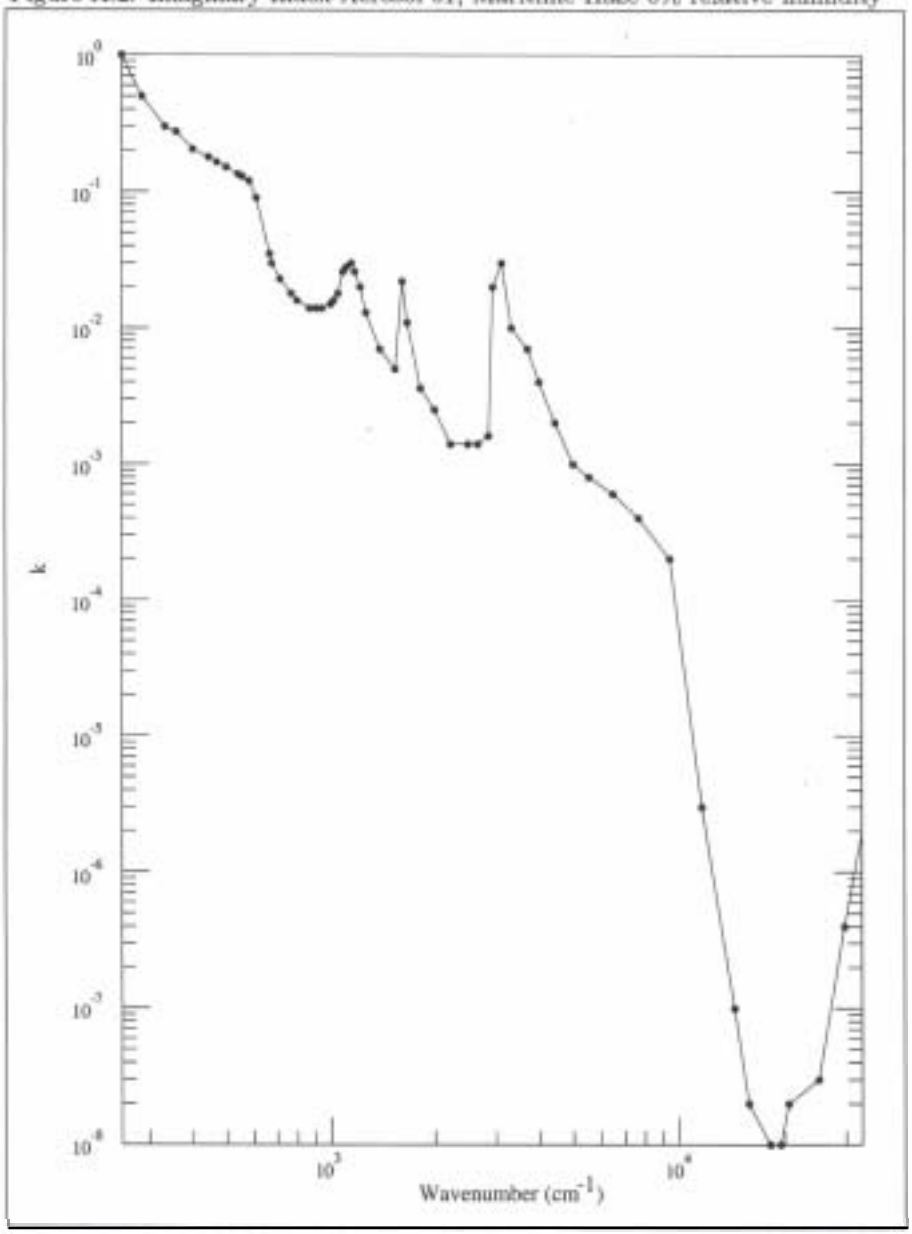

Figure A.3: Real Index Aerosol 02, Maritime Haze 50% relative humidity

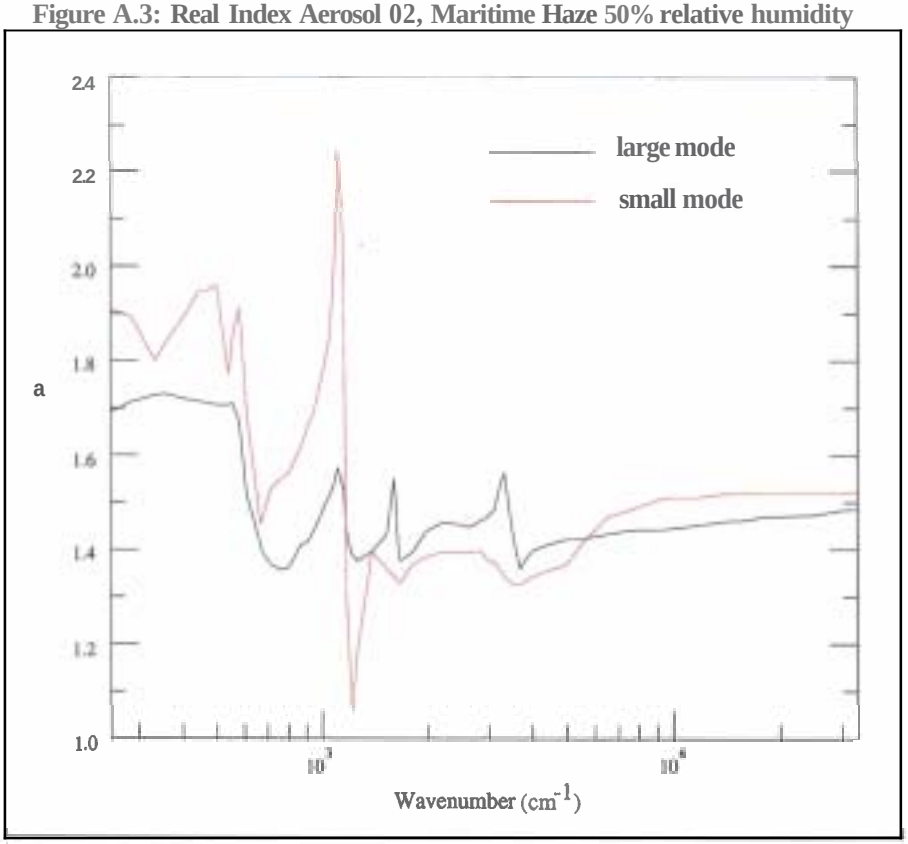

Figure A.4: Imaginary Index Aerosol 02, Maritime Haze 50% relative humidity

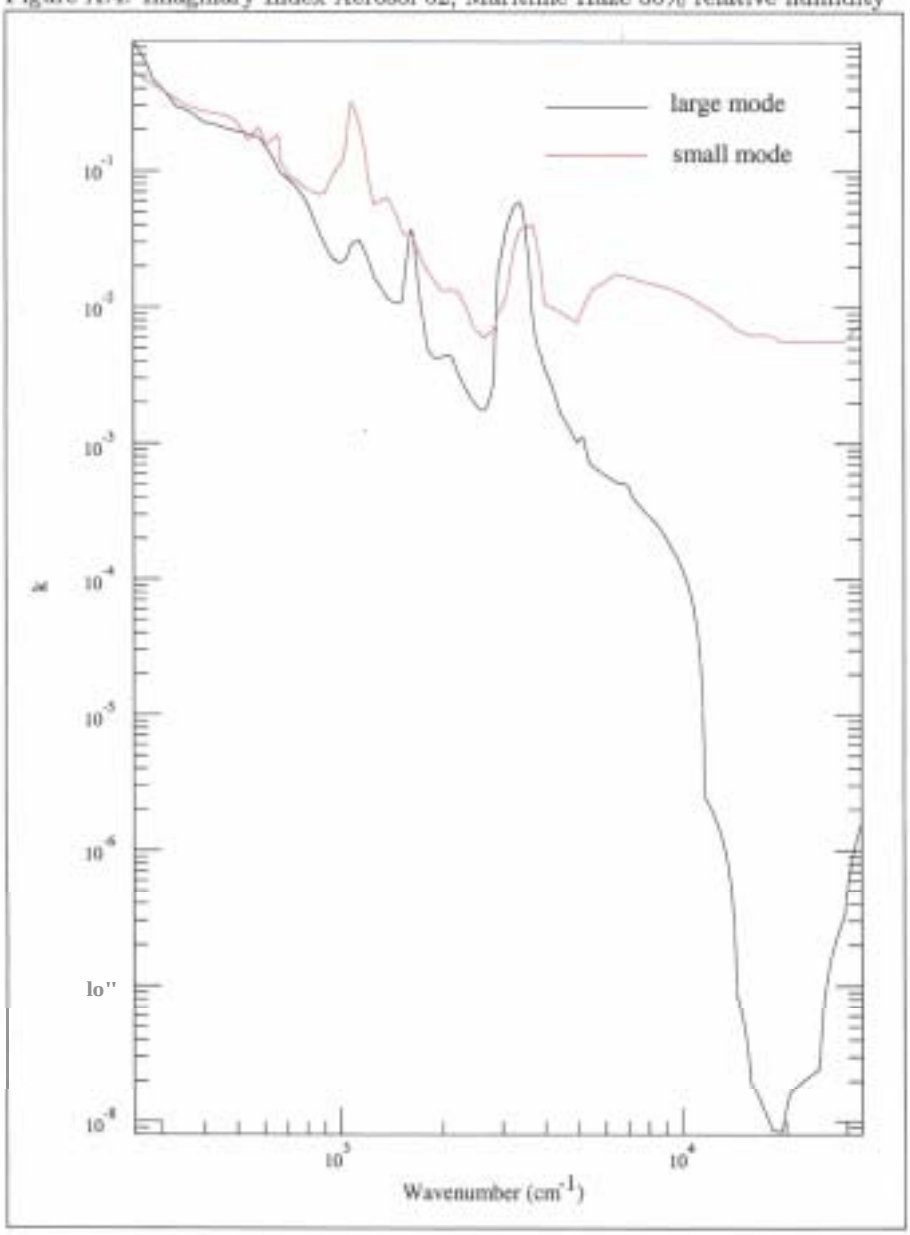

Figure A.5: Real Index Aerosol 03, Maritime Haze 70% relative humidity

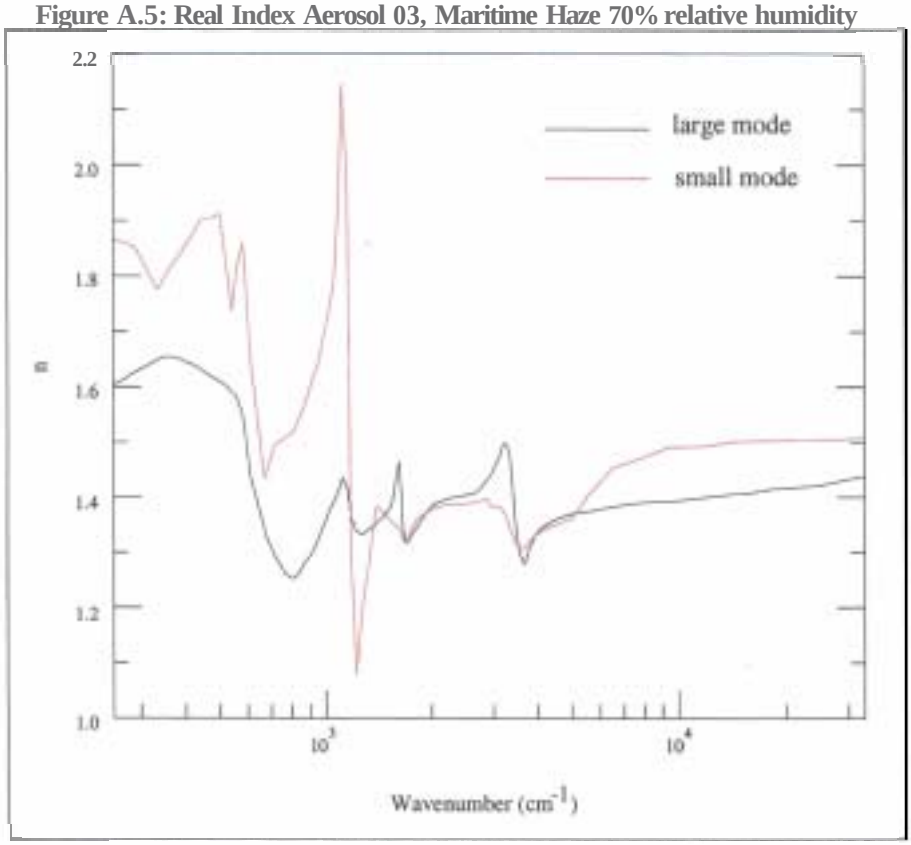

Figure A.6: Imaginary Index Aerosol 03, Maritime Haze 70% relative humidity

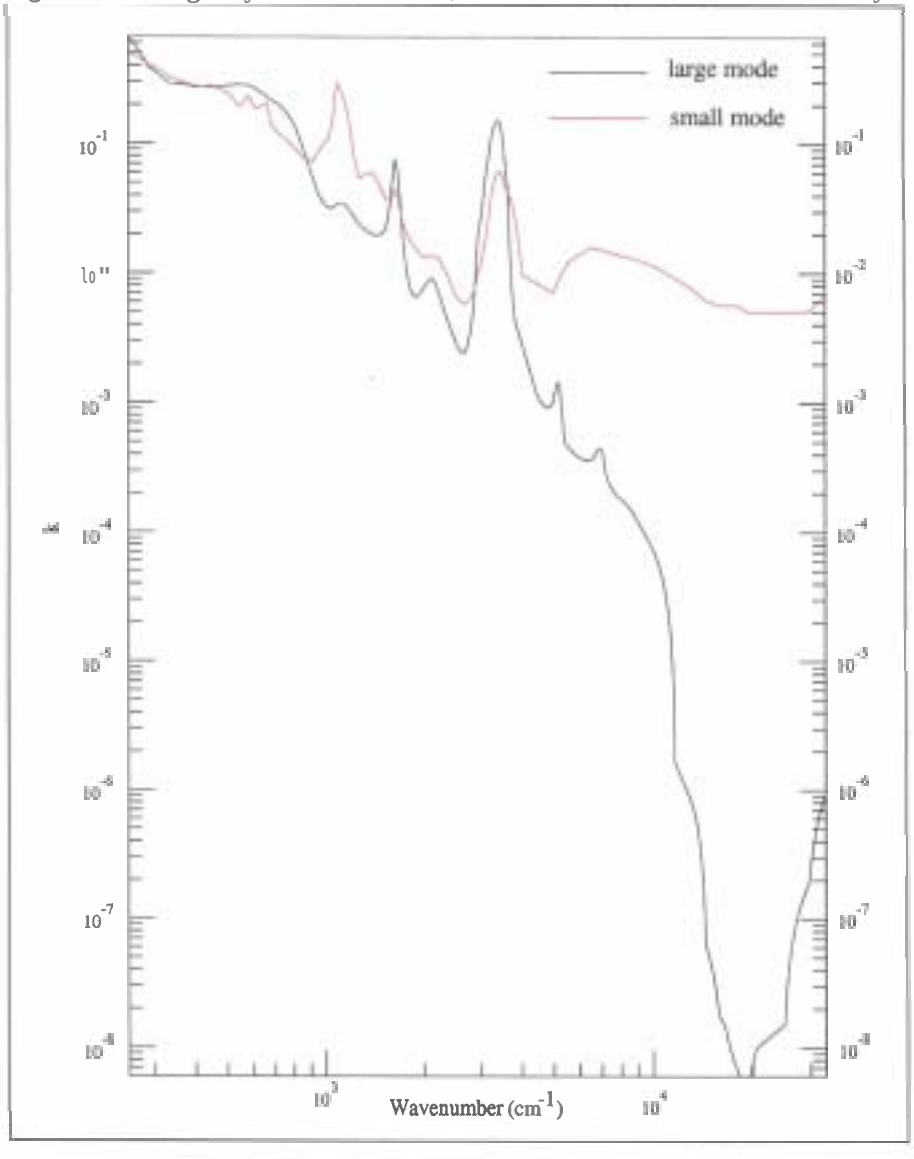

Figure A.7: Real Index Aerosol 04, Maritime Haze 80% relative humidity

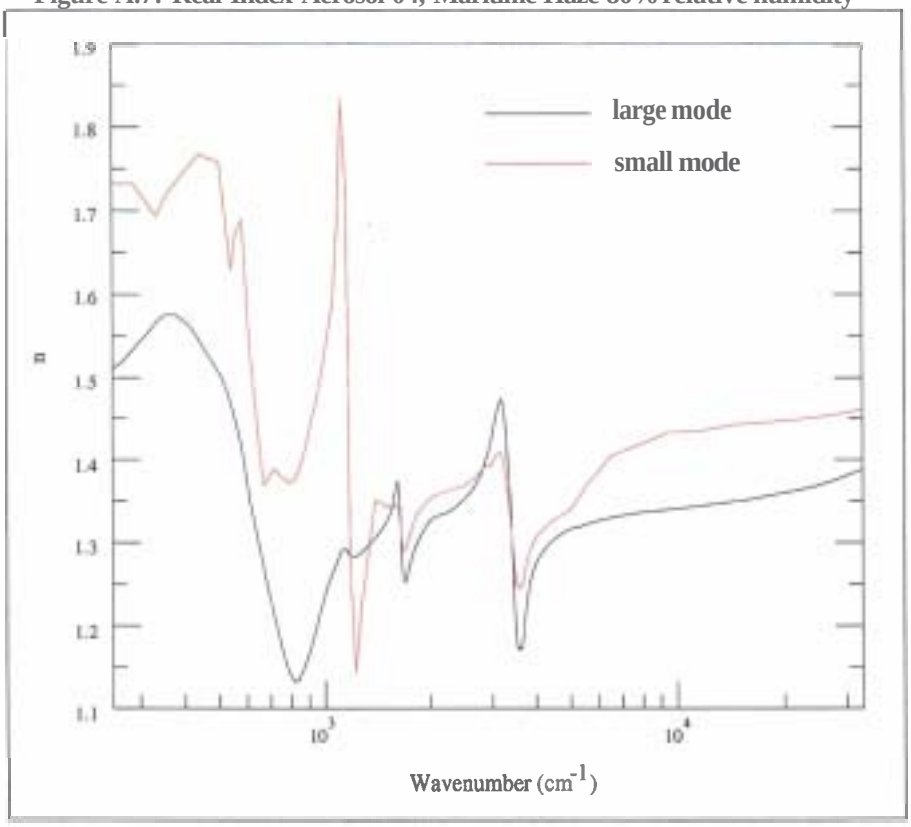

Figure A.8: Imaginary Index Aerosol 04, Maritime Haze 80% relative humidity

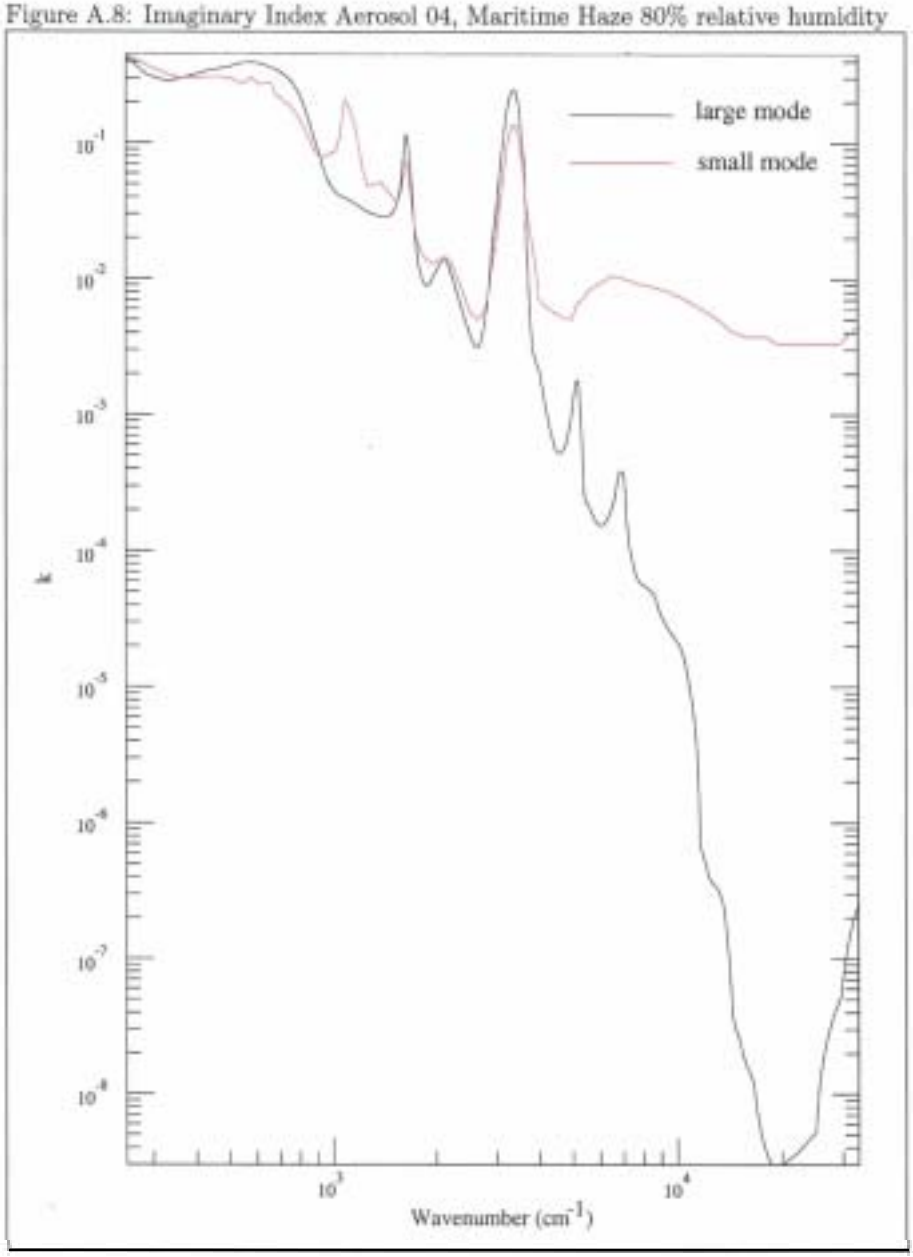

Figure A.9: Red Index Aerosol 05, Maritime Haze 90% relative humidity

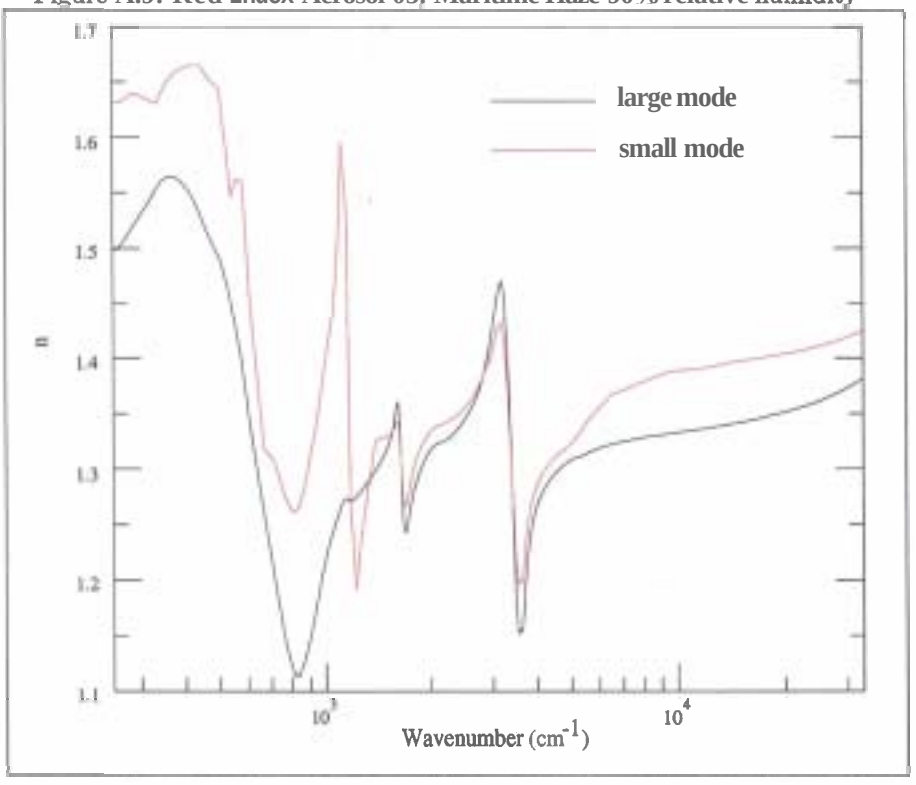

Figure A.lO: Imaginary Index Aerosol 05, Maritime Haze 90% relative humidity

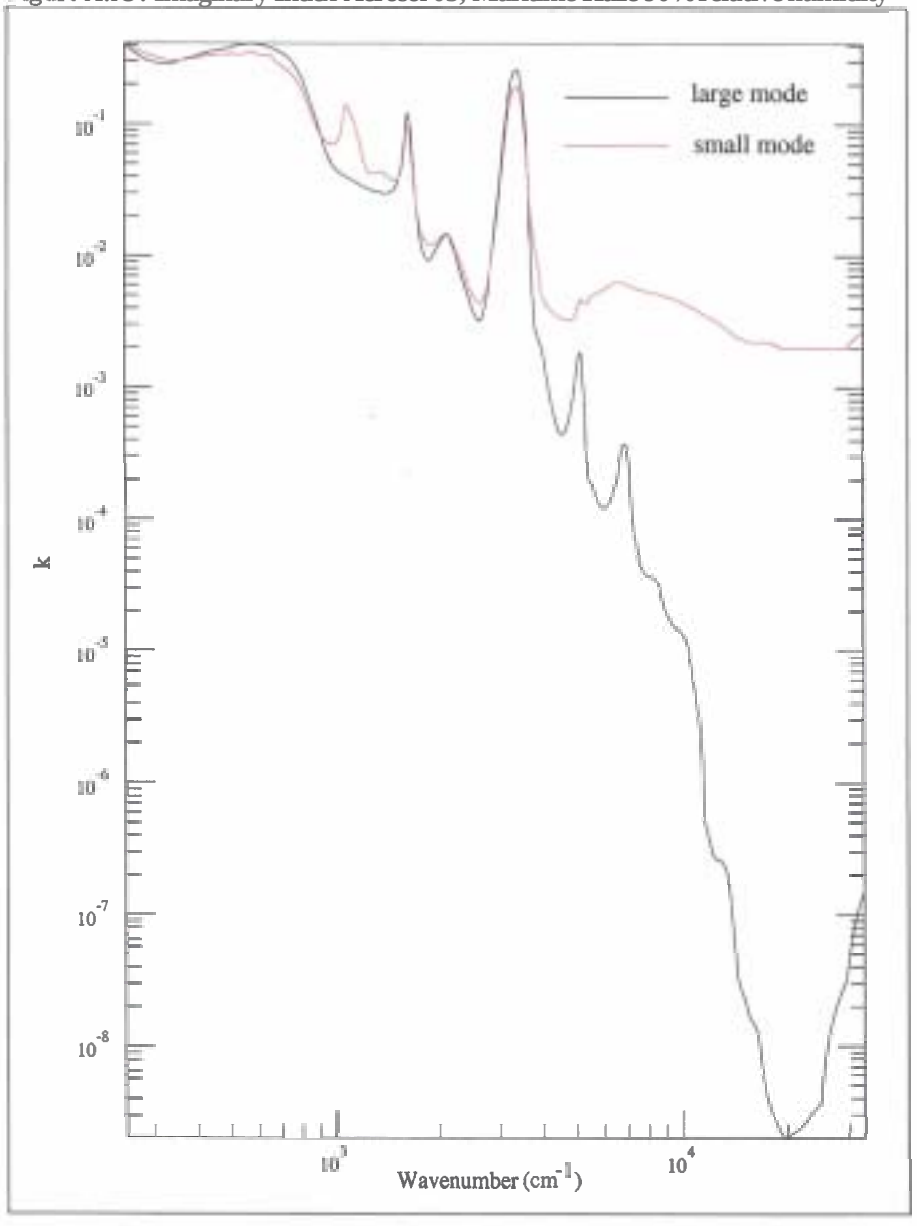

Figure A.11: Real Index Aerosol 06, Maritime Haze 95% relative humidity

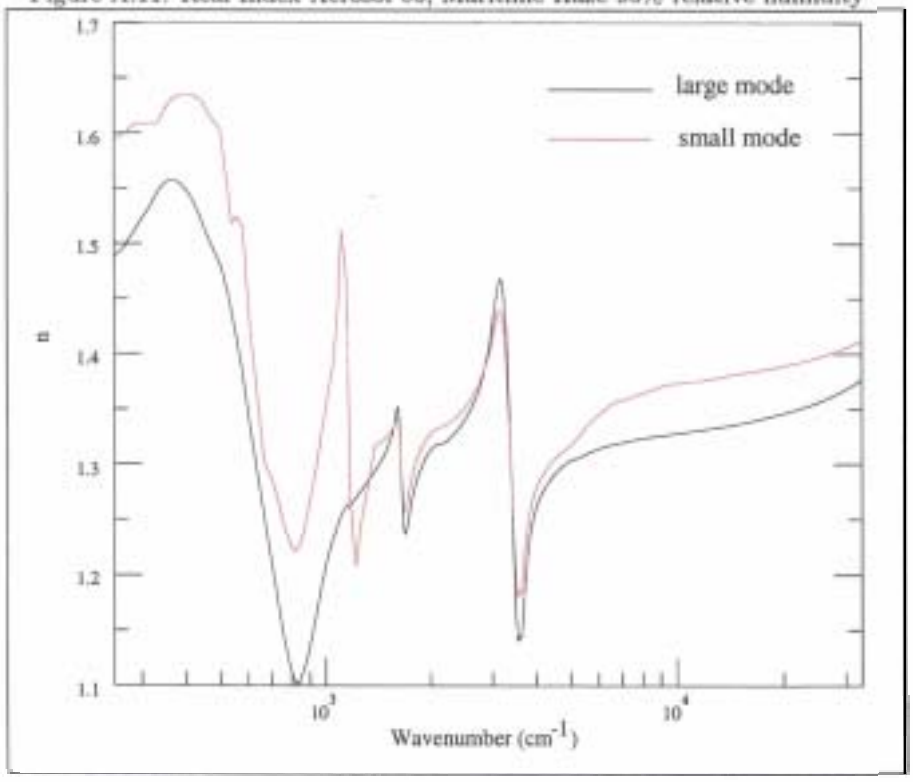

Figure A.12: Imaginary Index Aerosol 06, Maritime Haze 95% relative humidity

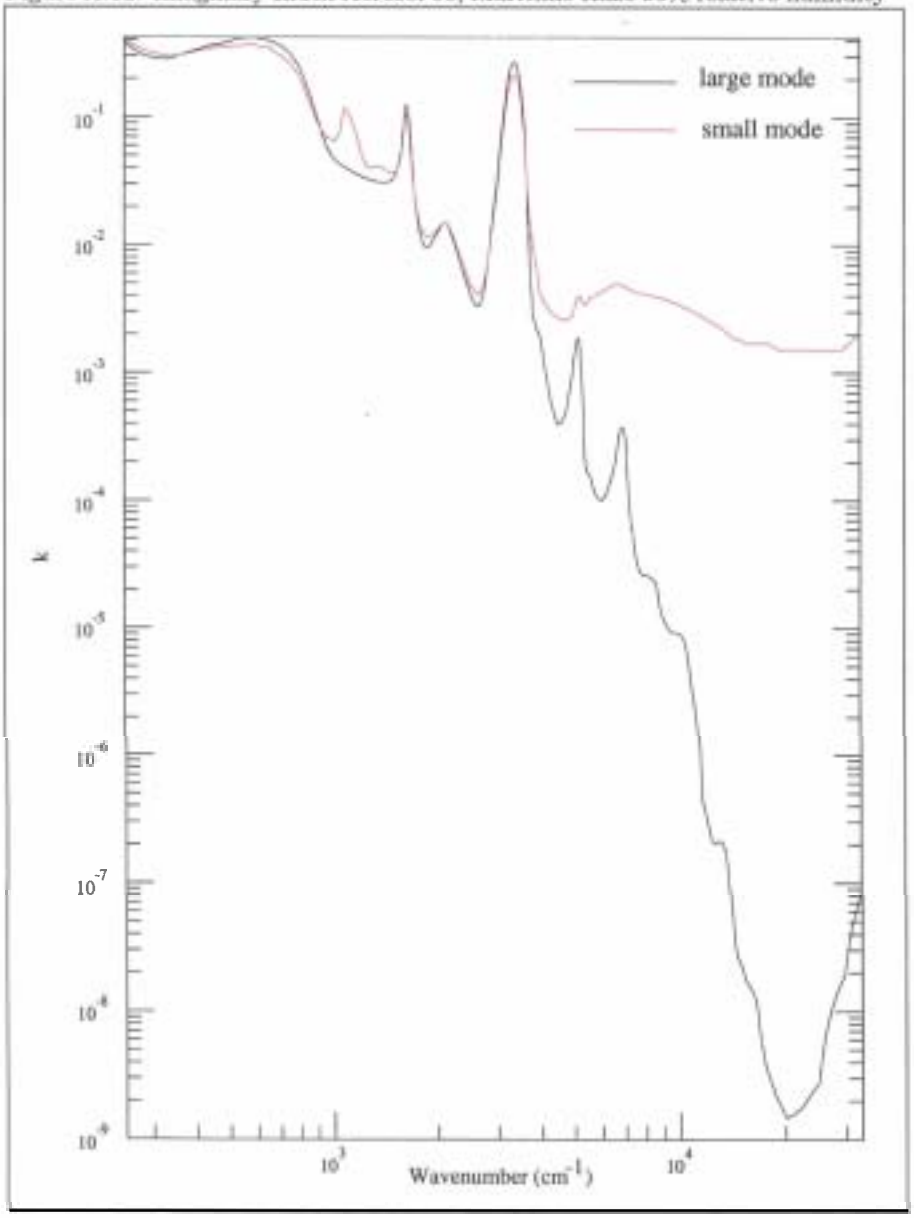

Figure A.13: Real Index Aerosol 07, Maritime Haze 98% relative humidity

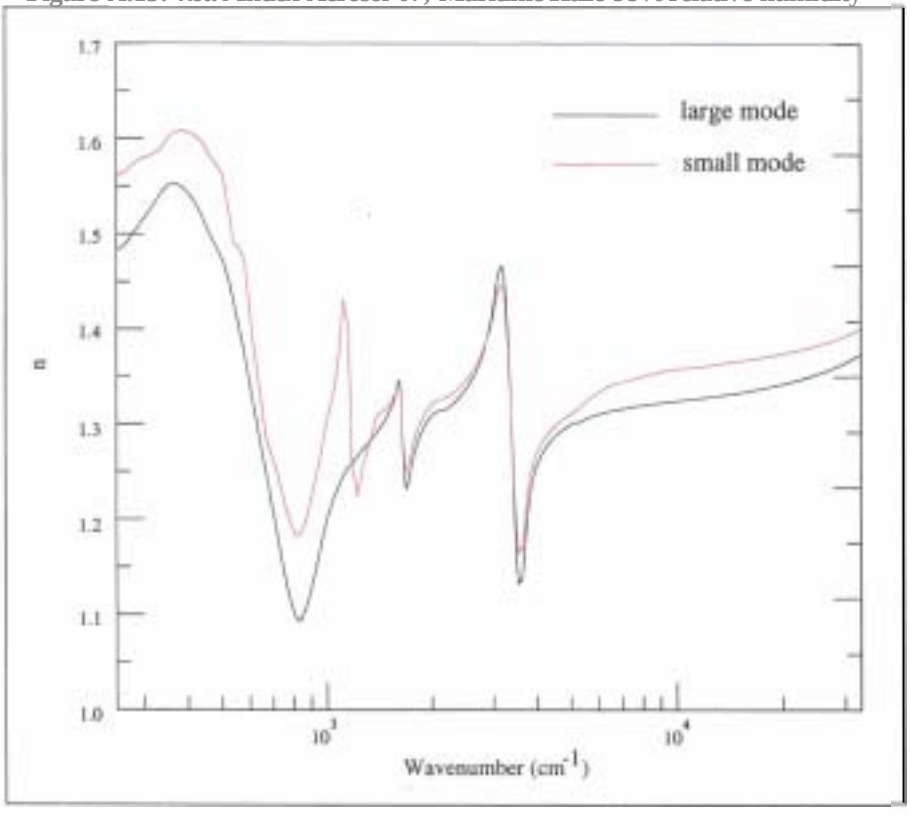

Figure A.14: Imaginary Index Aerosol 07, Maritime Haze 98% relative humidity

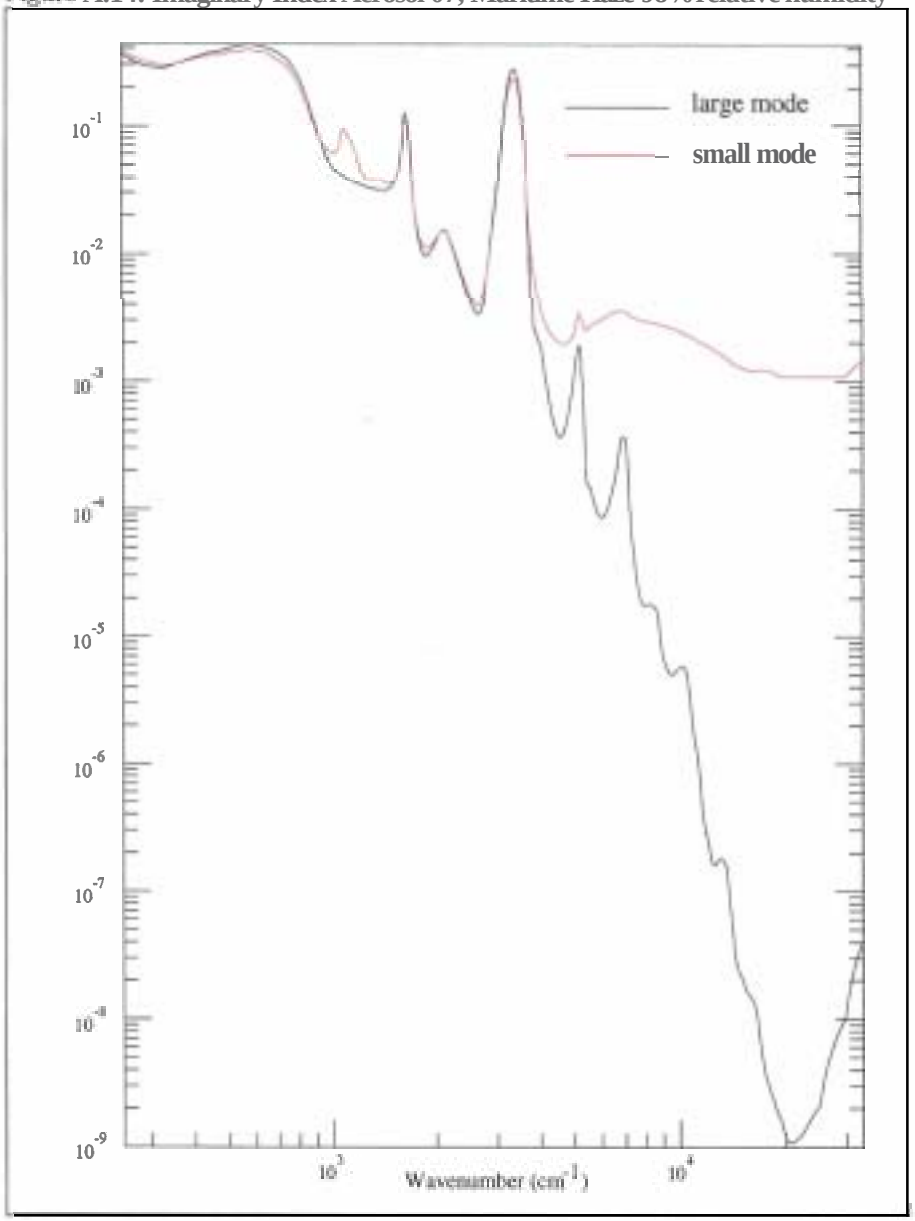

Figure A.15: Real Index Aerosol 08, Maritime Haze 99% relative humidity

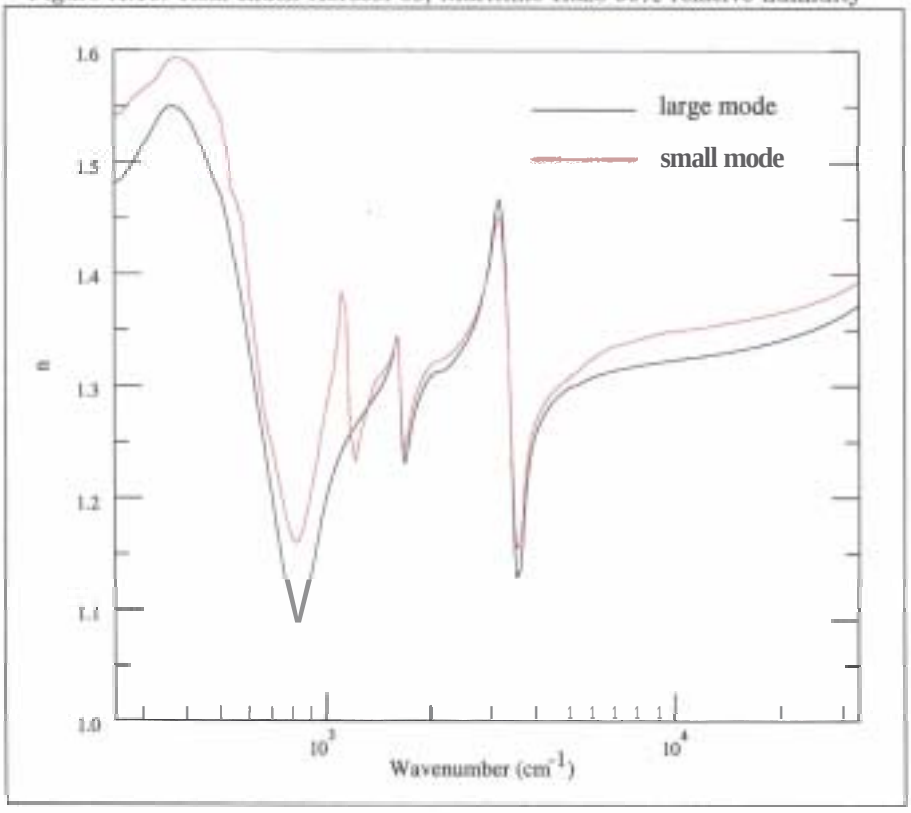

Figure A.16: Imaginary Index Aerosol 08, Maritime Haze 99% relative humidity

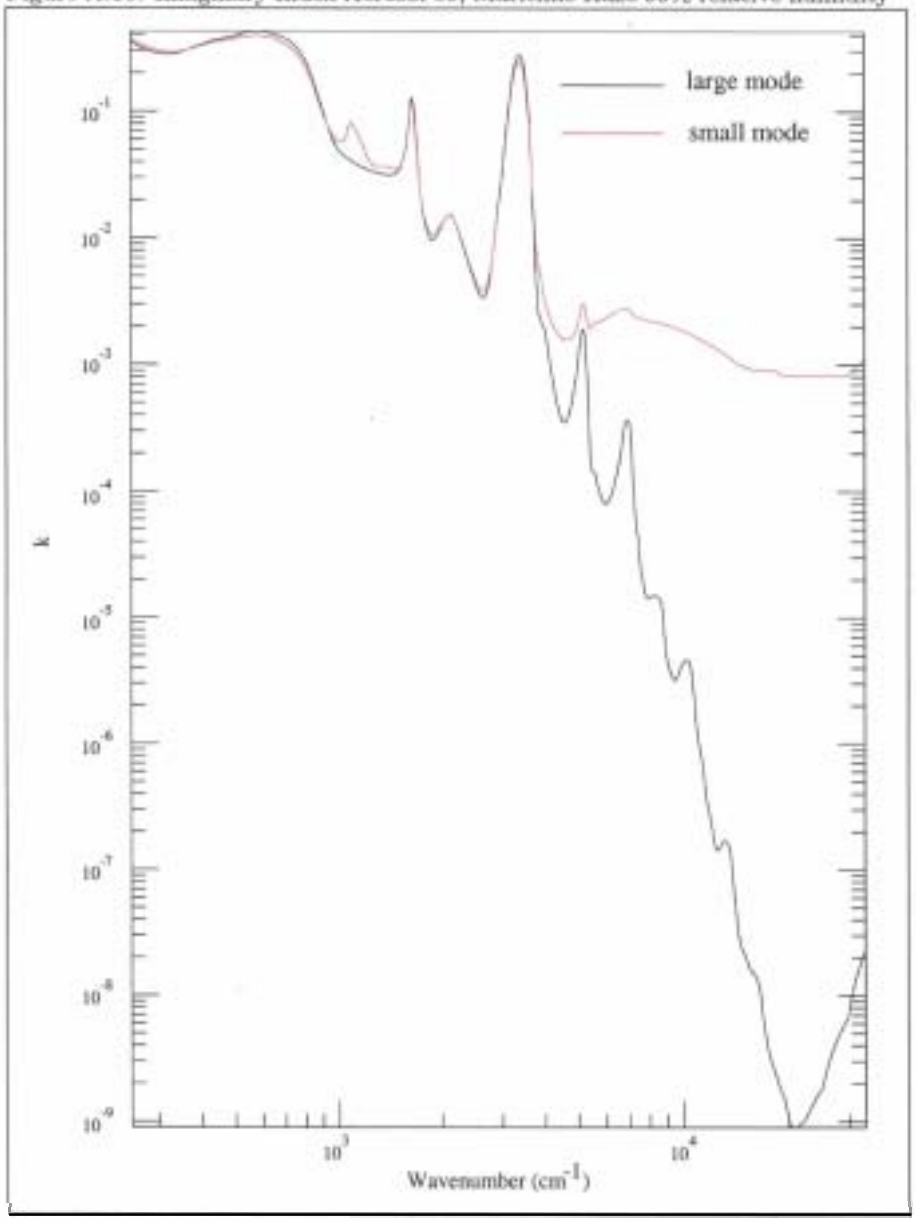

Figure A.17: Real Index Aerosol 09, Urban Haze 0% relative humidity

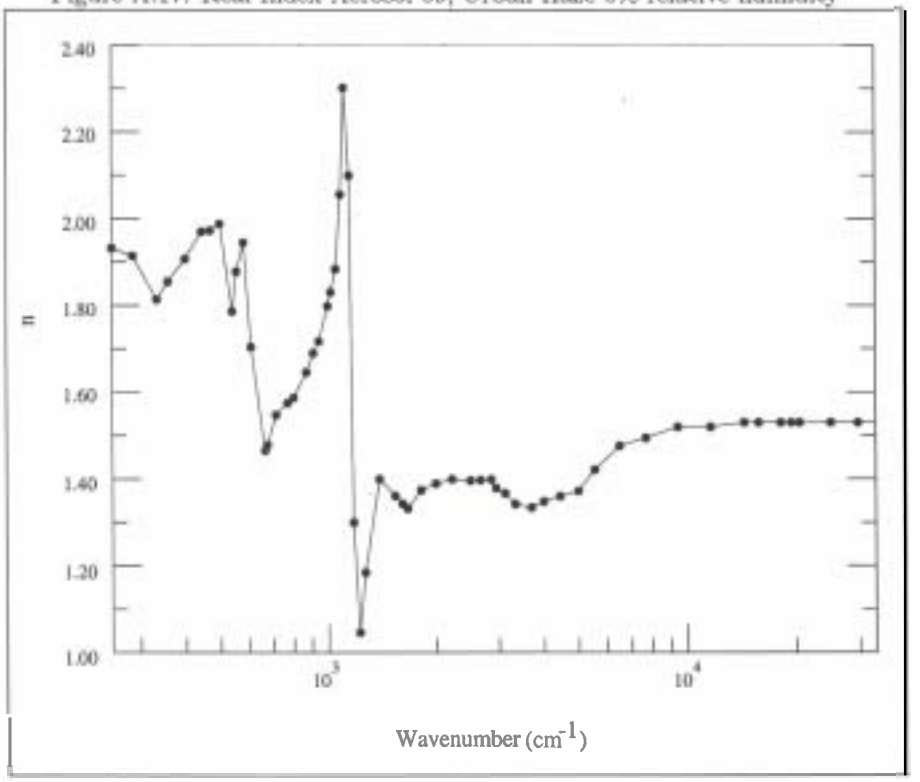

A.2 Indices of Refraction of Urban Aerosols

Figure A.18: Imaginary Index Aerosol 09, Urban Haze 0% relative humidity

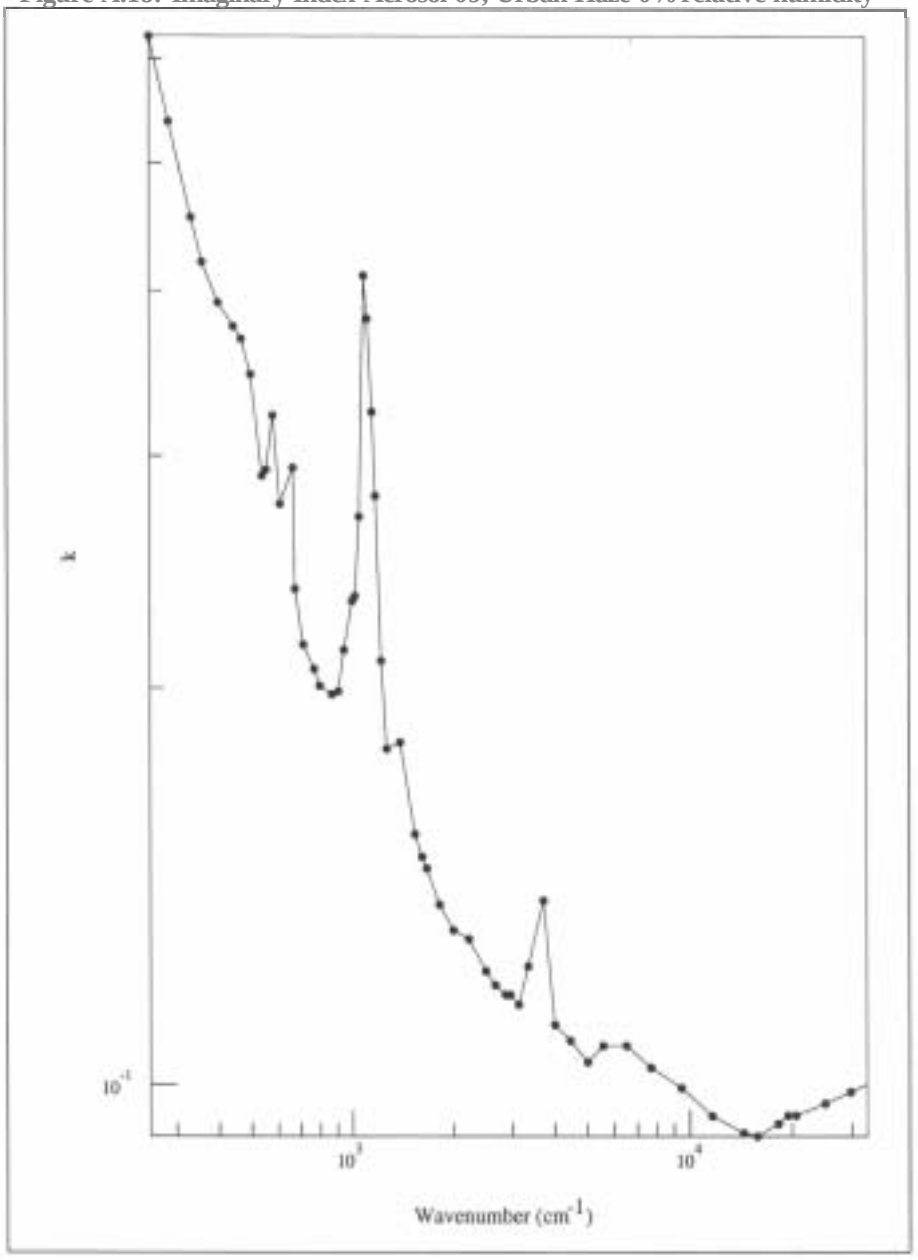

Figure A.19: Real Index Aerosol 10, Urban Haze 50% relative humidity

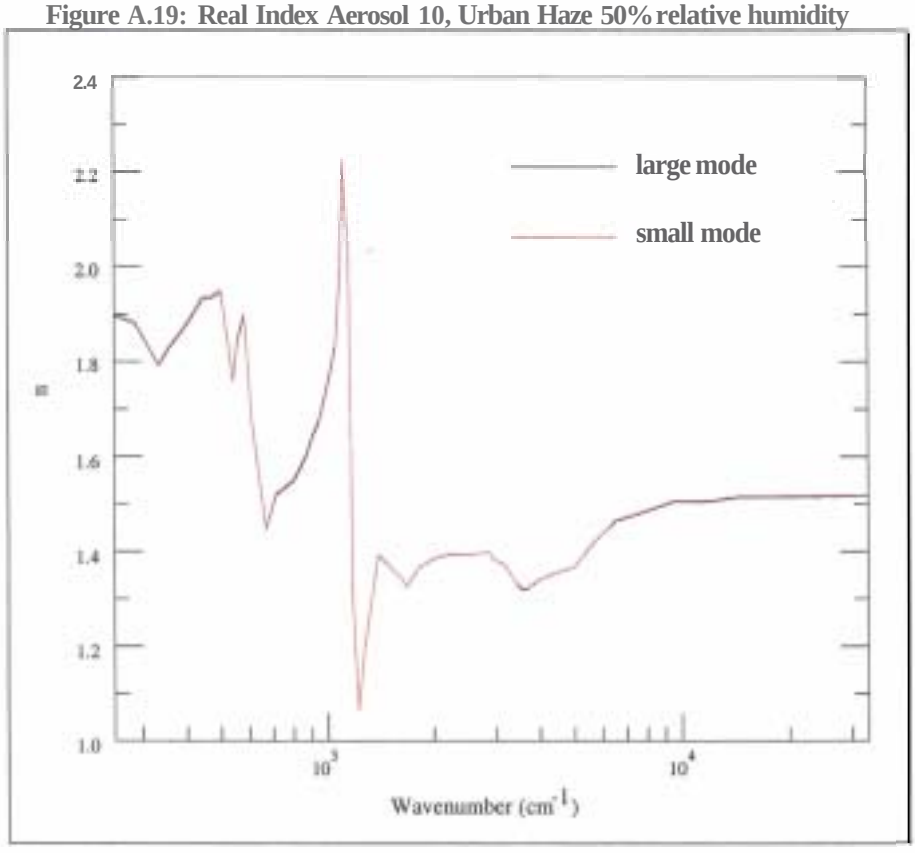

Figure A.20: Imaginary Index Aerosol 10, Urban Haze 50% relative humidity

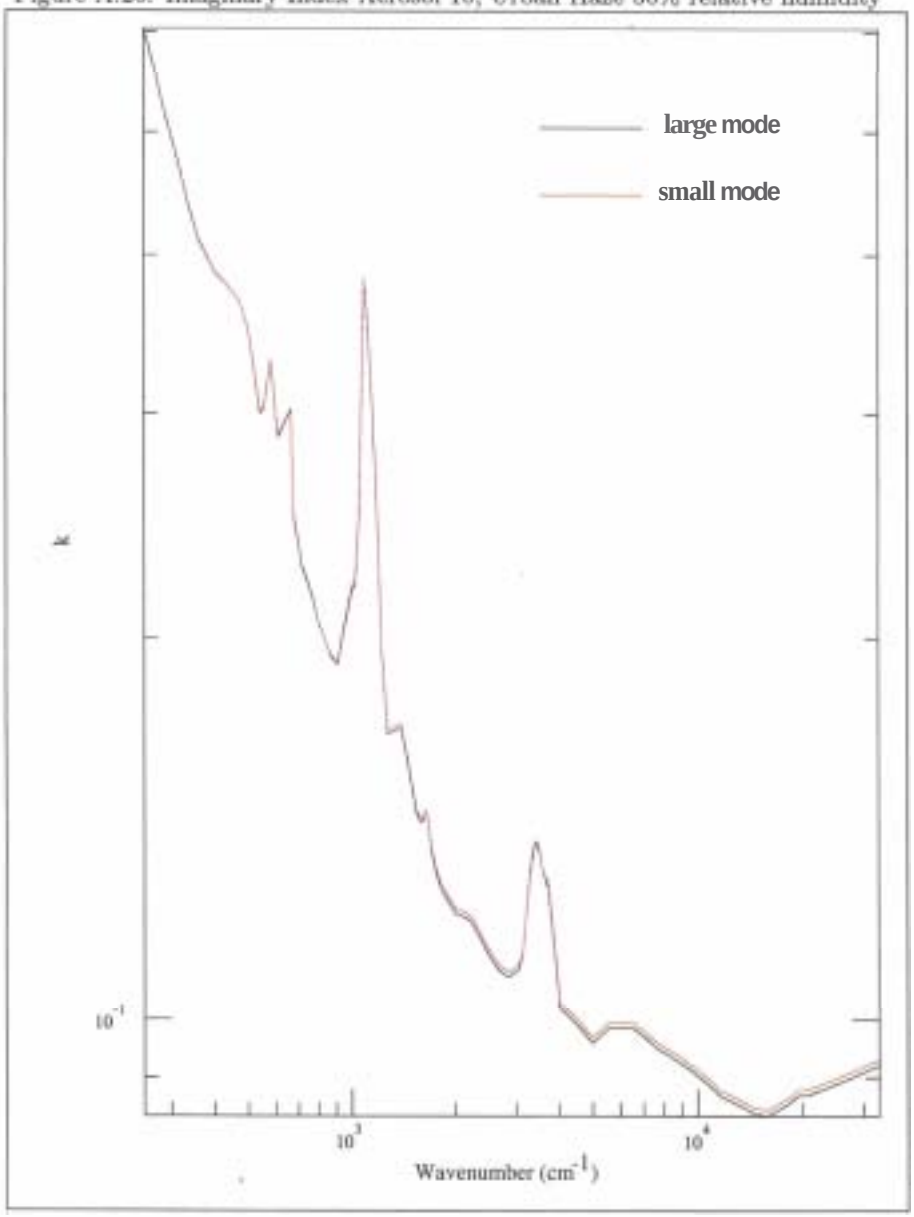

Figure A.21: Real Index Aerosol 11, Urban Haze 70% relative humidity

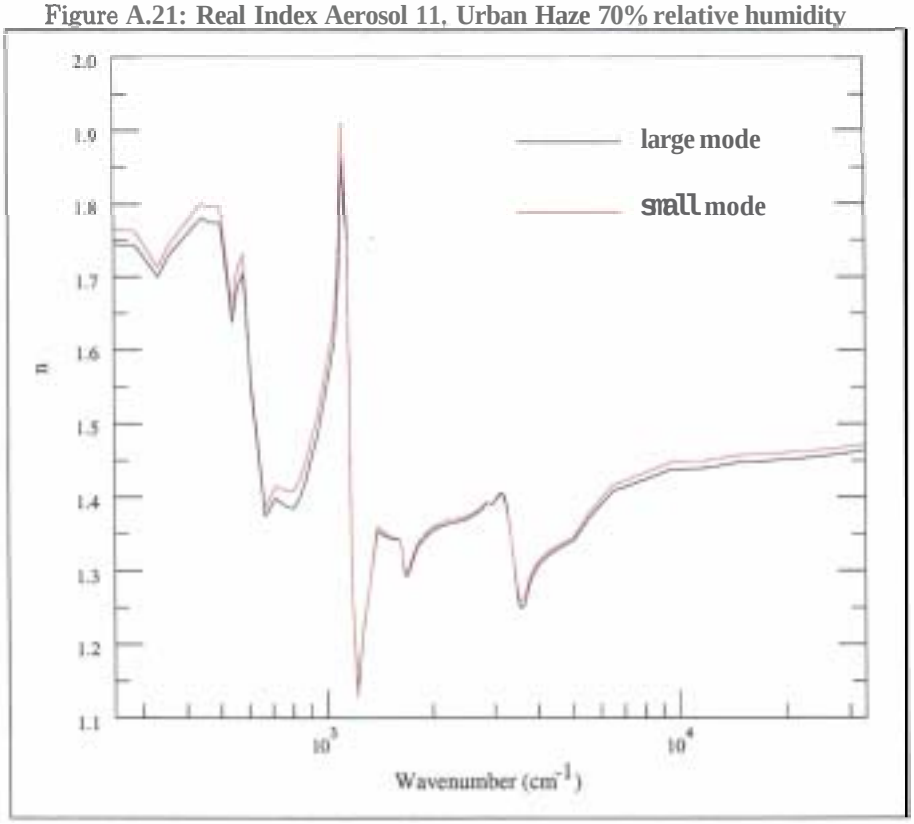

Figure A.22: Imaginary Index Aerosol 11, Urban Haze 70% relative humidity

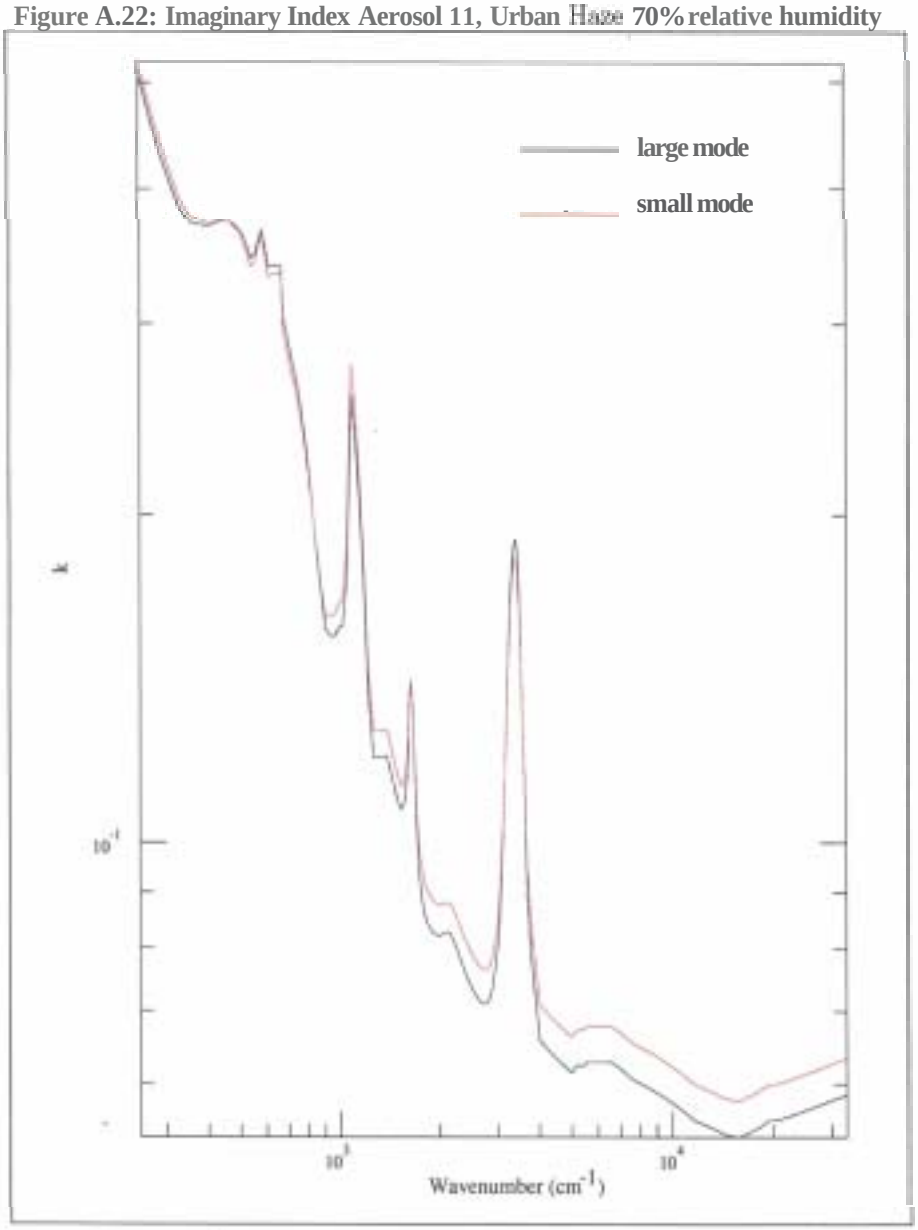

Figure **A.23: Real Index Aerosol 12, Urban Haze 80% relative humidity**

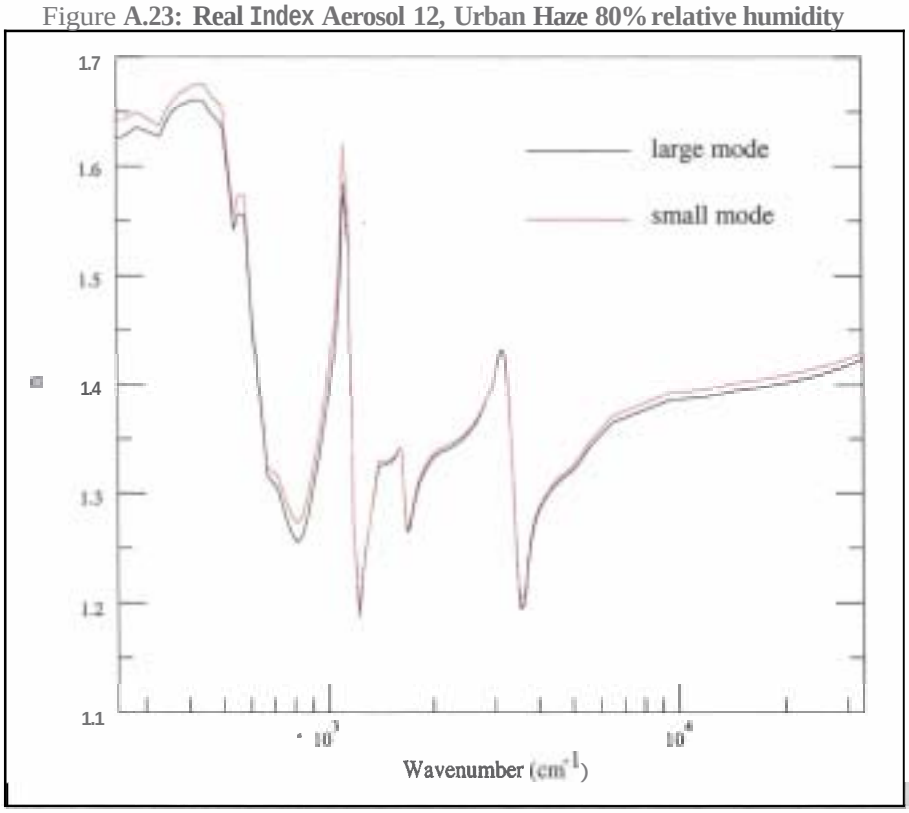

Fie A.24: Imaginary Index Aerosol 12, Urban Haze 80% relative humidity

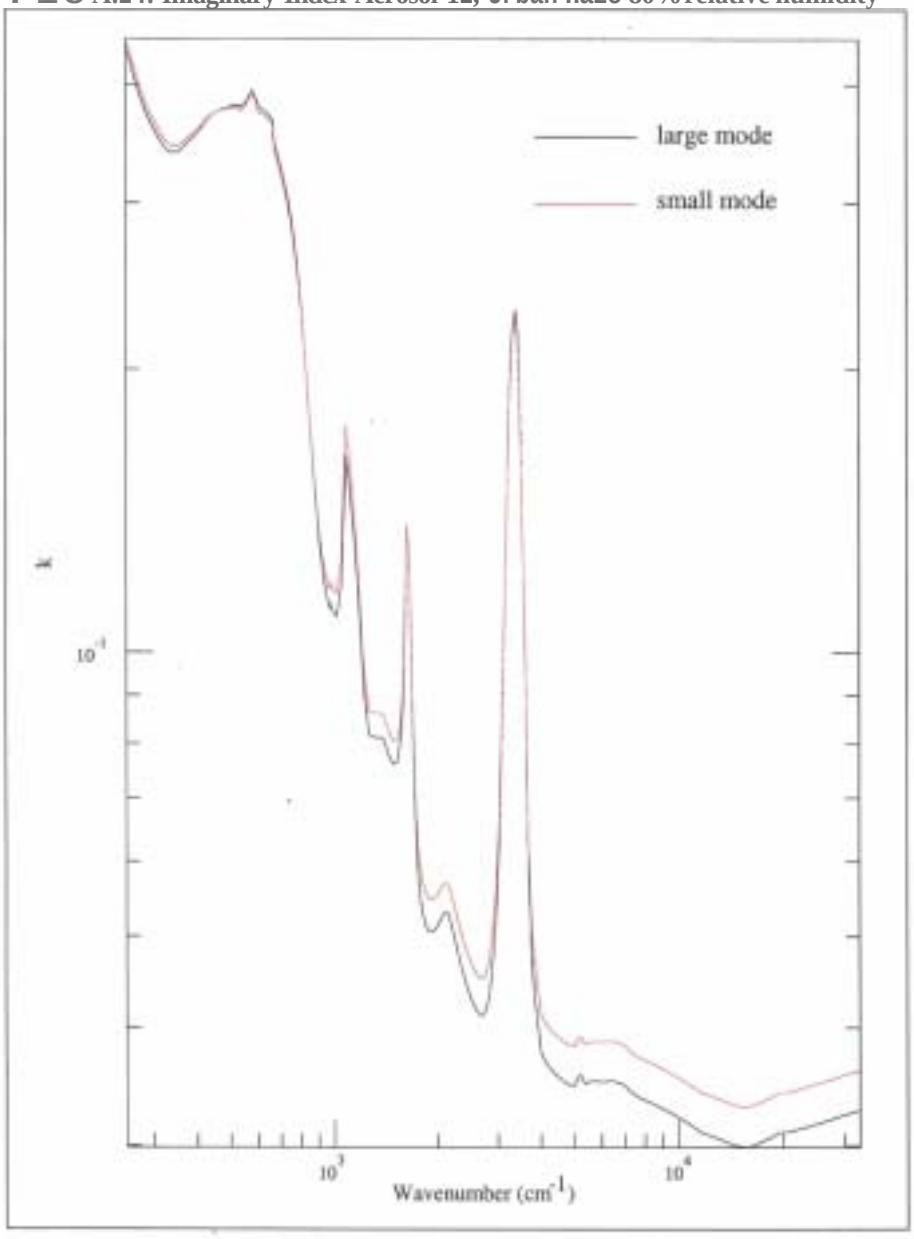

Figure A.25: Real Index Aerosol 13, Urban Haze 90% relative humidity

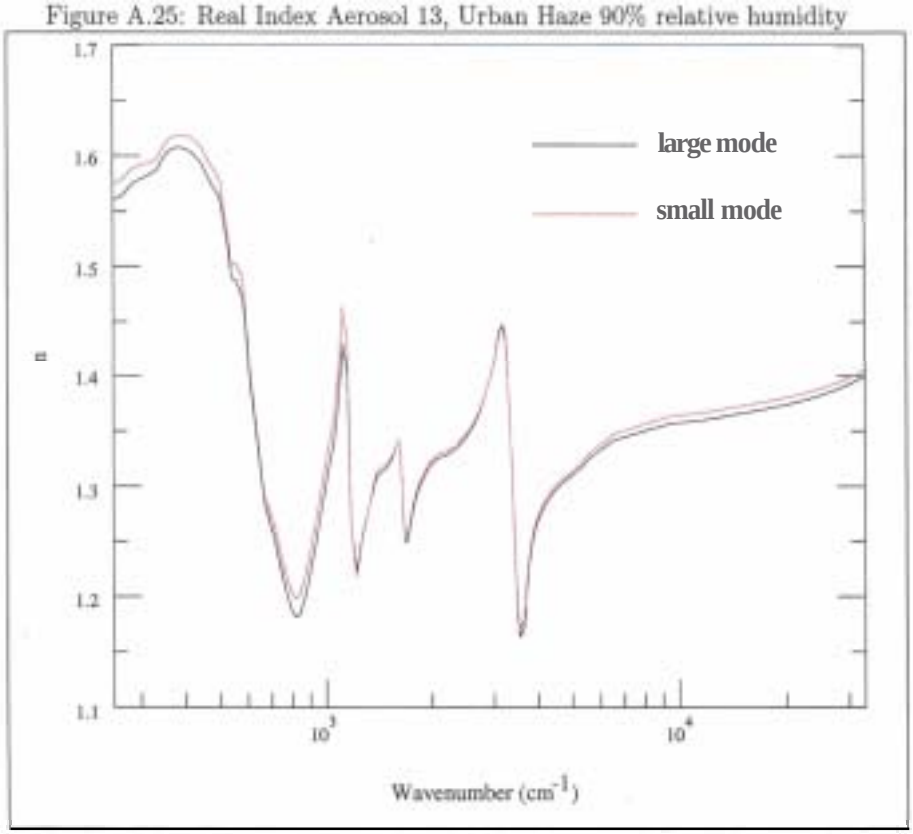

Figure A.26: Imaginary Index Aerosol 13, Urban Haze 90% relative humidity

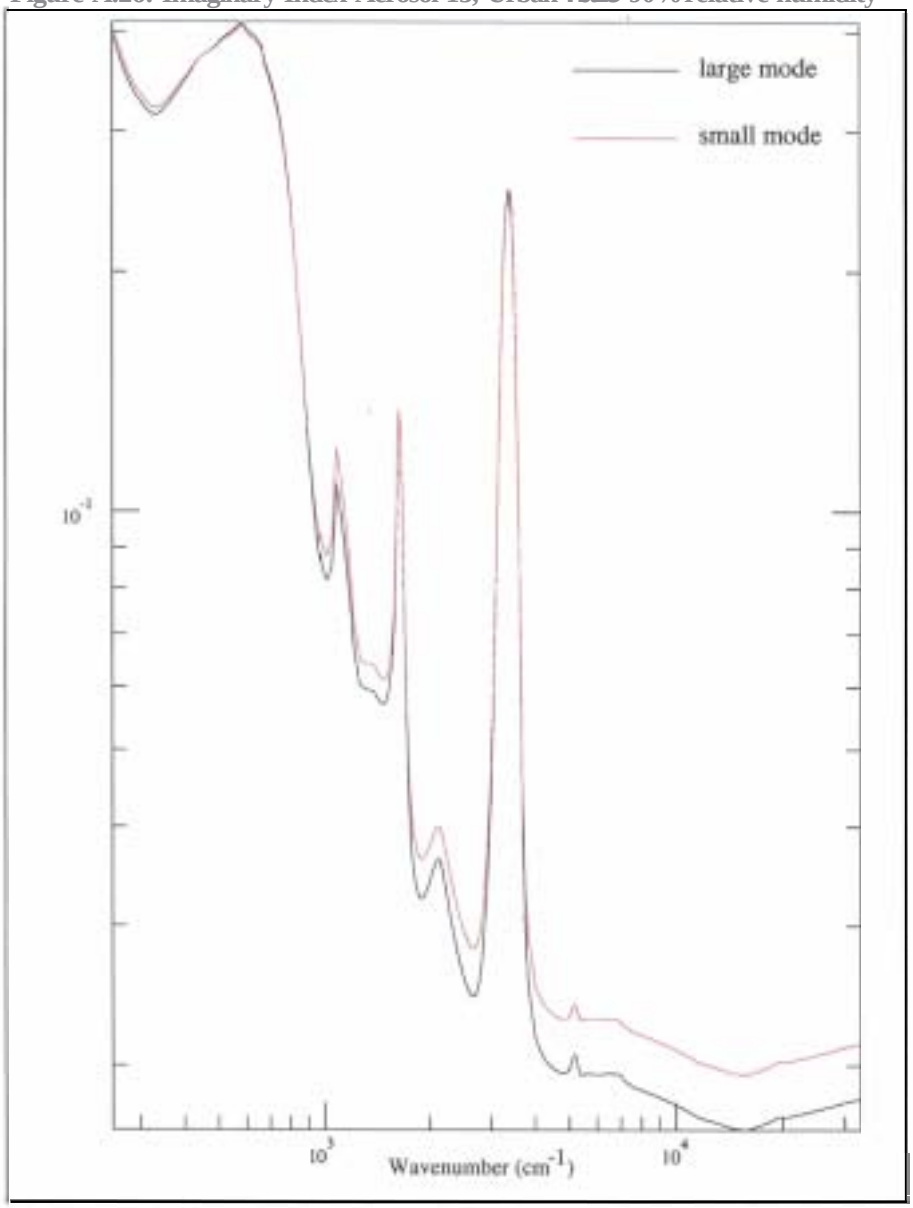

Figure A.27: Real Index Aerosol 14, Urban Haze 95% relative humidity

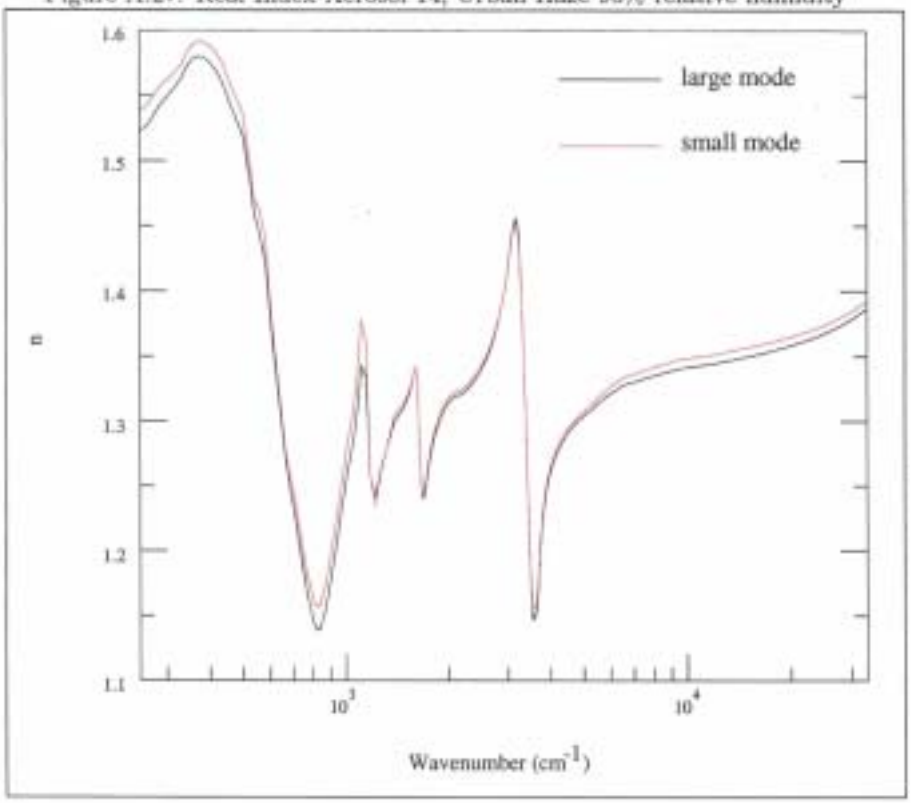

Figure A.28: Imaginary Index Aerosol 14, Urban Haze 95% relative humidity

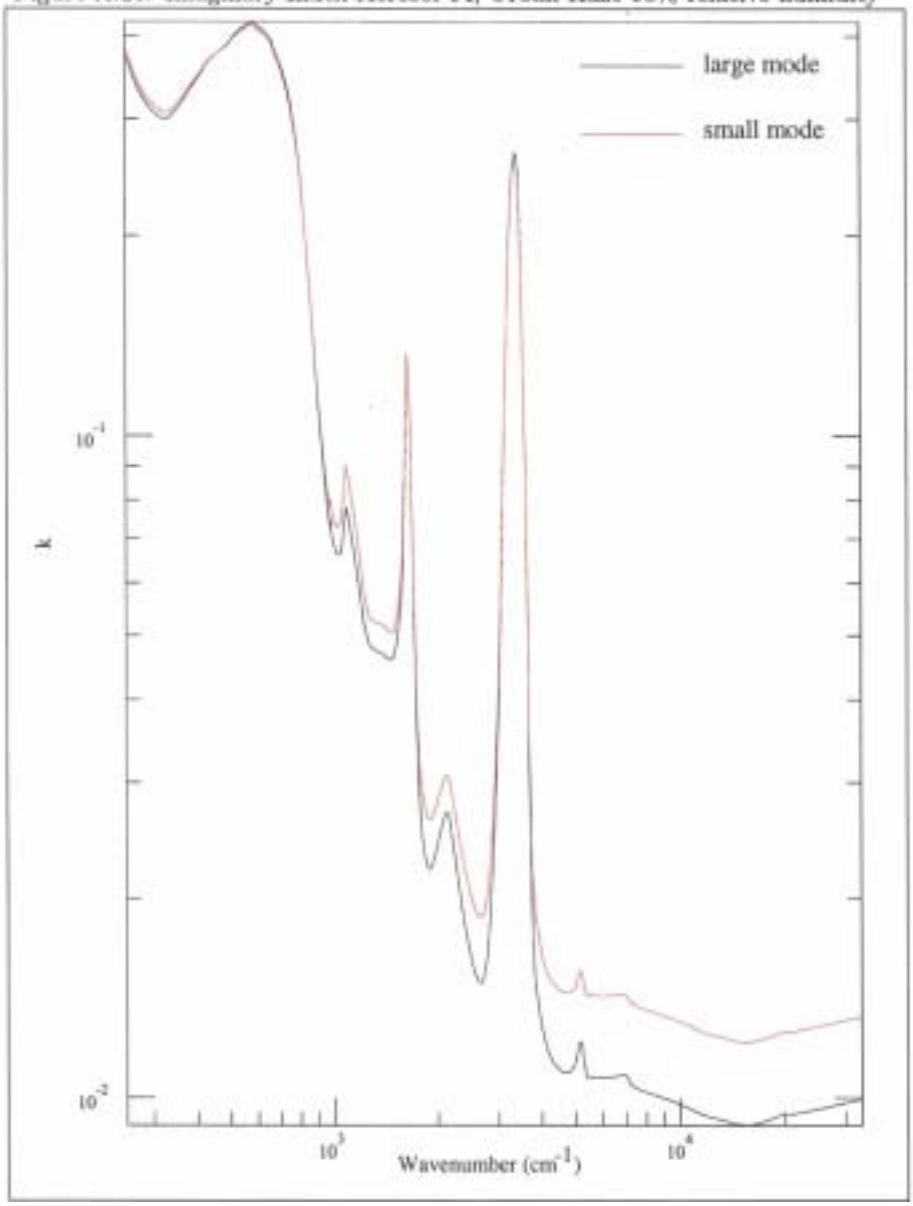

Figure A.29: Real Index Aerosol 15, Urban Haze 98% relative humidity

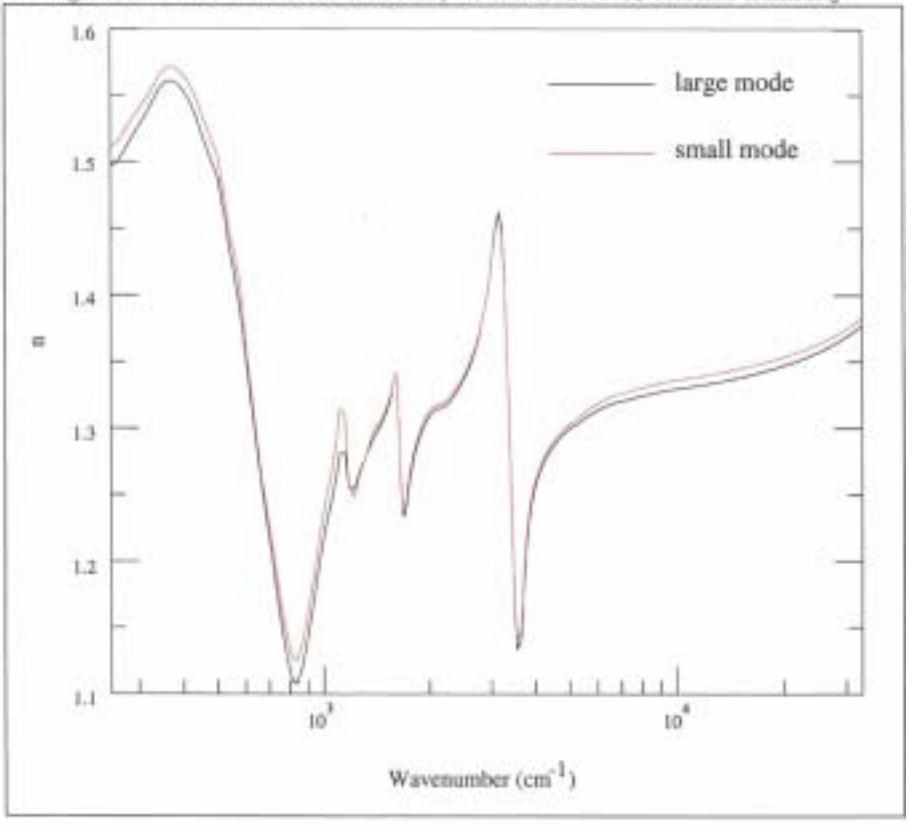

Figure A.30: Imaginary Index Aerosol 15, Urban Haze 98% relative humidity

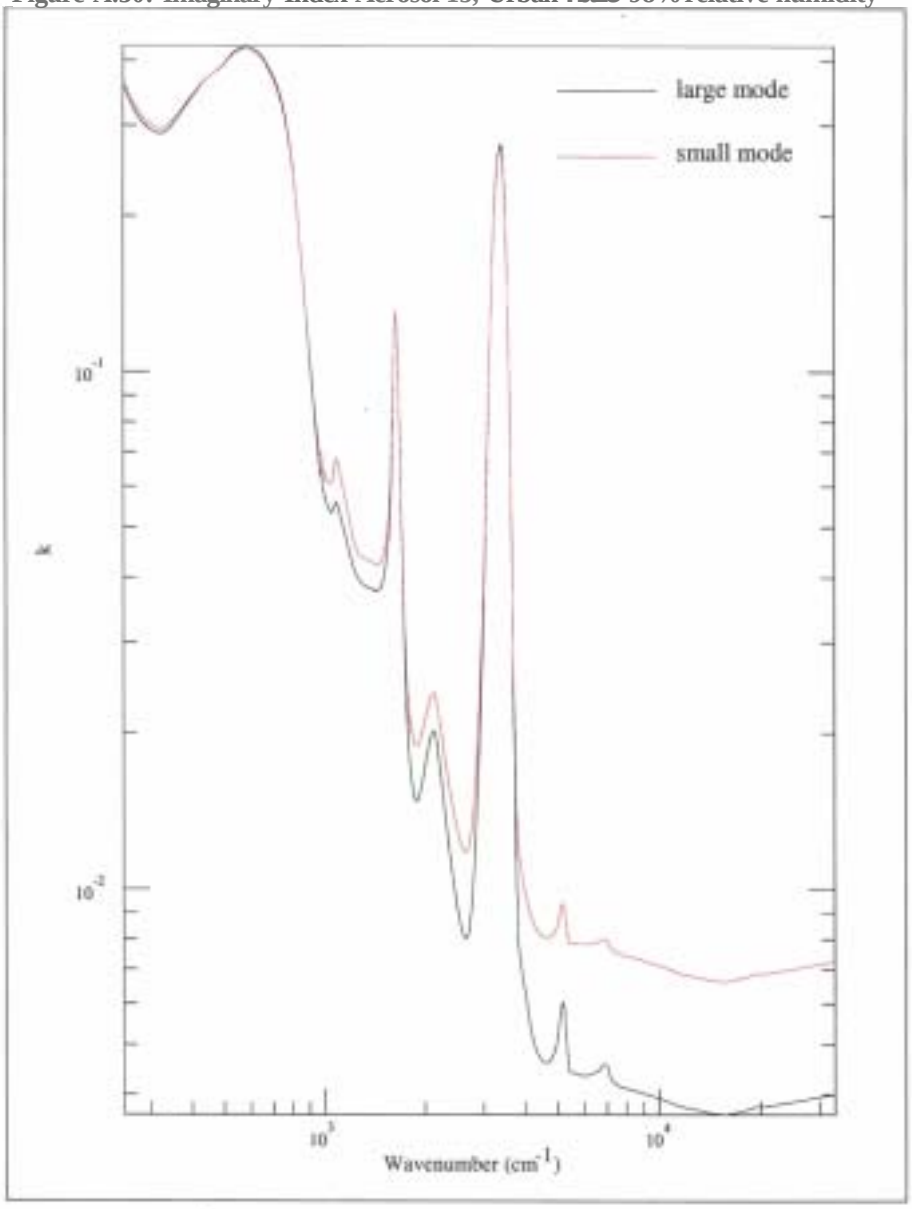

Figure A.31: Real Index Aerosol 16, Urban Haze 99% relative humidity

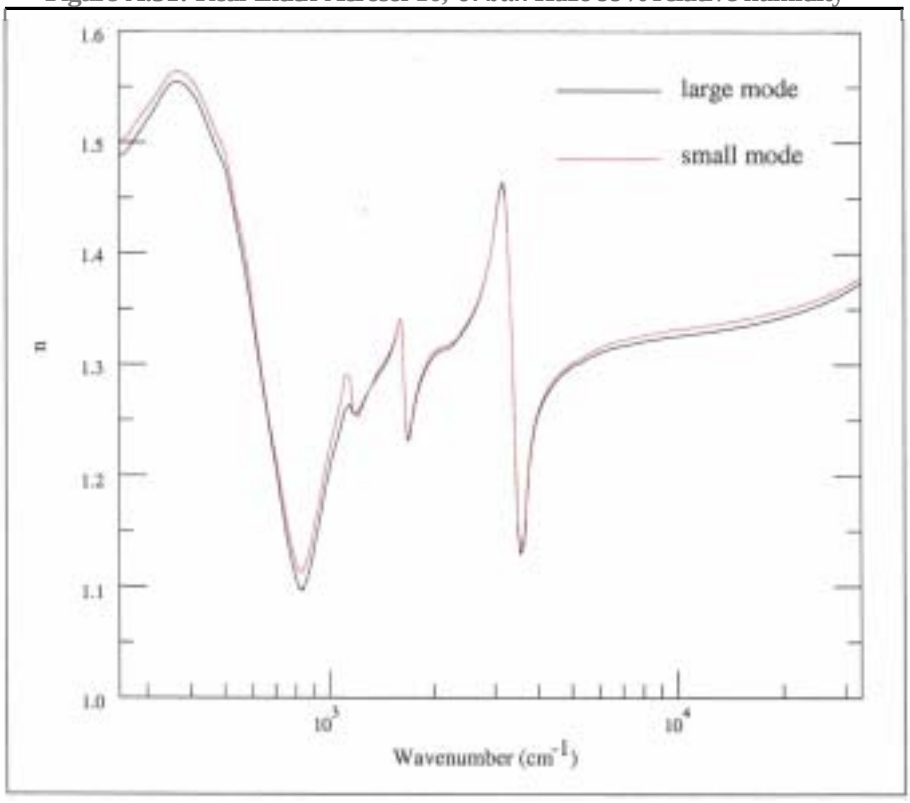

Figure A.32: Imaginary Index Aerosol 16, Urban Haze 99% relative humidity

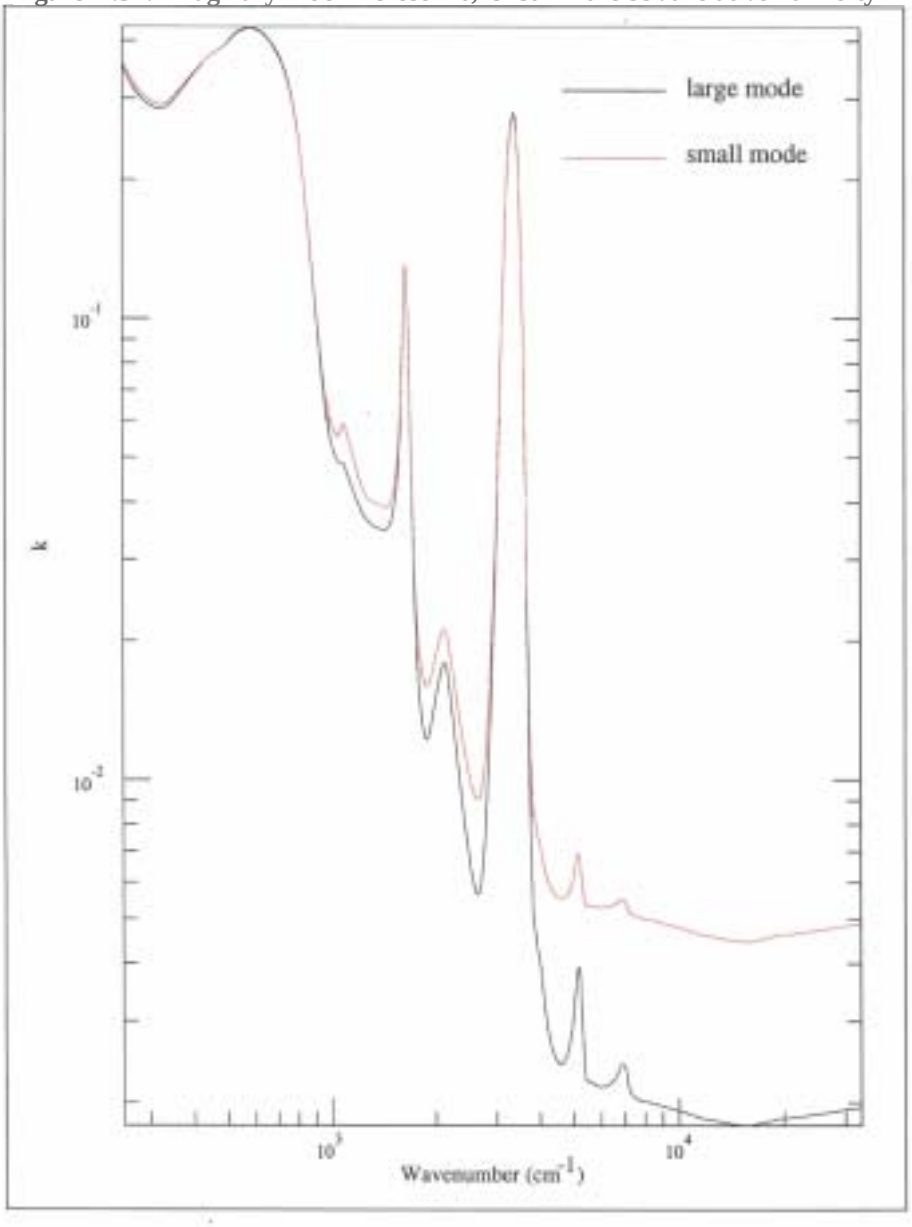

Figure **A.33:** Real Index Aerosol 17, Rural Haze 0% relative humidity

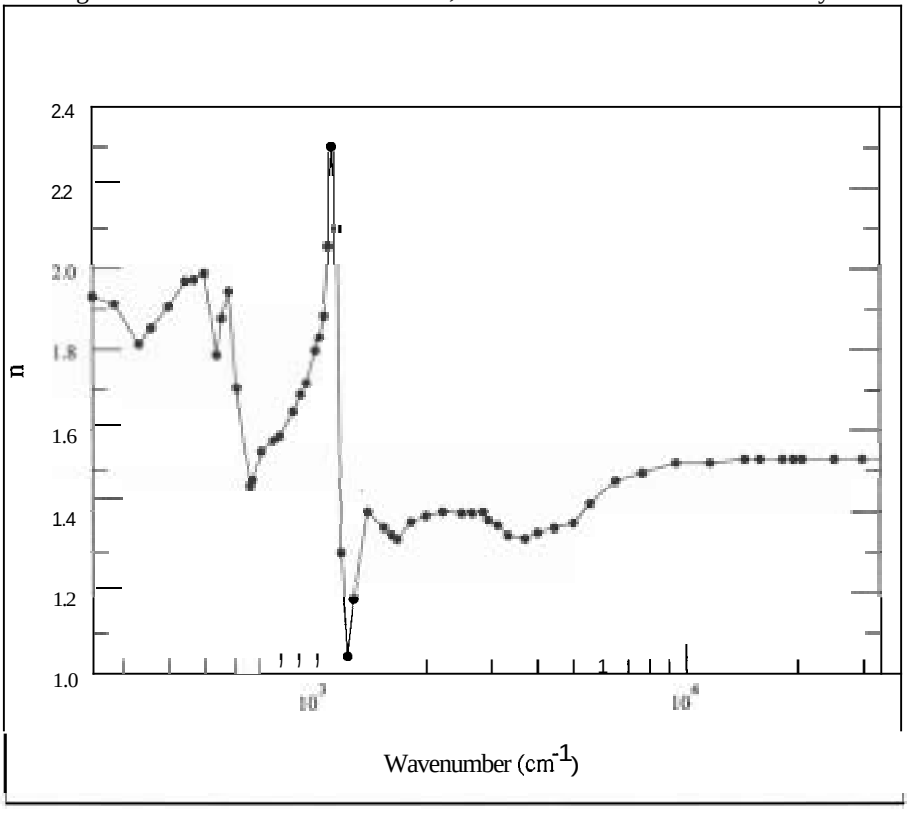

A.3 Indices of Refraction of Rural Aerosols

Figure A.34: Imaginary Index Aerosol 17, Rural Haze 0% relative humidity

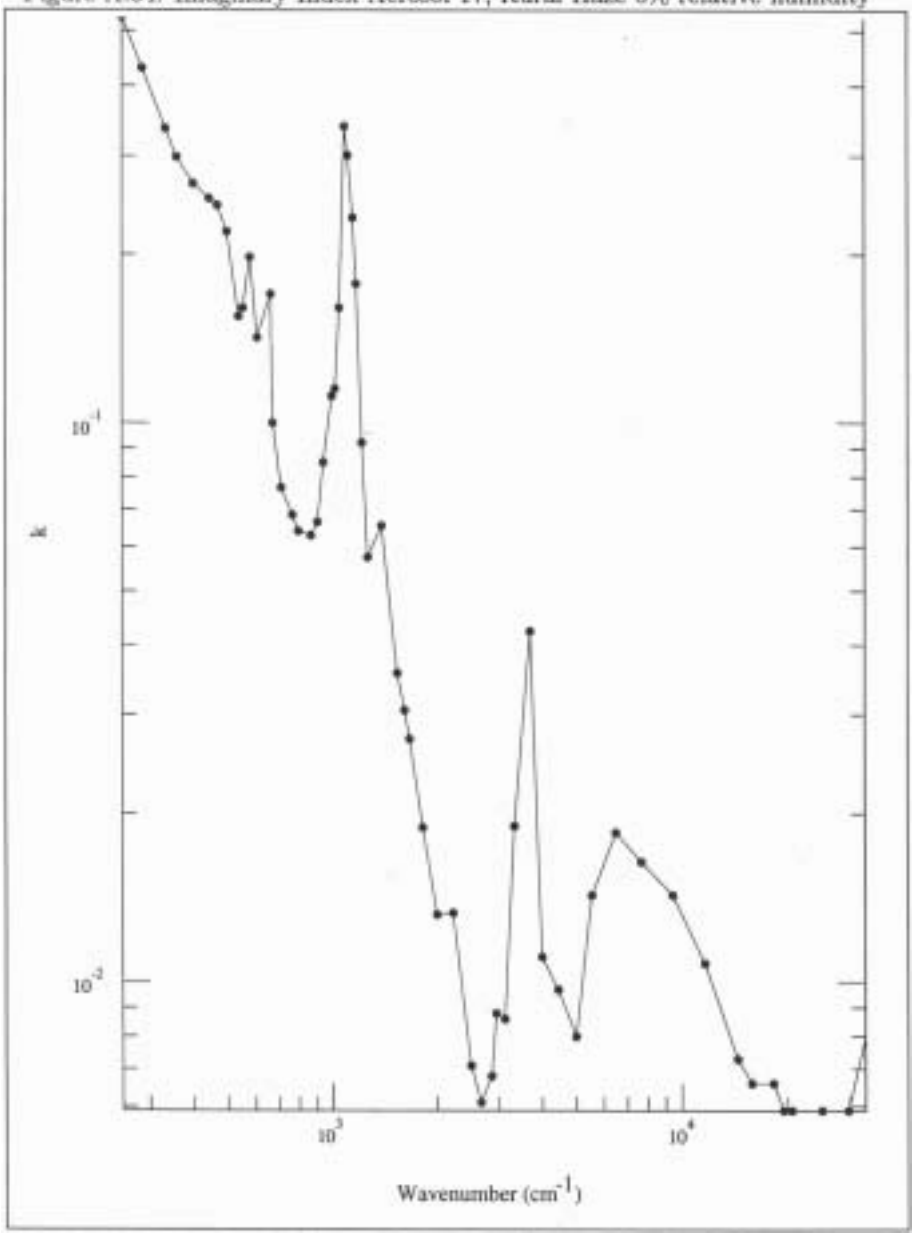

Figure A.35: Real Index Aerosol 18, Rural Haze 50% relative humidity

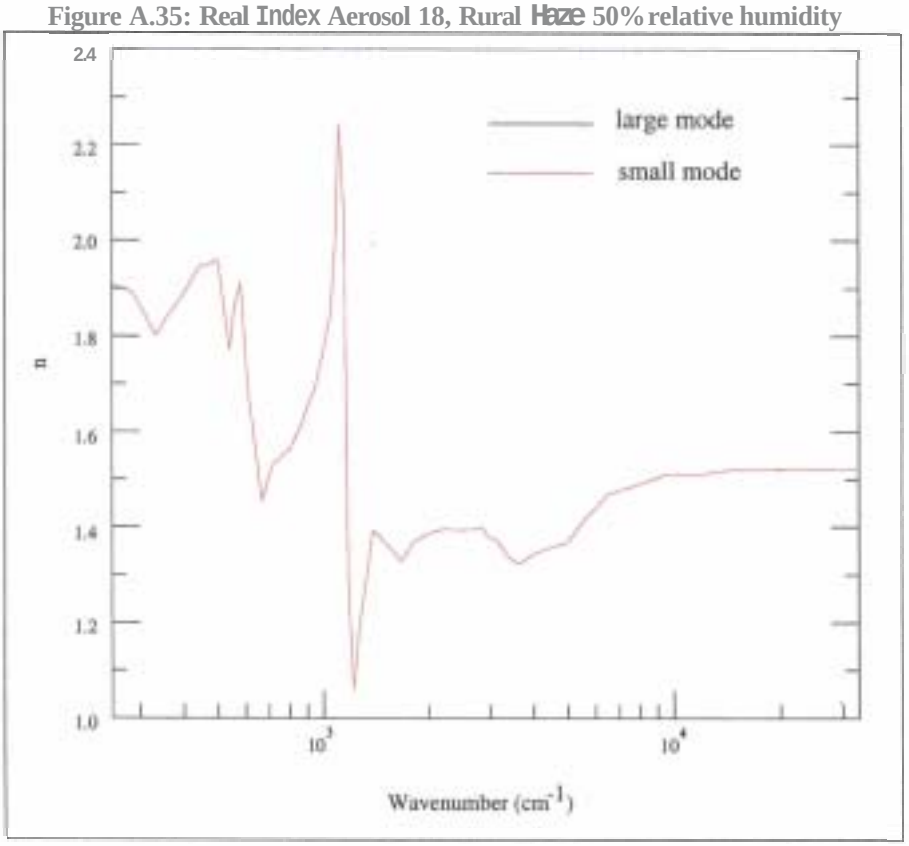

Figure A.36: Imaginary Index Aerosol 18, Rural Haze 50% relative humidity

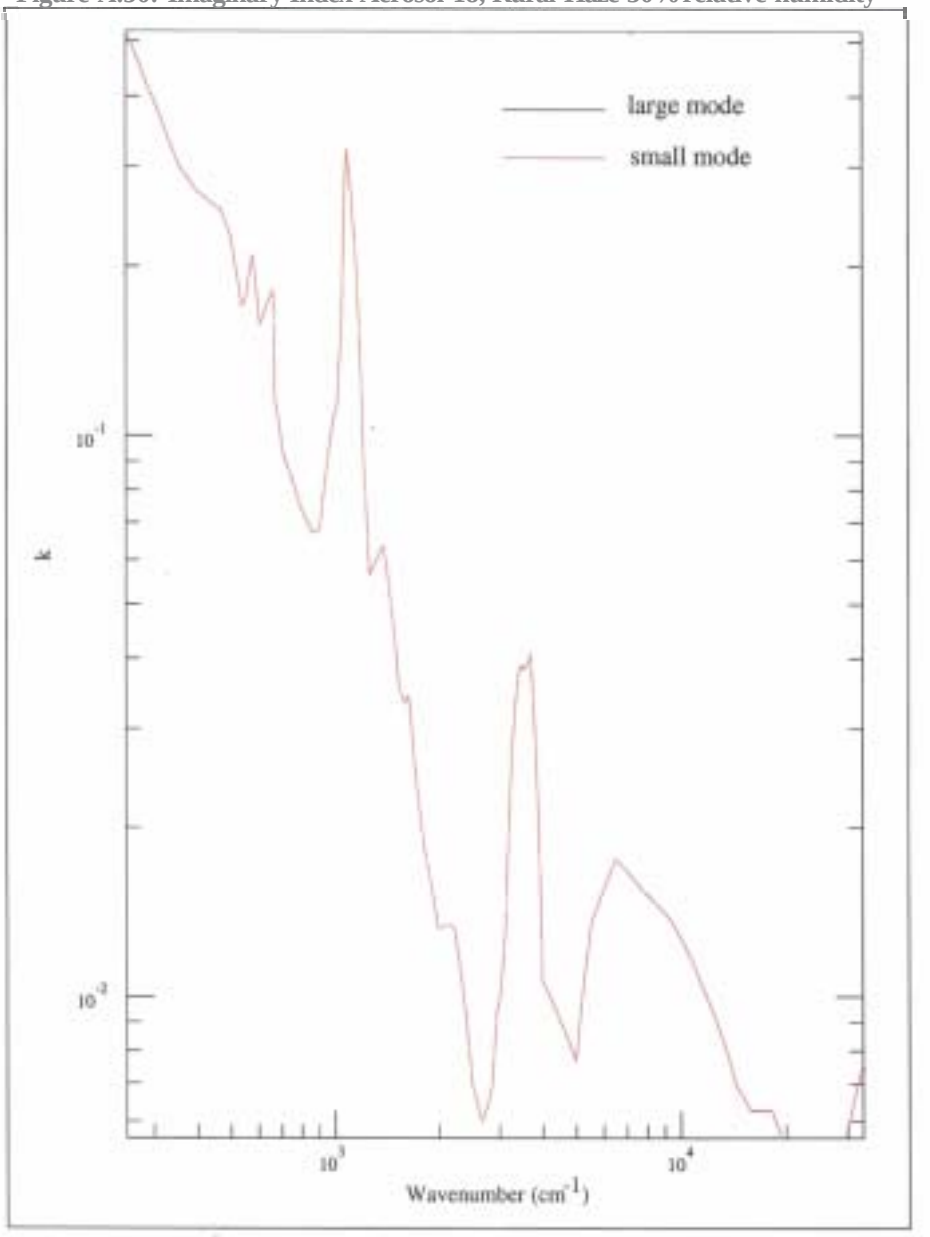

Figure A.37: Real Index Aerosol 19, Rural Haze 70% relative humidity

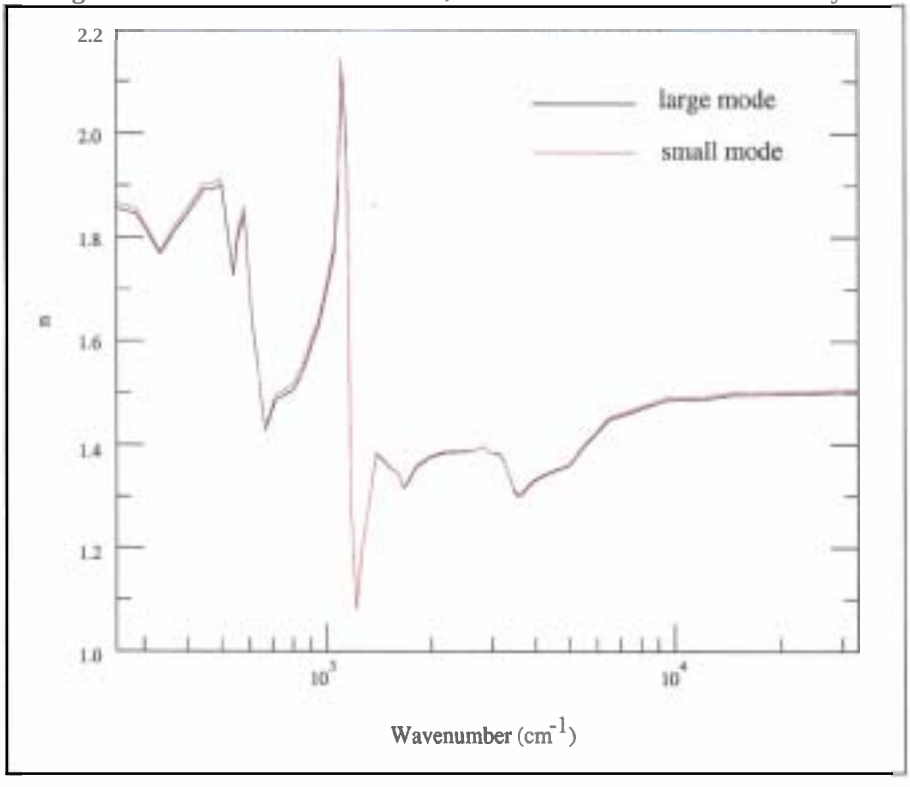

Figure A.38: Imaginary Index Aerosol 19, Rural Haze 70% relative humidity

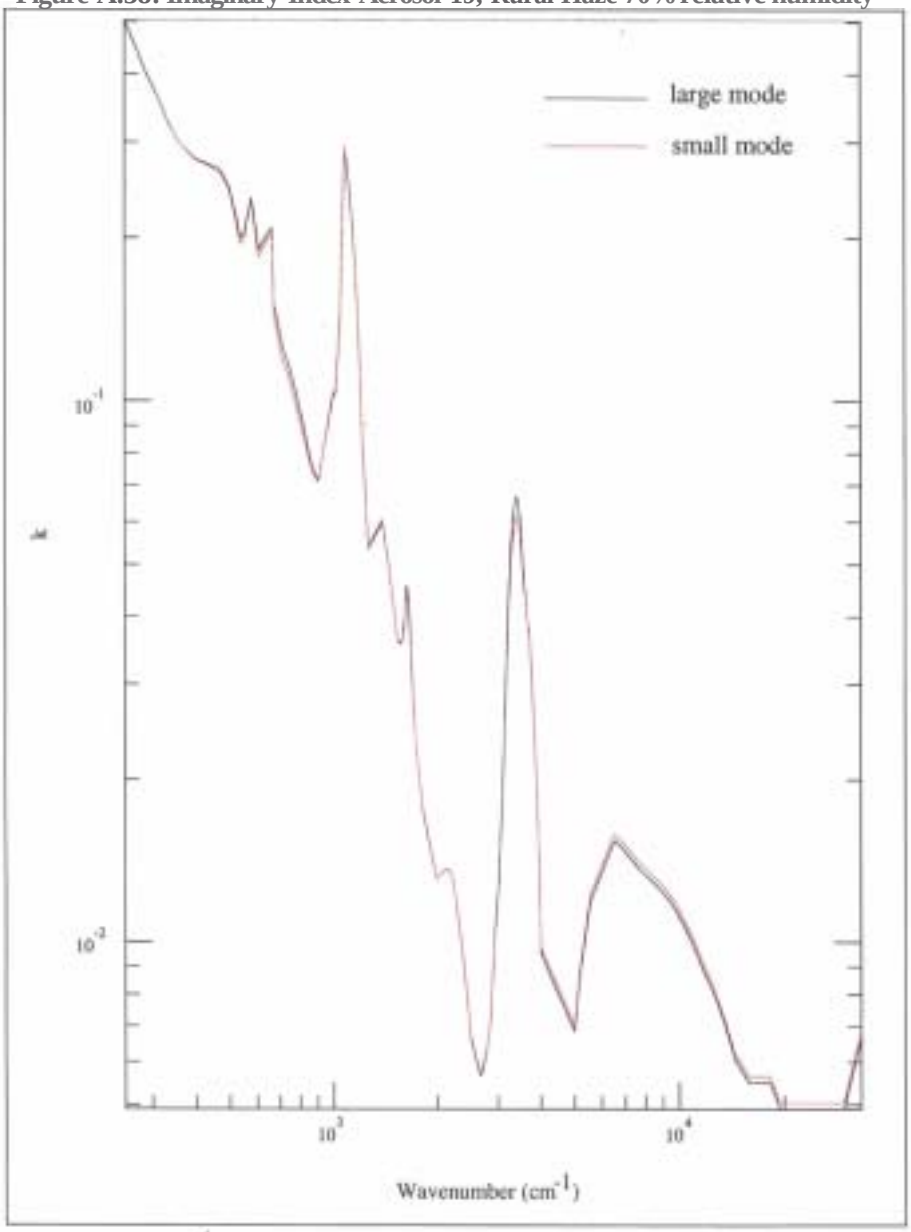

Figure A.39: Real Index Aerosol 20, Rural Haze 80% relative humidity

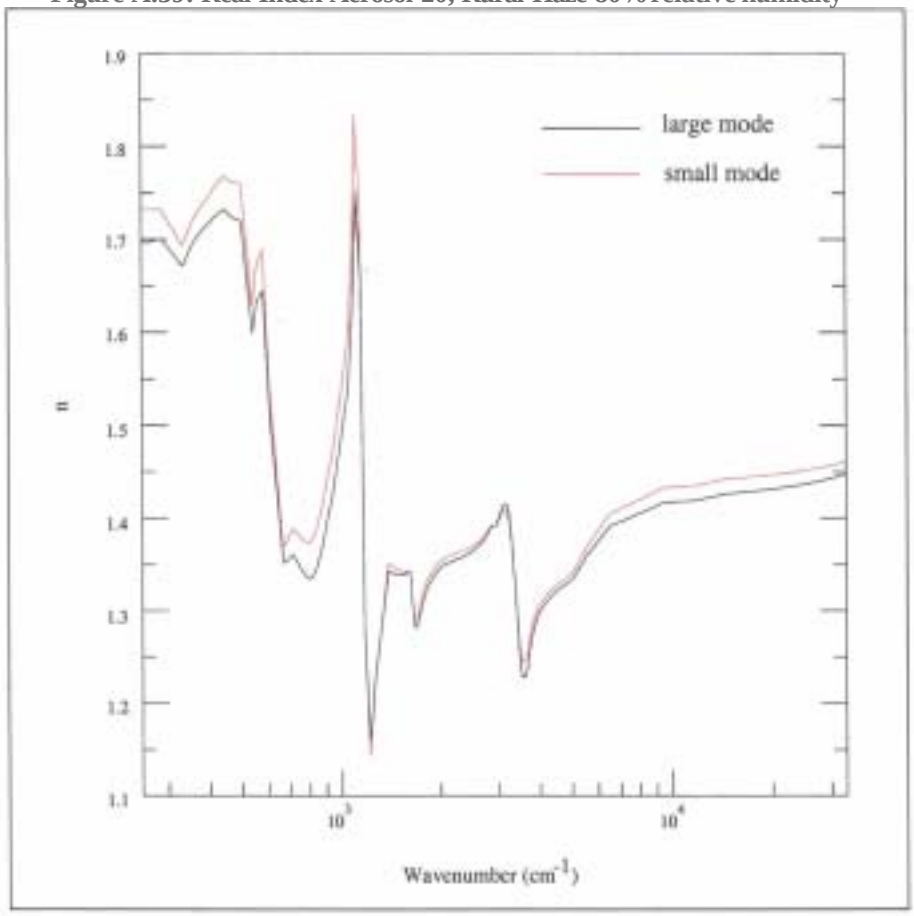

Figure A.40: Imaginary Index Aerosol 20, Rural Haze 80% relative humidity

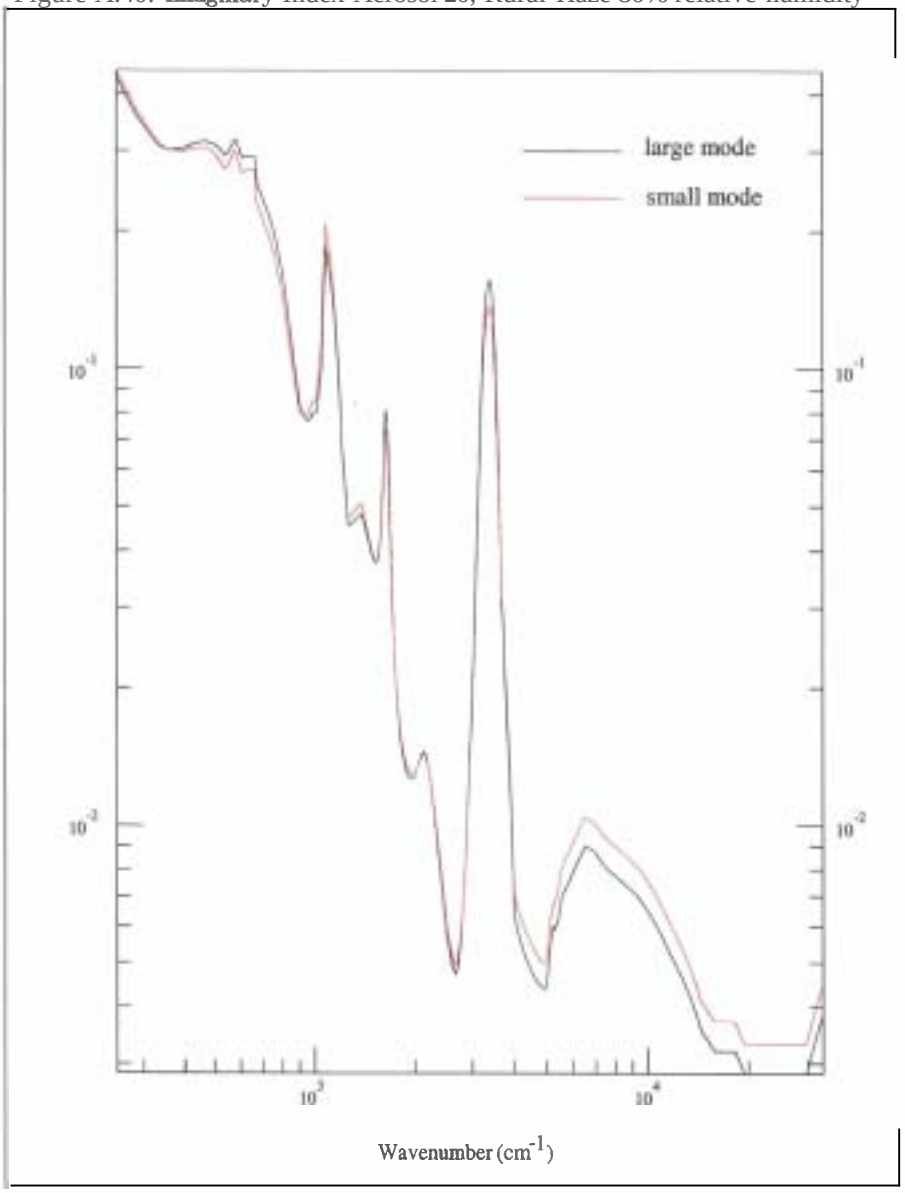

Figure A.41: Real Index Aerosol 21, Rural Haze 90% relative humidity

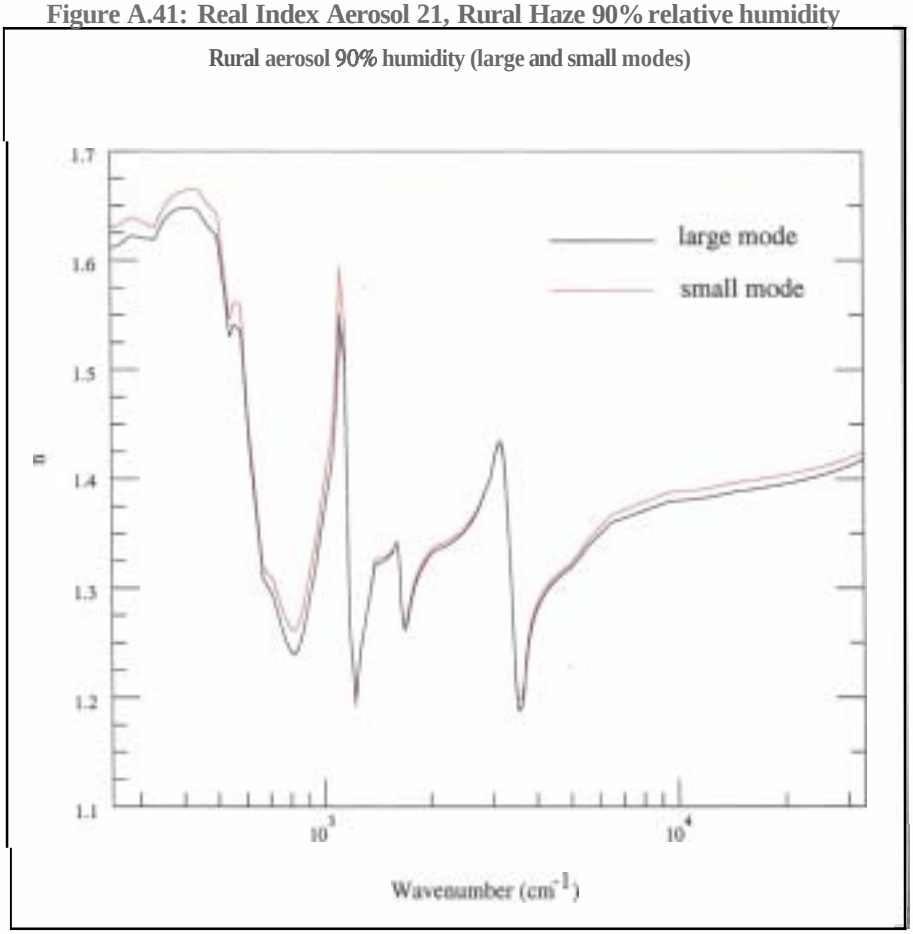

Figure A.42: Imaginary Index Aerosol 21, Rural Haze 90% relative humidity

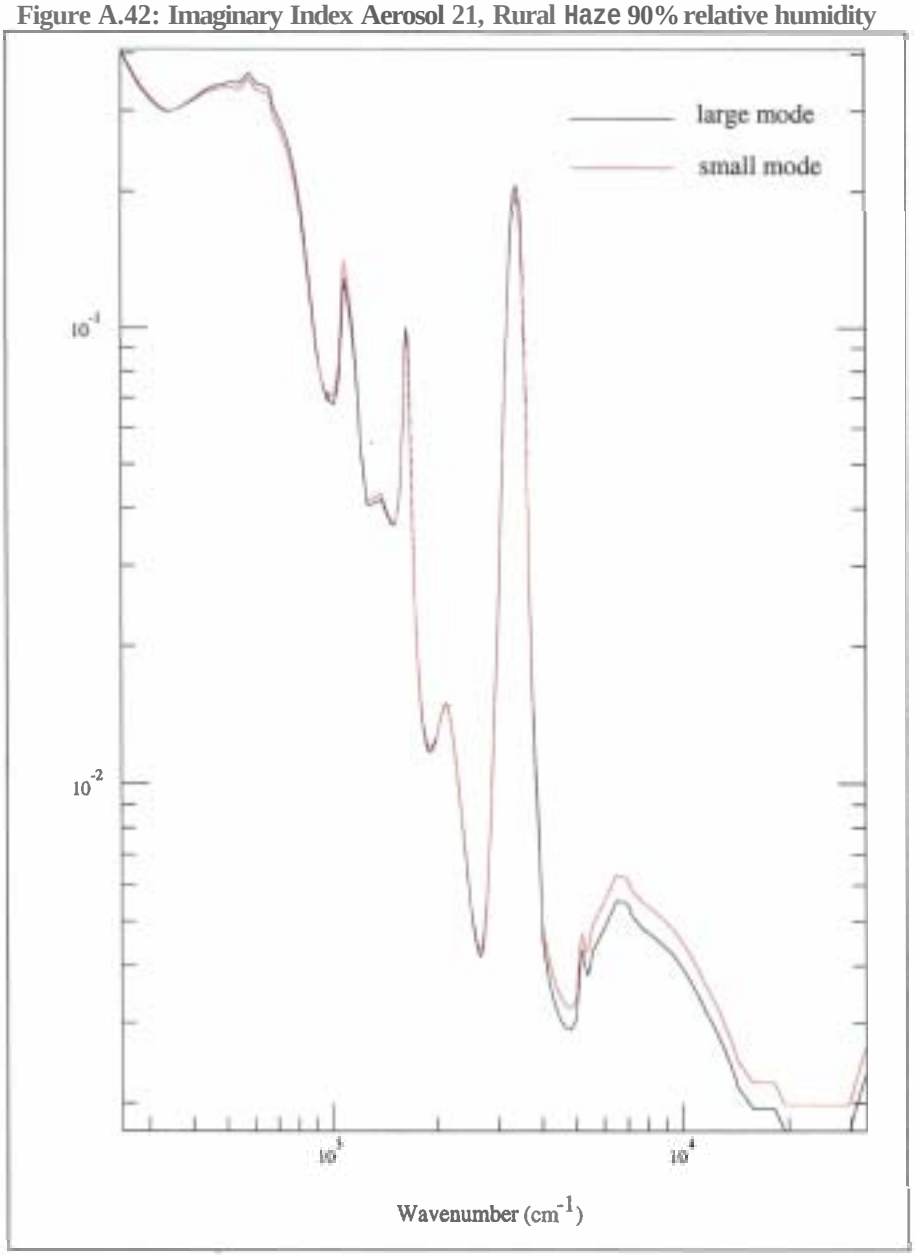

Figure A.43: Real Index Aerosol 22, Rural Haze 95% relative humidity

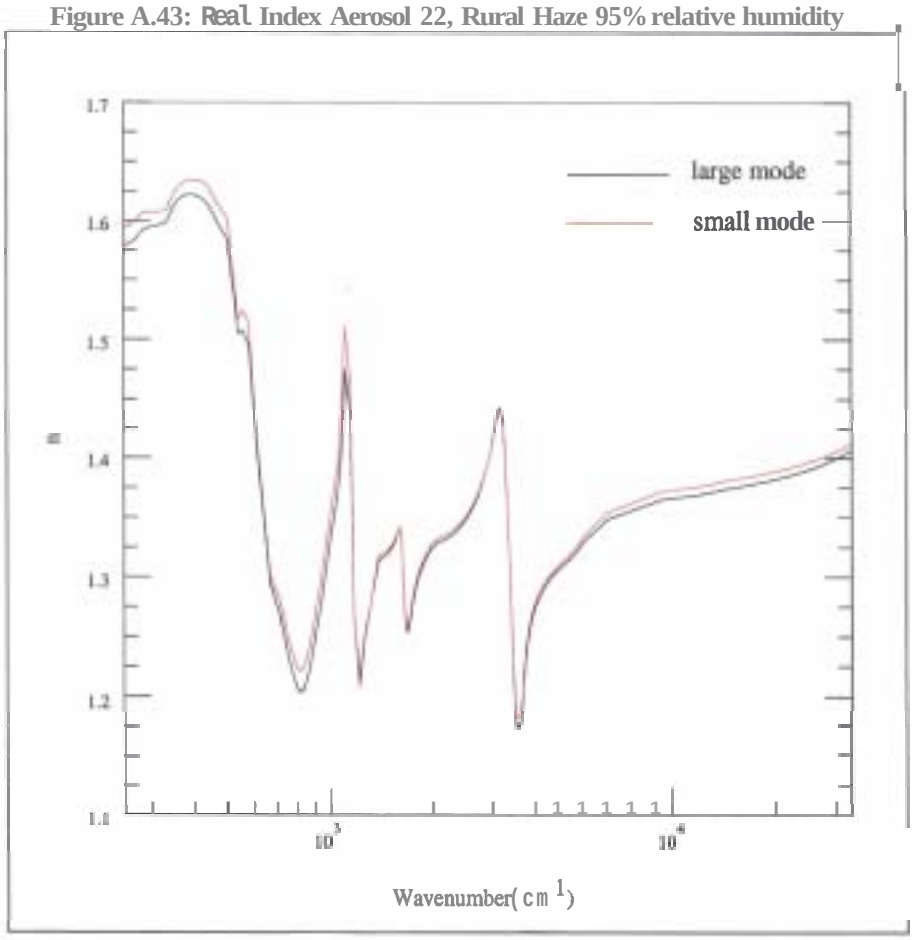

Figure A.44: Imaginary Index Aerosol 22, Rural Haze 95% relative humidity

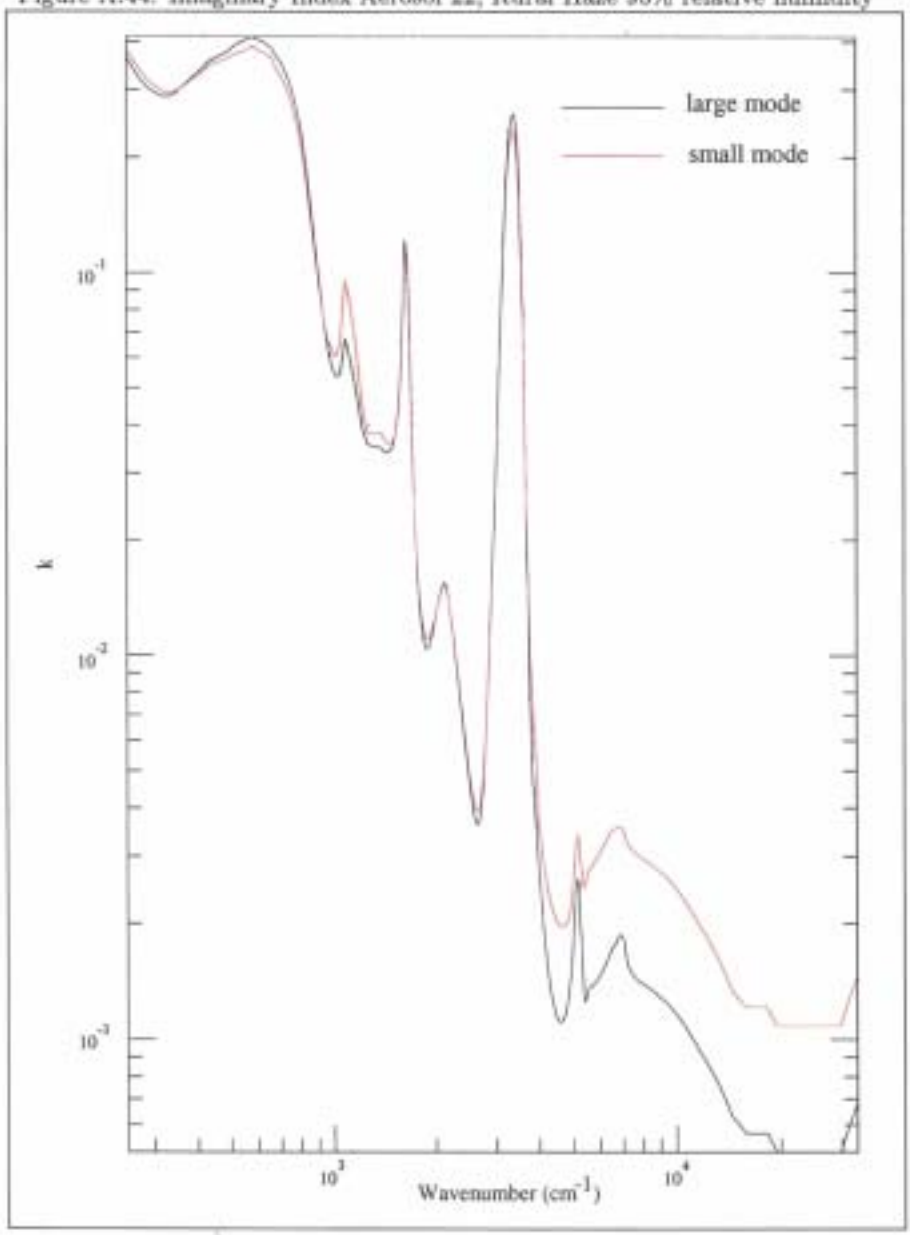

Figure A.45: Real Index Aerosol 23, Rural Haze 98% relative humidity

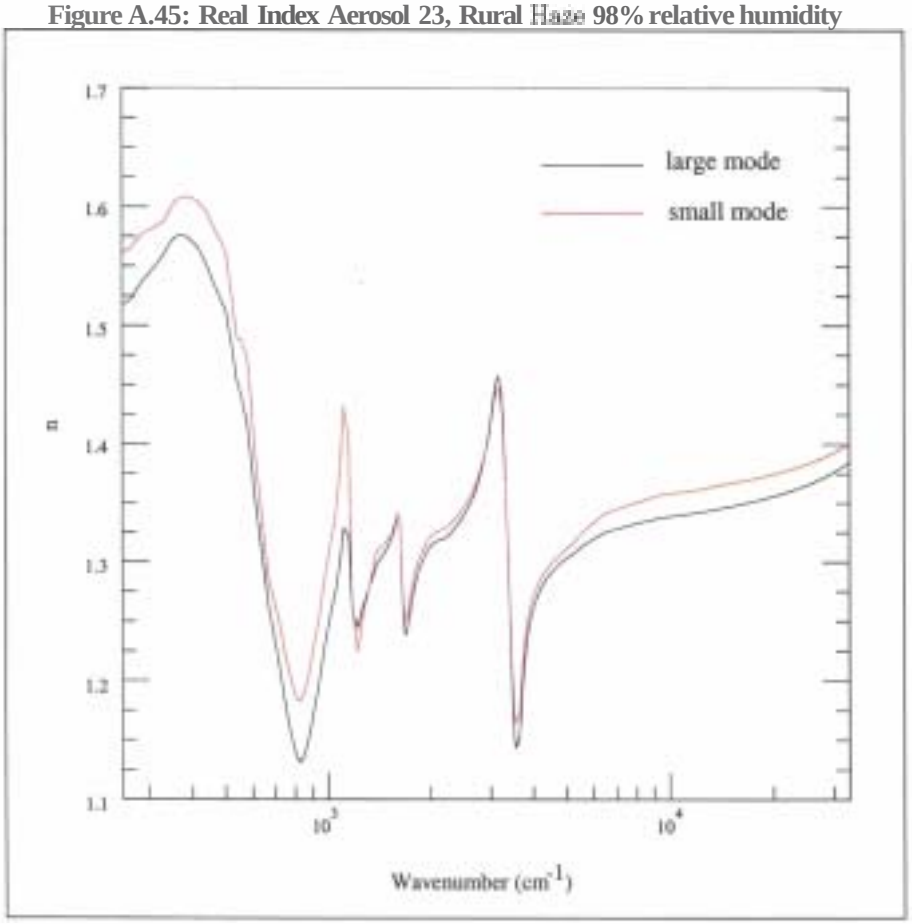

Figure A.46: Imaginary Index Aerosol 23, Rural Haze 98% relative humidity

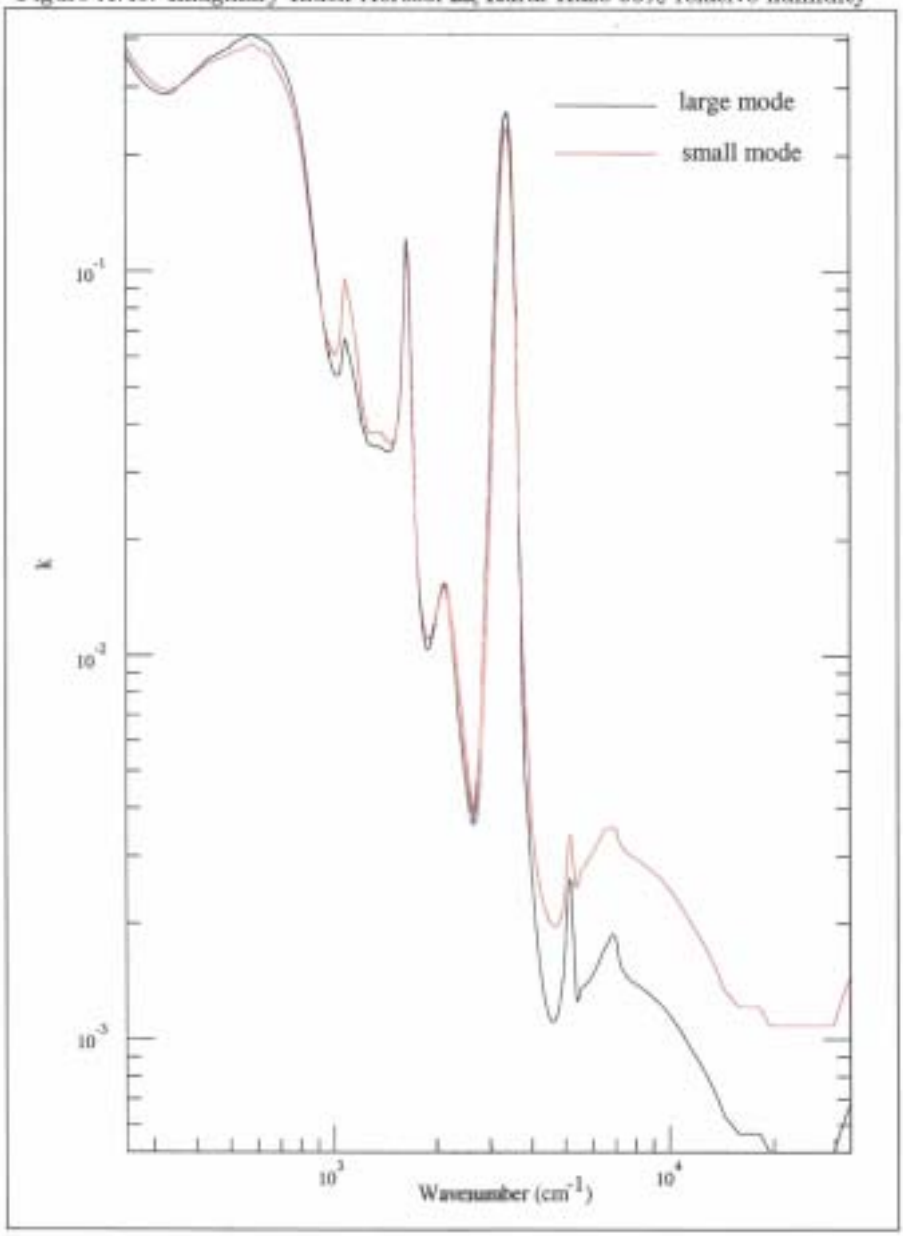

Figure A.47: Real Index Aerosol 24, Rural Haze 99% relative humidity

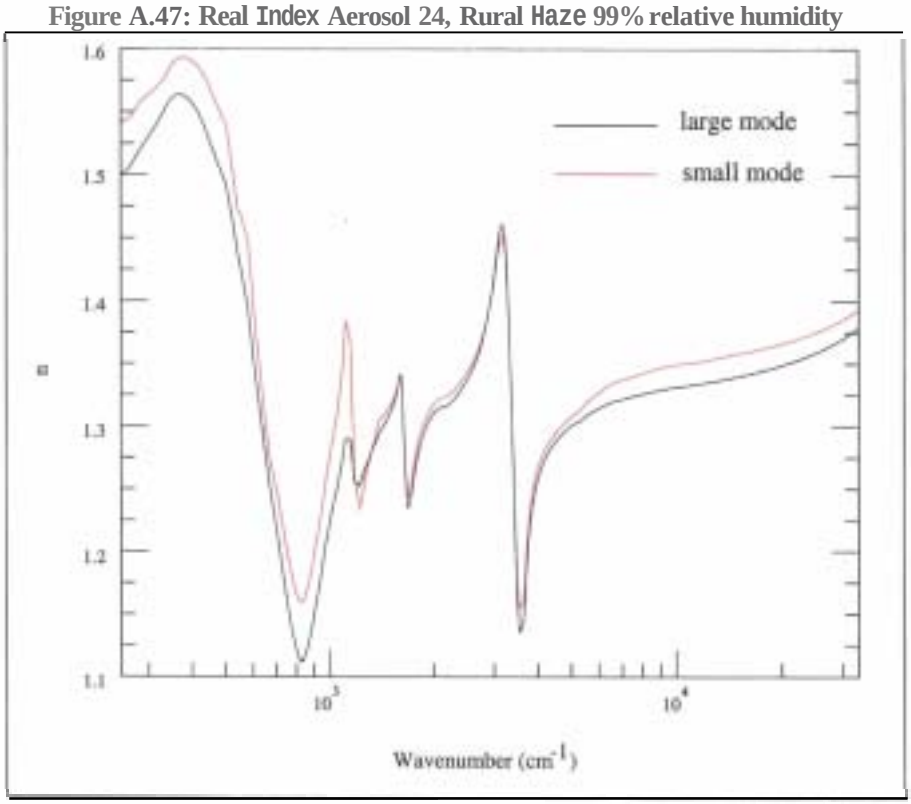

Figure A.48: Imaginary Index Aerosol 24, Rural Haze 99% relative humidity

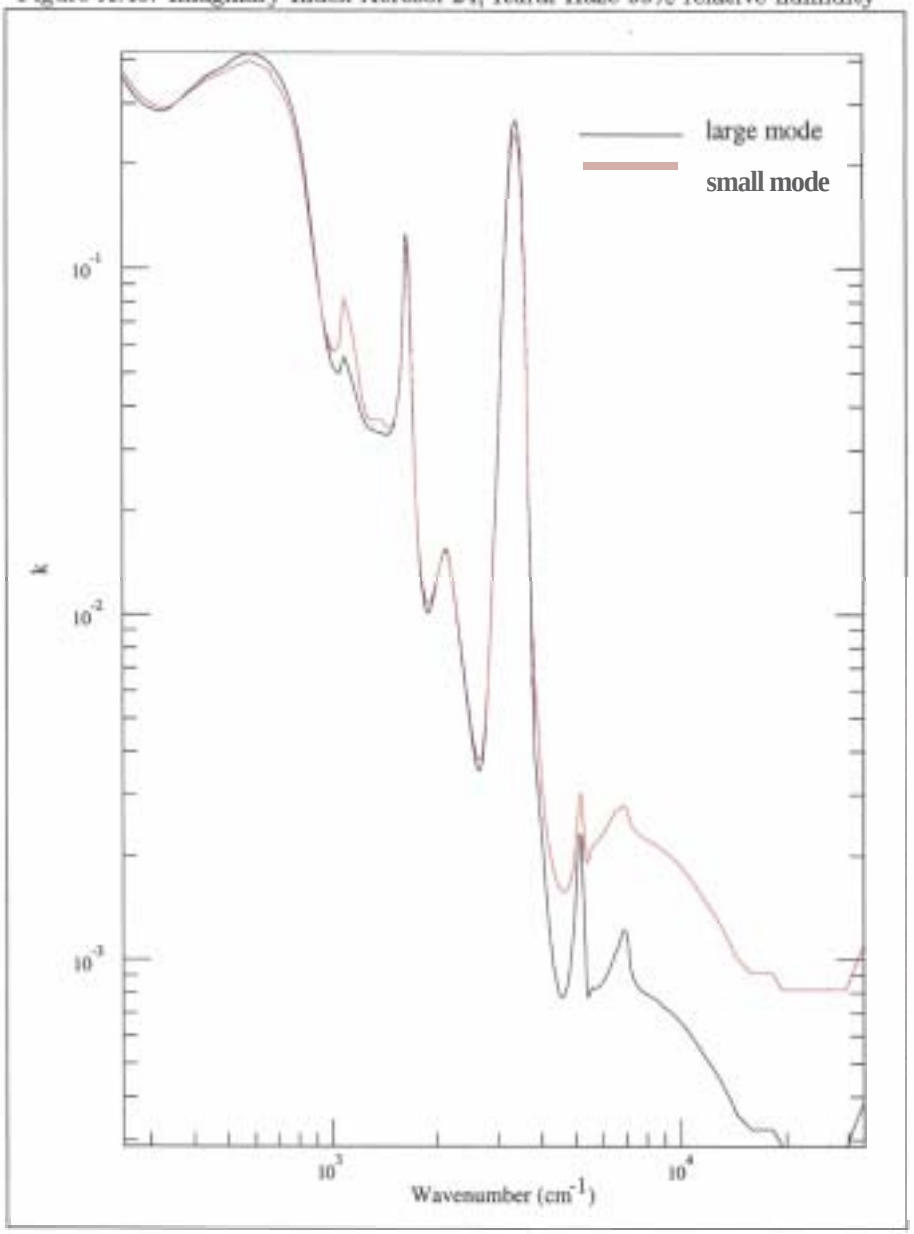

A.4 Indices of Refraction of Natural Fog

Since we are modeling the aerosol models 24 (Heavy Advection Fog) and 25 (Moderate Radiation Fog) as pure water, we do not repeat the REFWAT plots from figures A.51 and A.52 on pages 72 and 72.

A.5 Indices of Refraction of Fog Oil

Figure A.49: Real Index Aerosol 56, Fog Oil 50% relative humidity

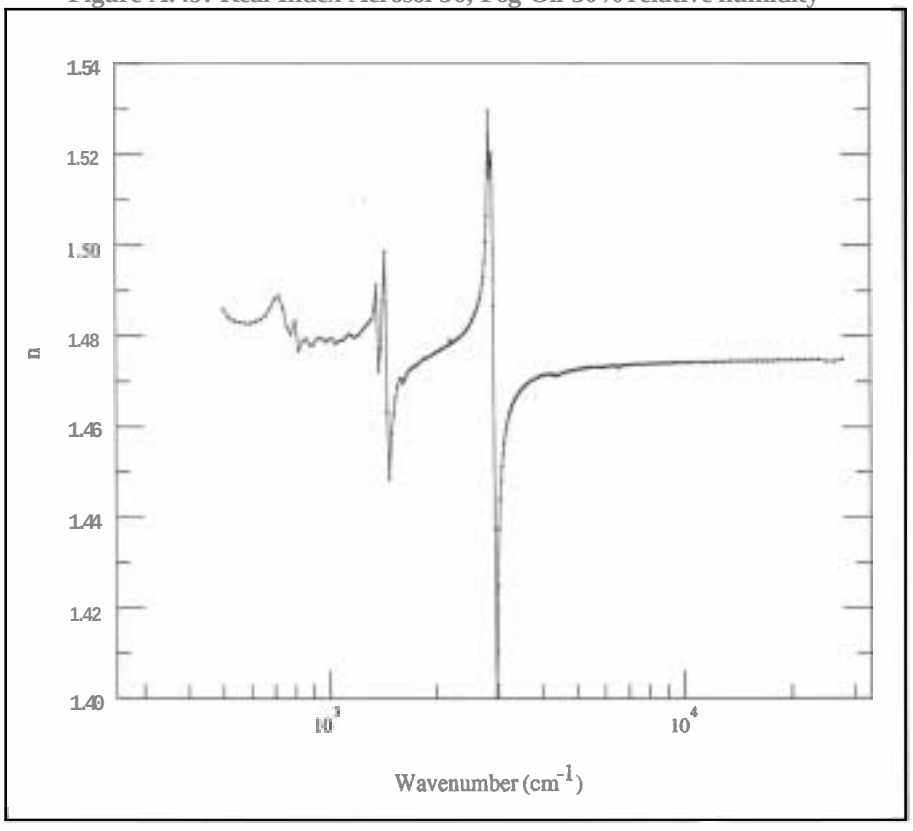

Figure A.50: Imaginary Index Aerosol 56, Fog Oil 50% relative humidity

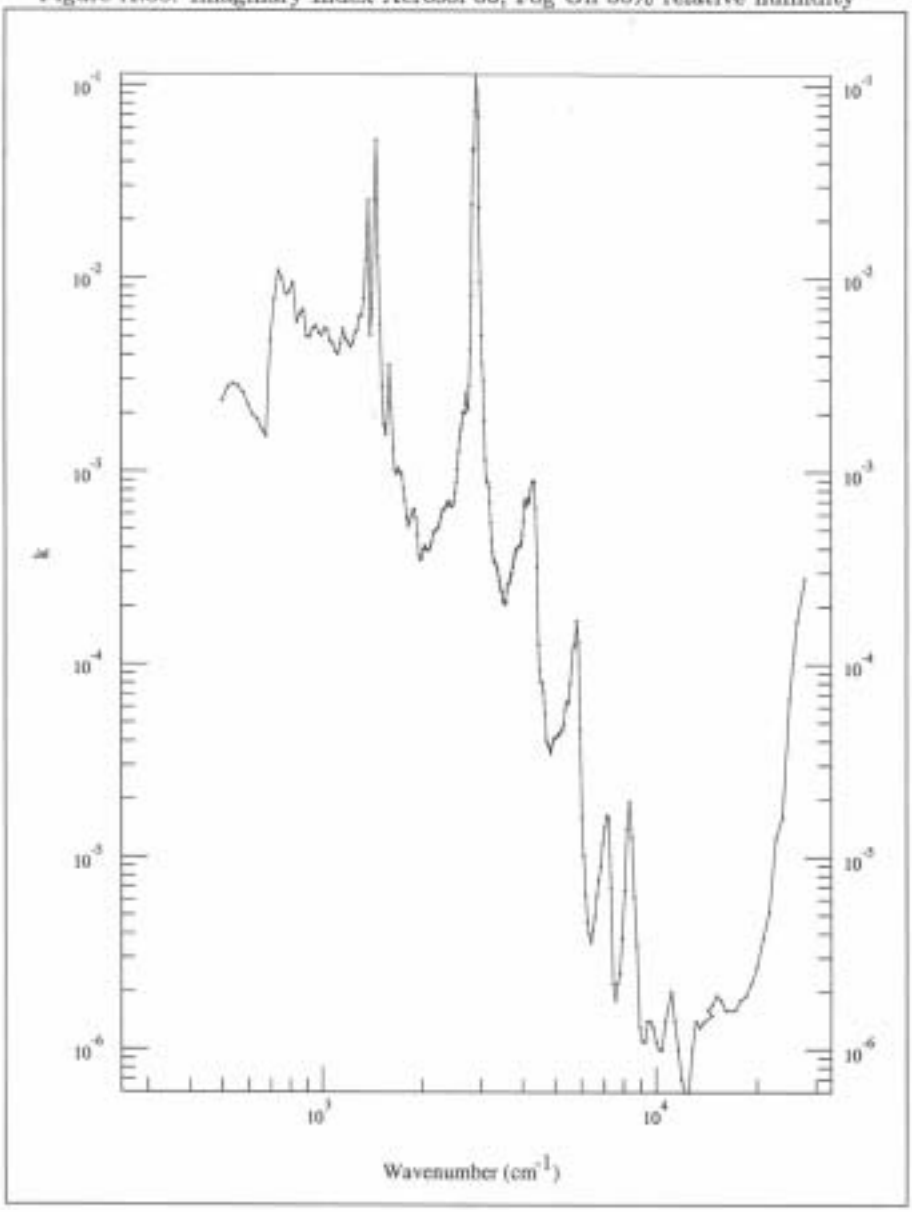

A.6 Indices of Refraction of Liquid Water

Figure A.51: Real Index H2O

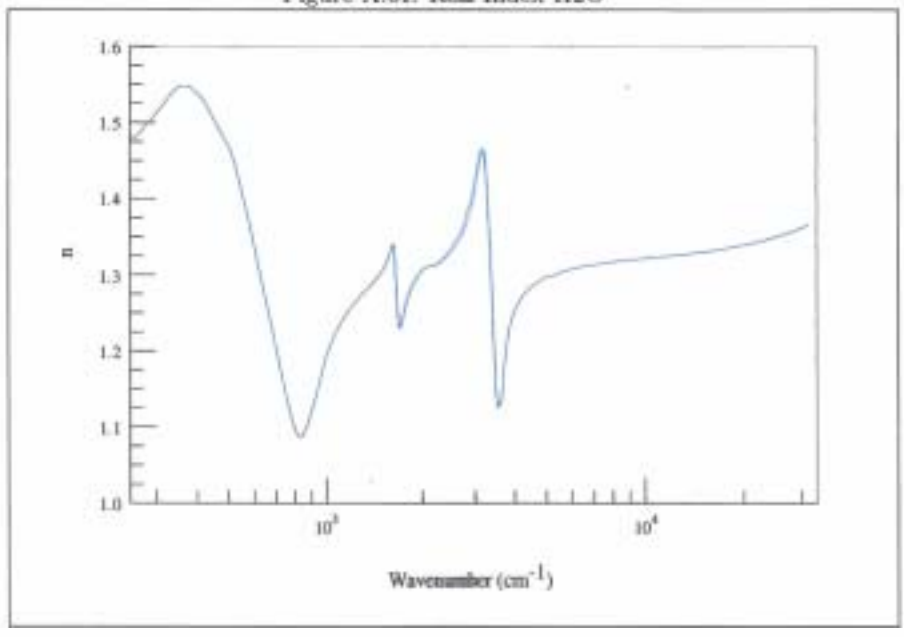

Figure A.52: Imaginary Index H2O

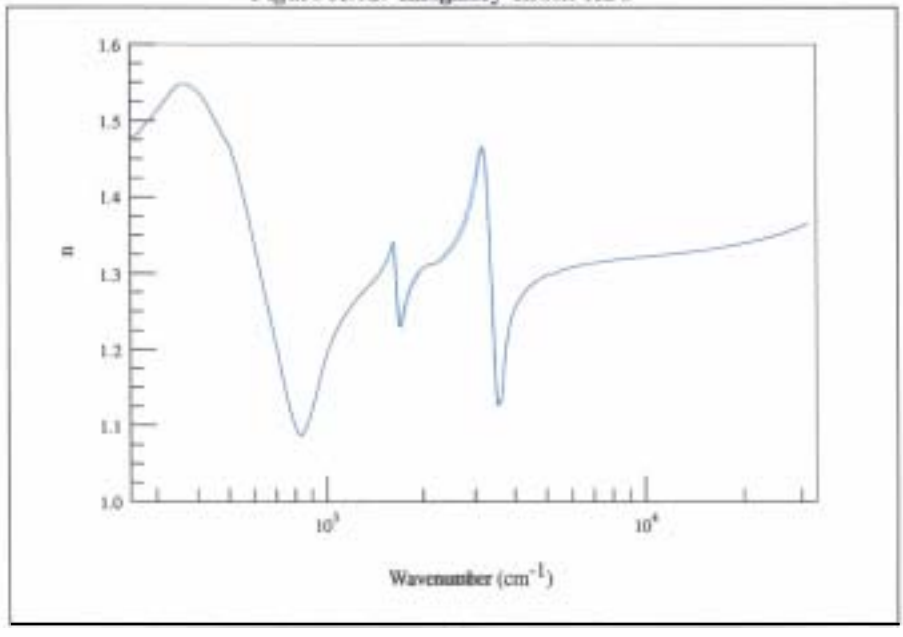

Appendix B

Aerosol Optical Properties

Figure B.1: Aerosol 01, Maritime Haze 0% relative humidity

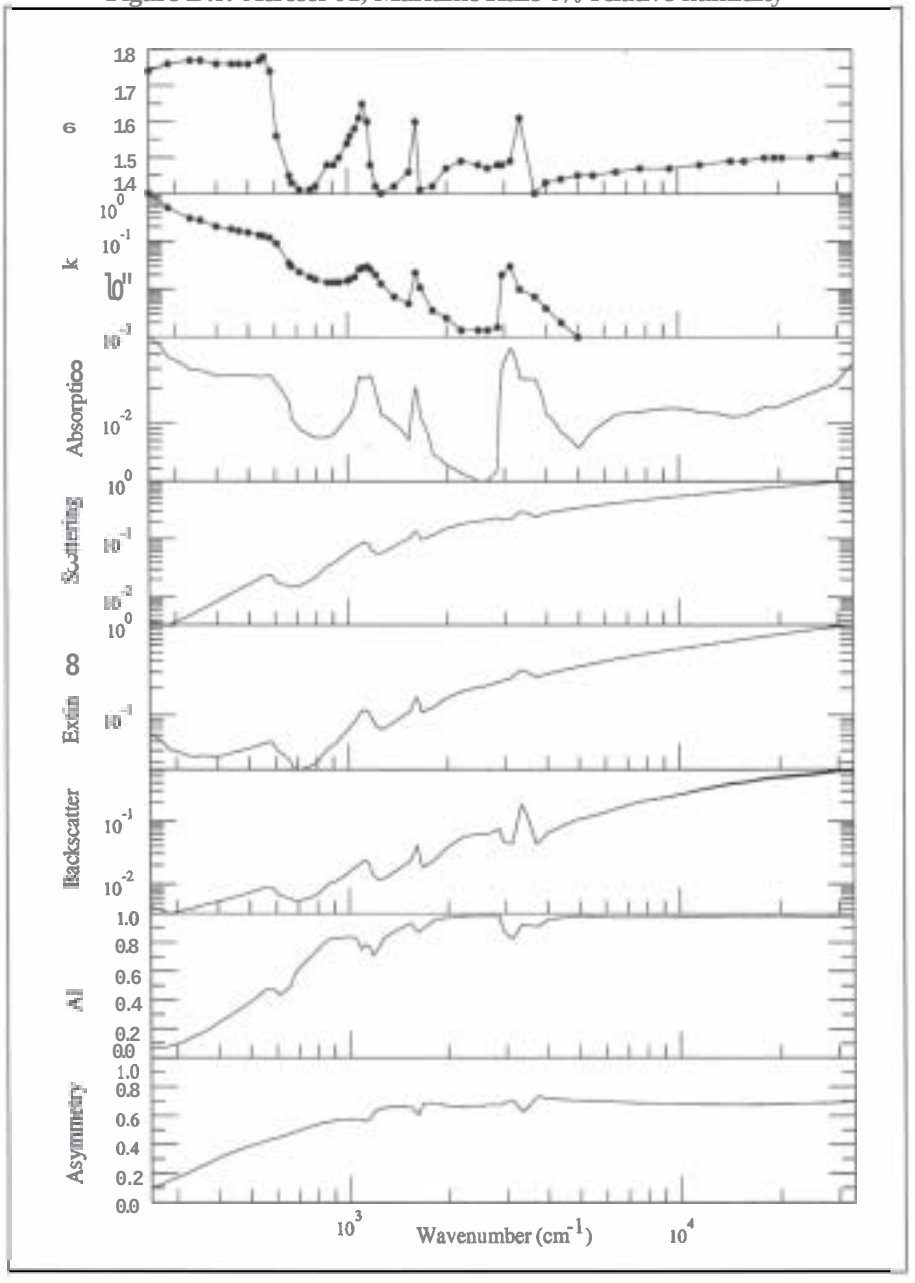

Figure B.2: Aerosol 02, Maritime Haze 50% relative humidity

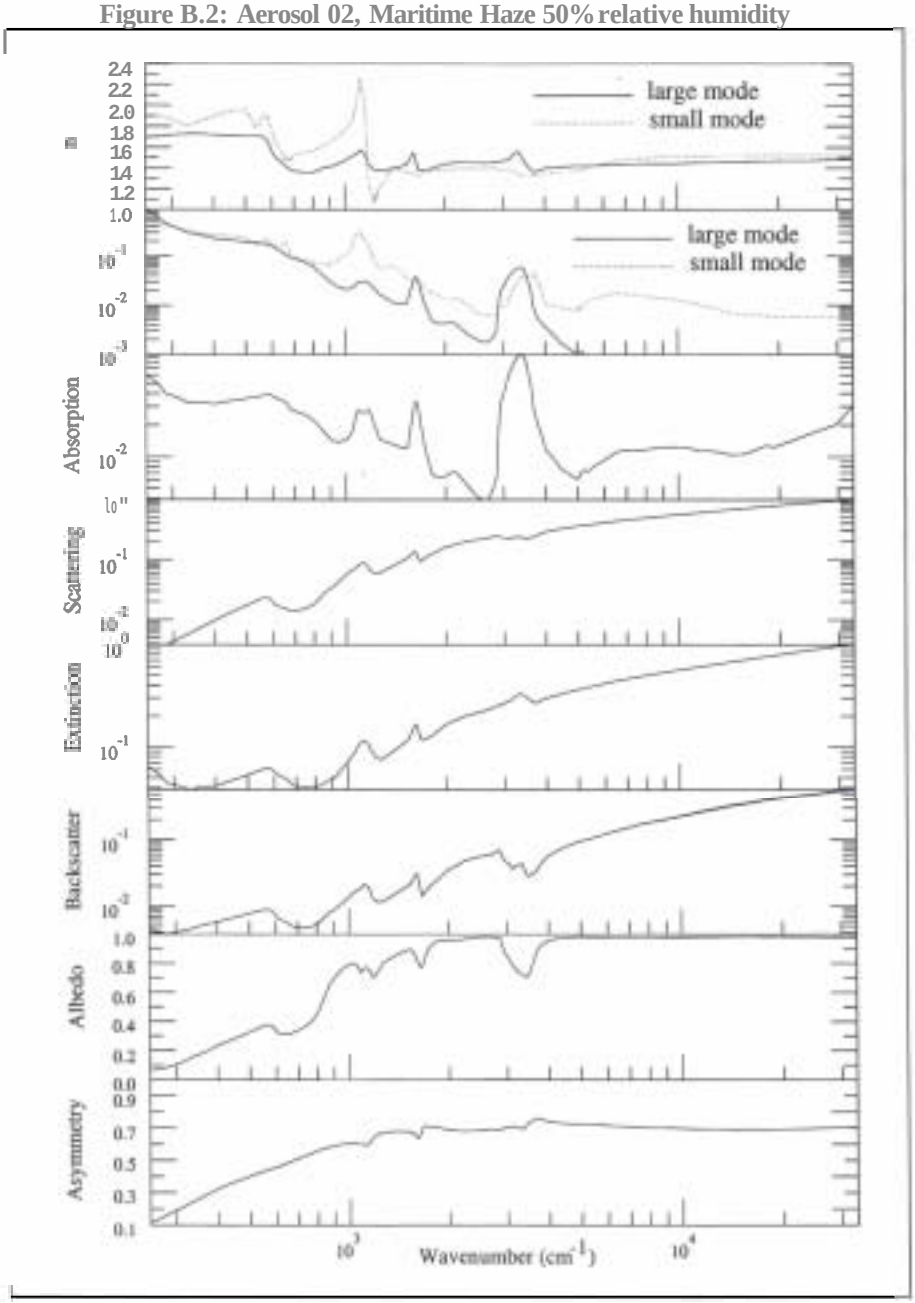

Figure B.3: Aerosol 03, Maritime Haze 70% relative humidity

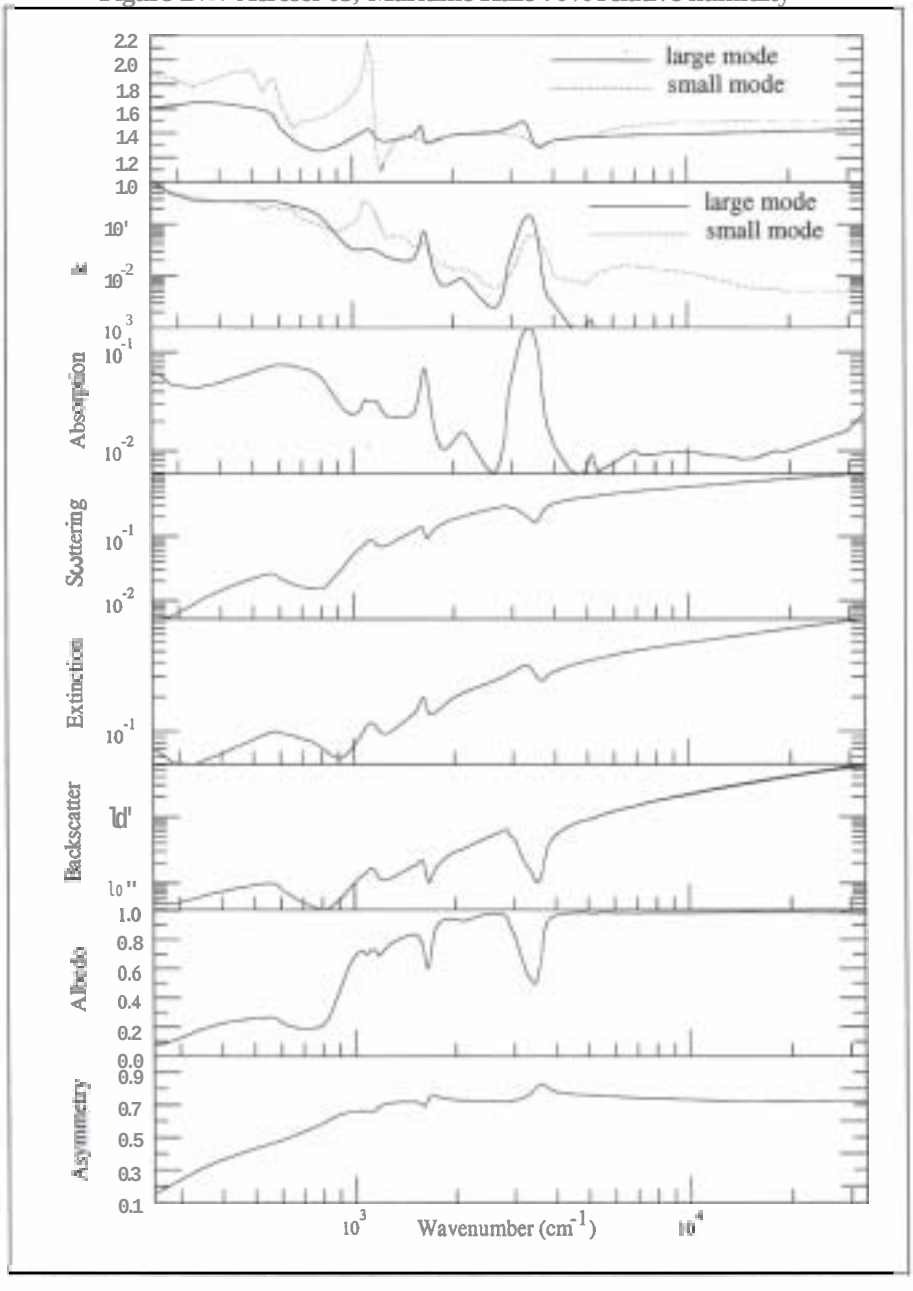

Figure B.4: Aerosol 04, Maritime Haze 80% relative humidity

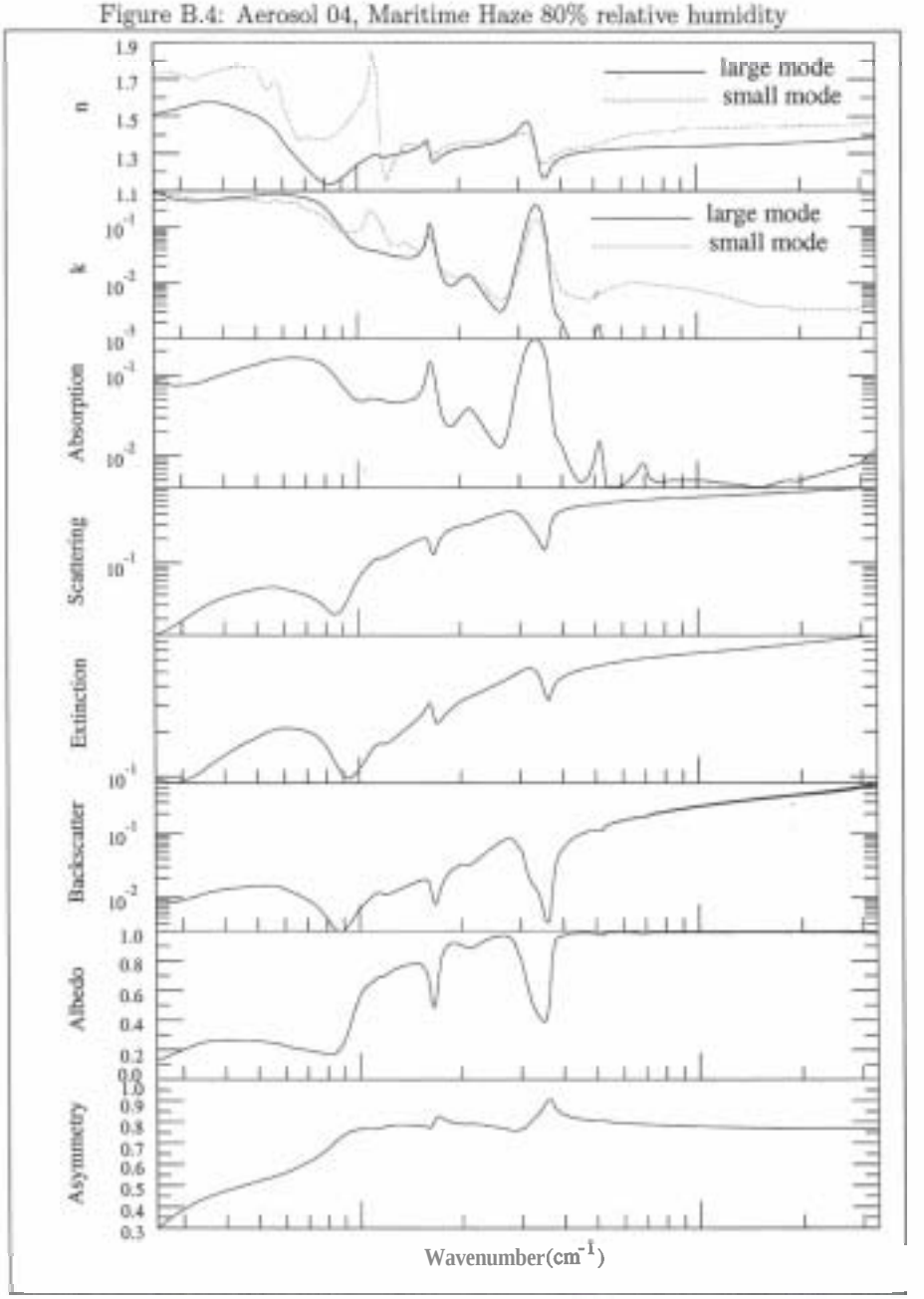

Figure B.5: Aerosol 05, Maritime Haze 90% relative humidity

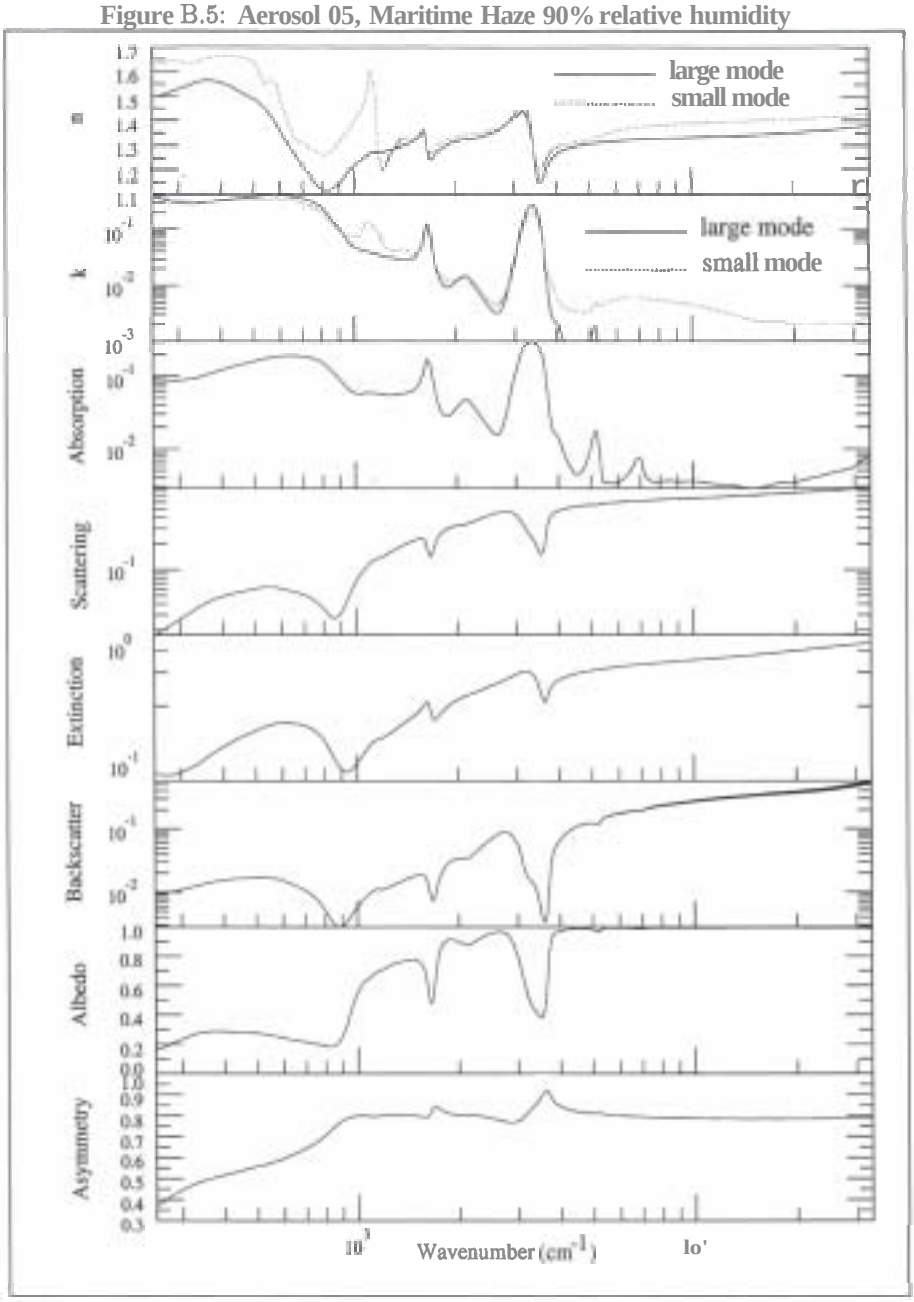

Figure B.6: Aerosol 06, Maritime Haze 95% relative humidity

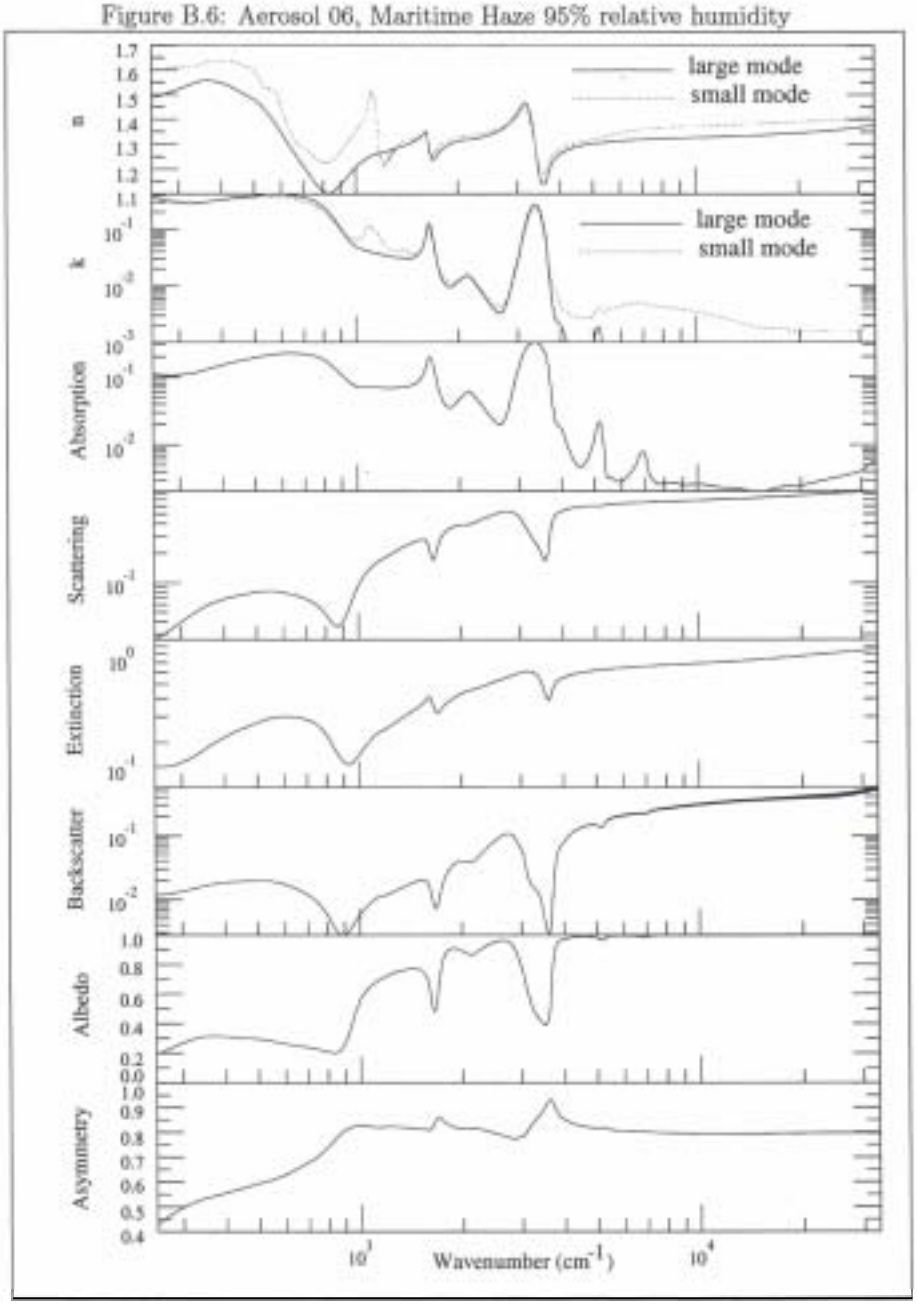

Figure **B.7:** Aerosol **07,** Maritime Haze 98% relative humidity

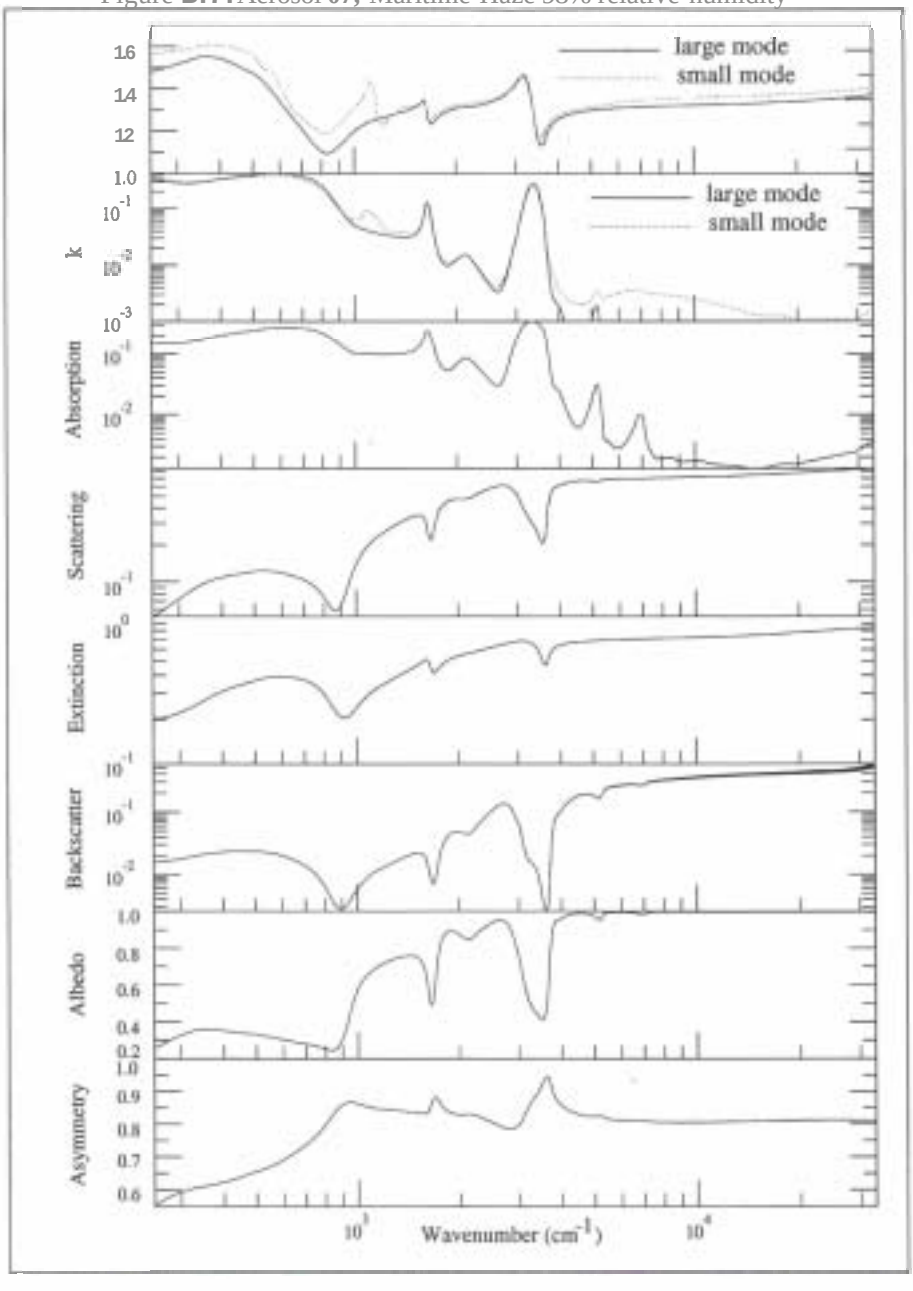

Finure B.8: Aerosol 08, Maritime Haze 99% relative humidity

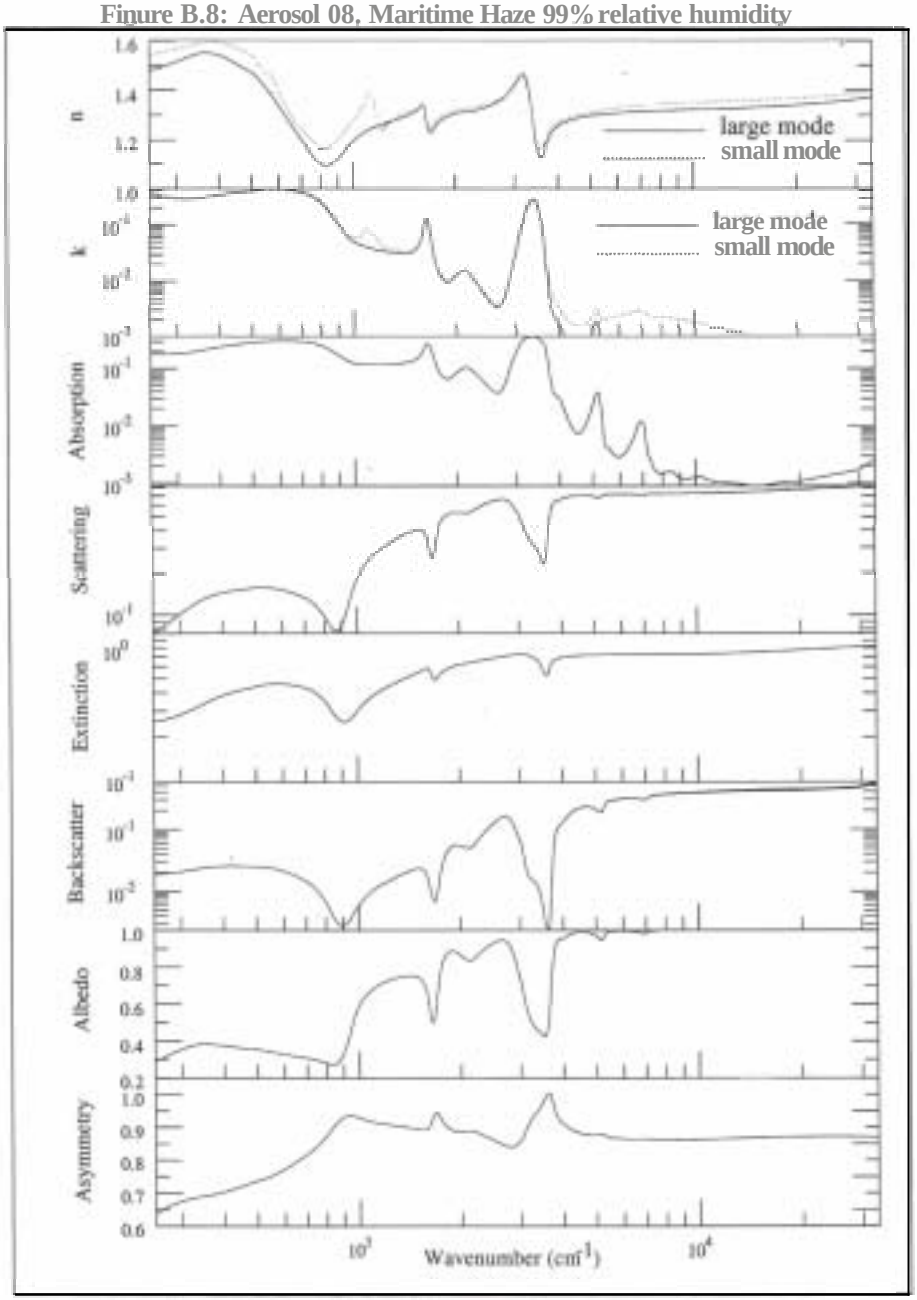

Figure B.9: Aerosol 09, Urban Haze 0% relative humidity

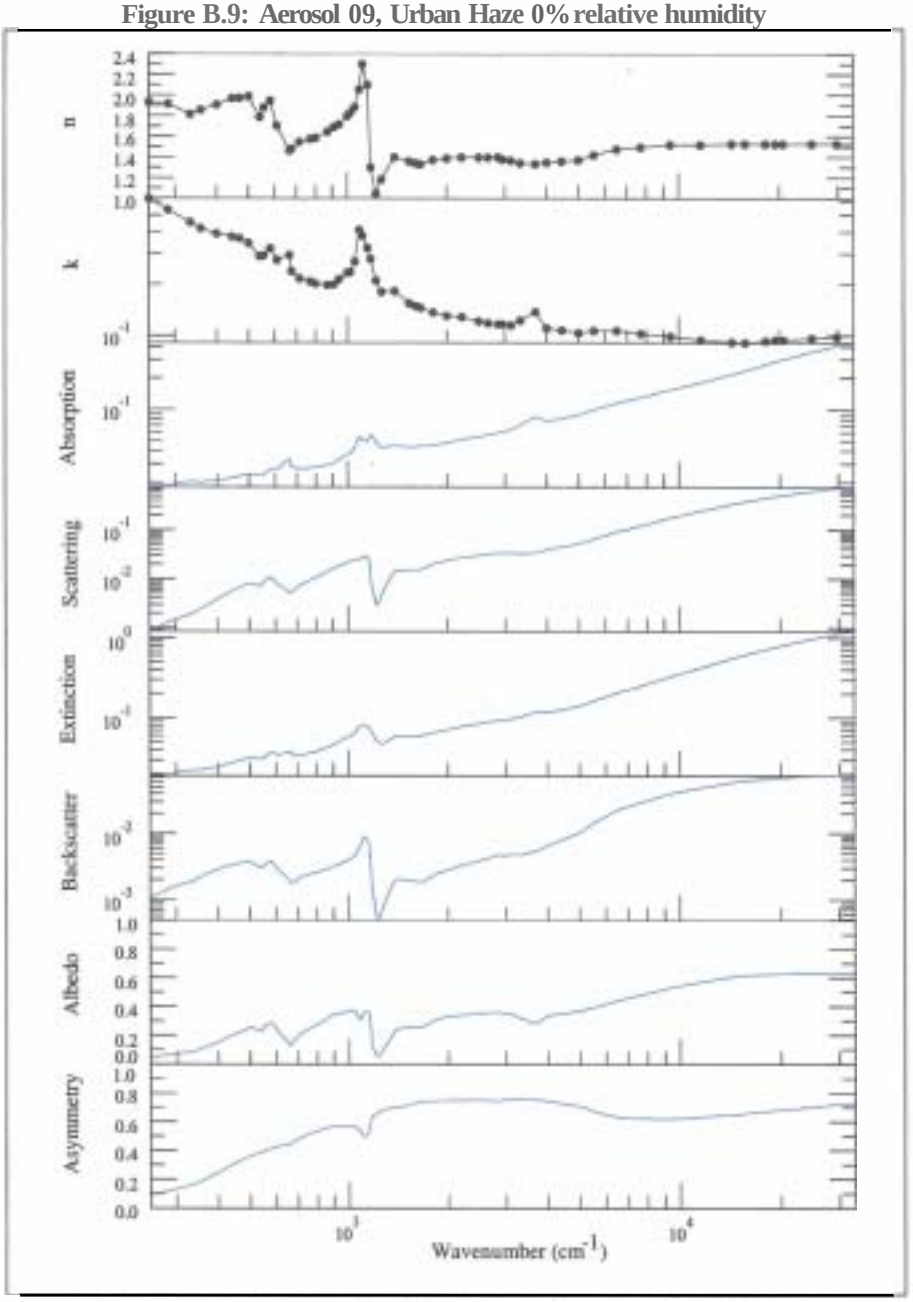

Figure B.lO: Aerosol 10, Urban Haze 50% relative humidity

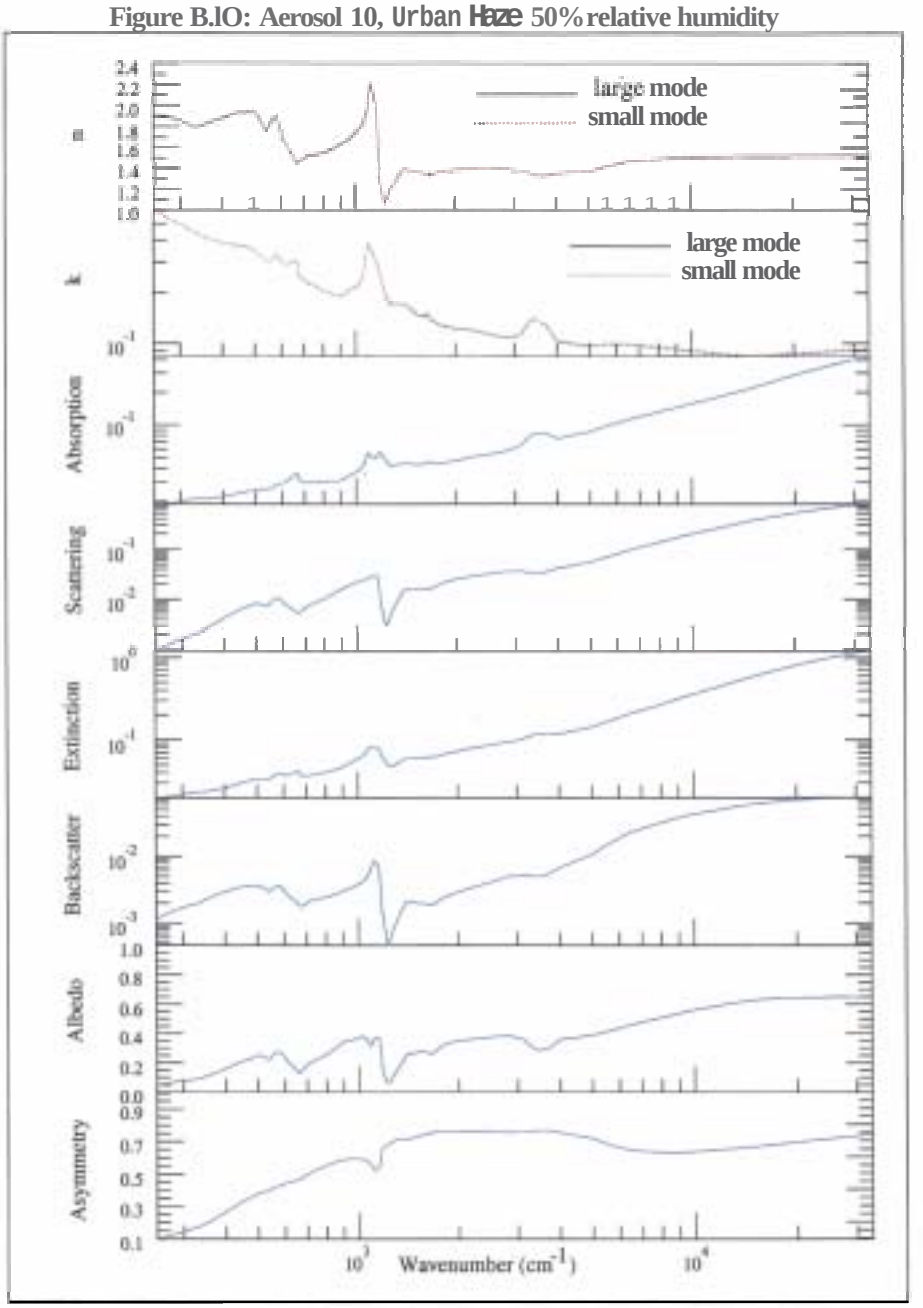

Figure B.11: Aerosol 11, Urban Haze 70% relative humidity

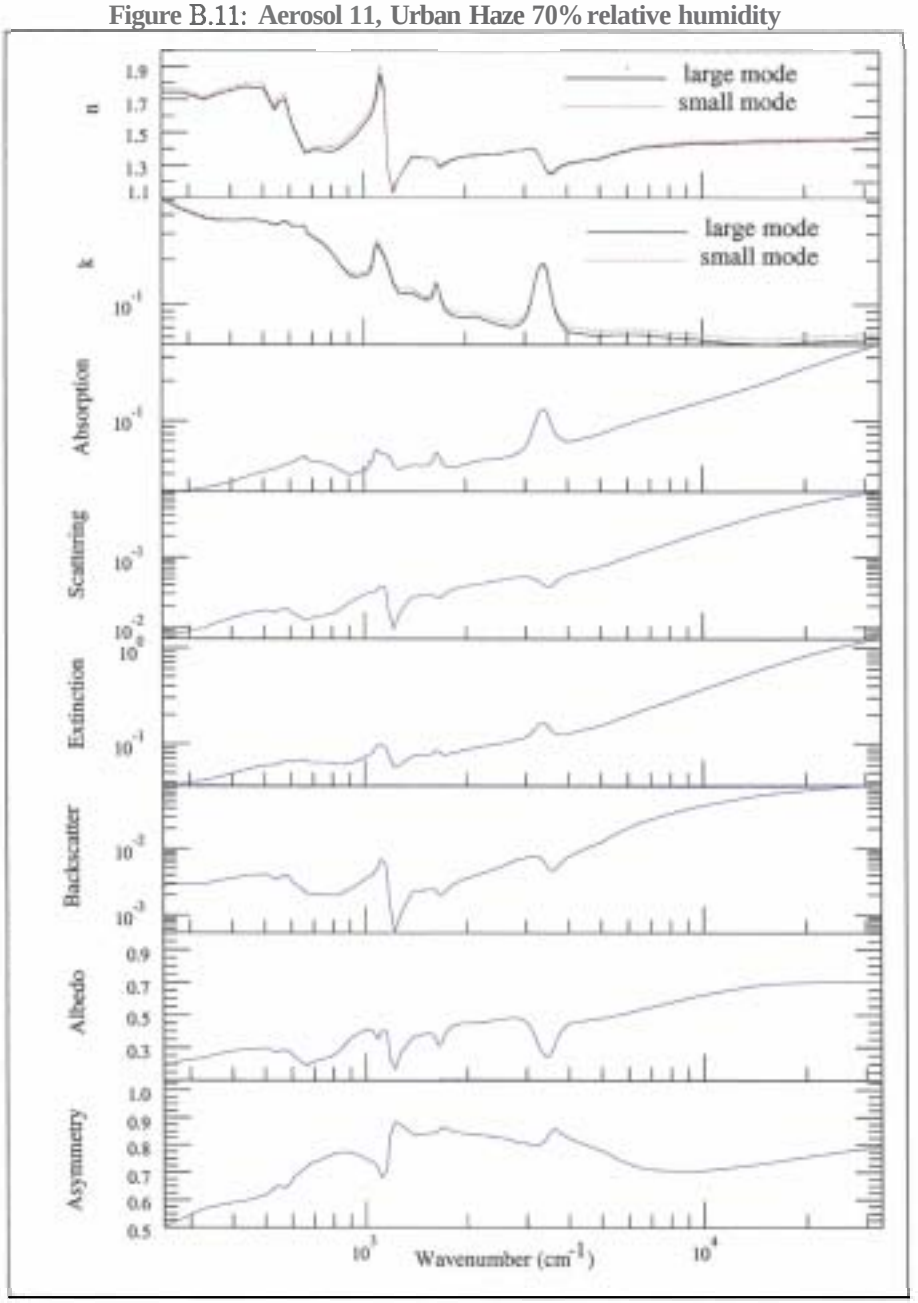

Figure B.12: Aerosol 12, Urban **Haze 80% relative humidity**

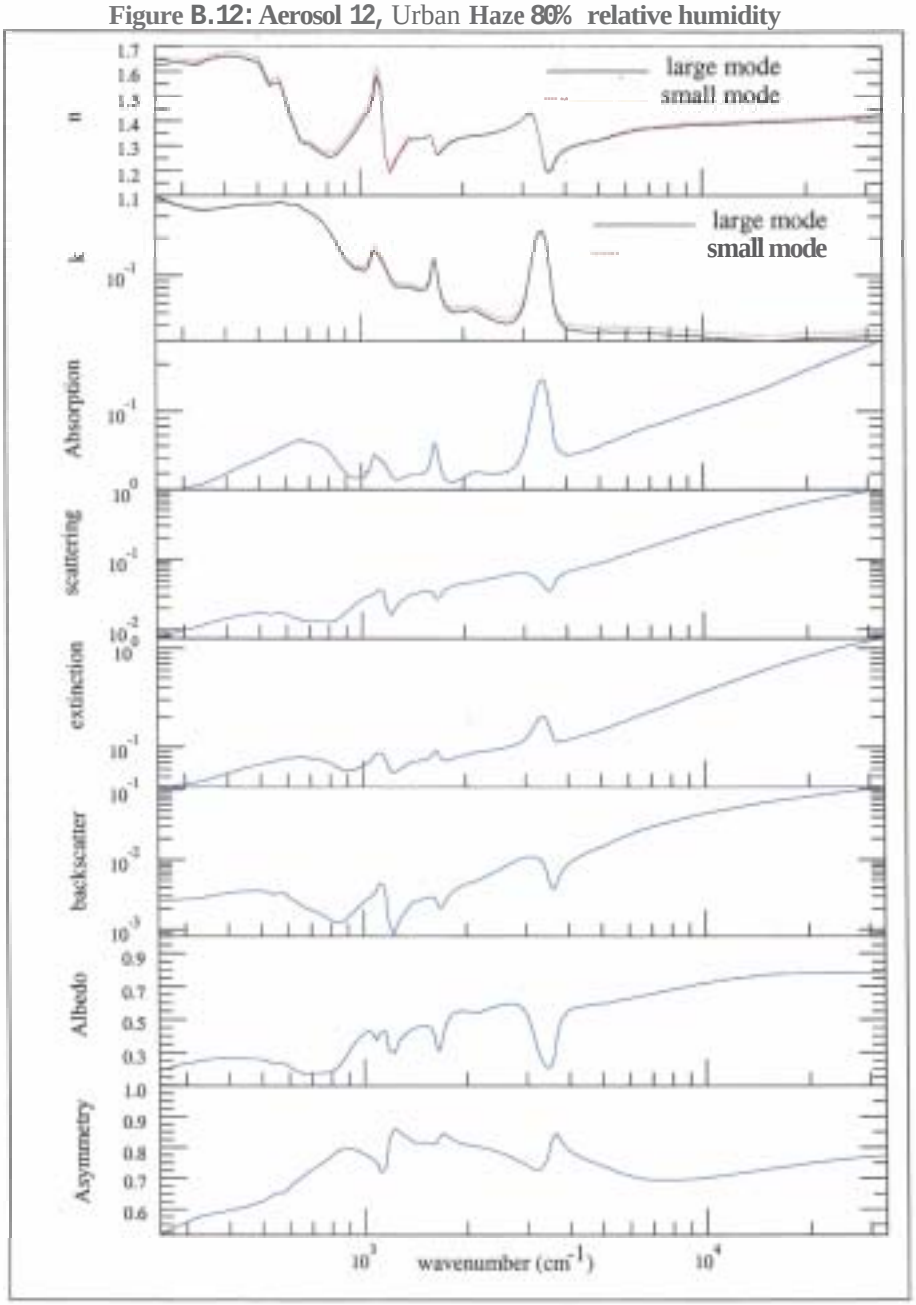

Figure B.13: Aerosol 13, Urban Haze 90% relative humidity

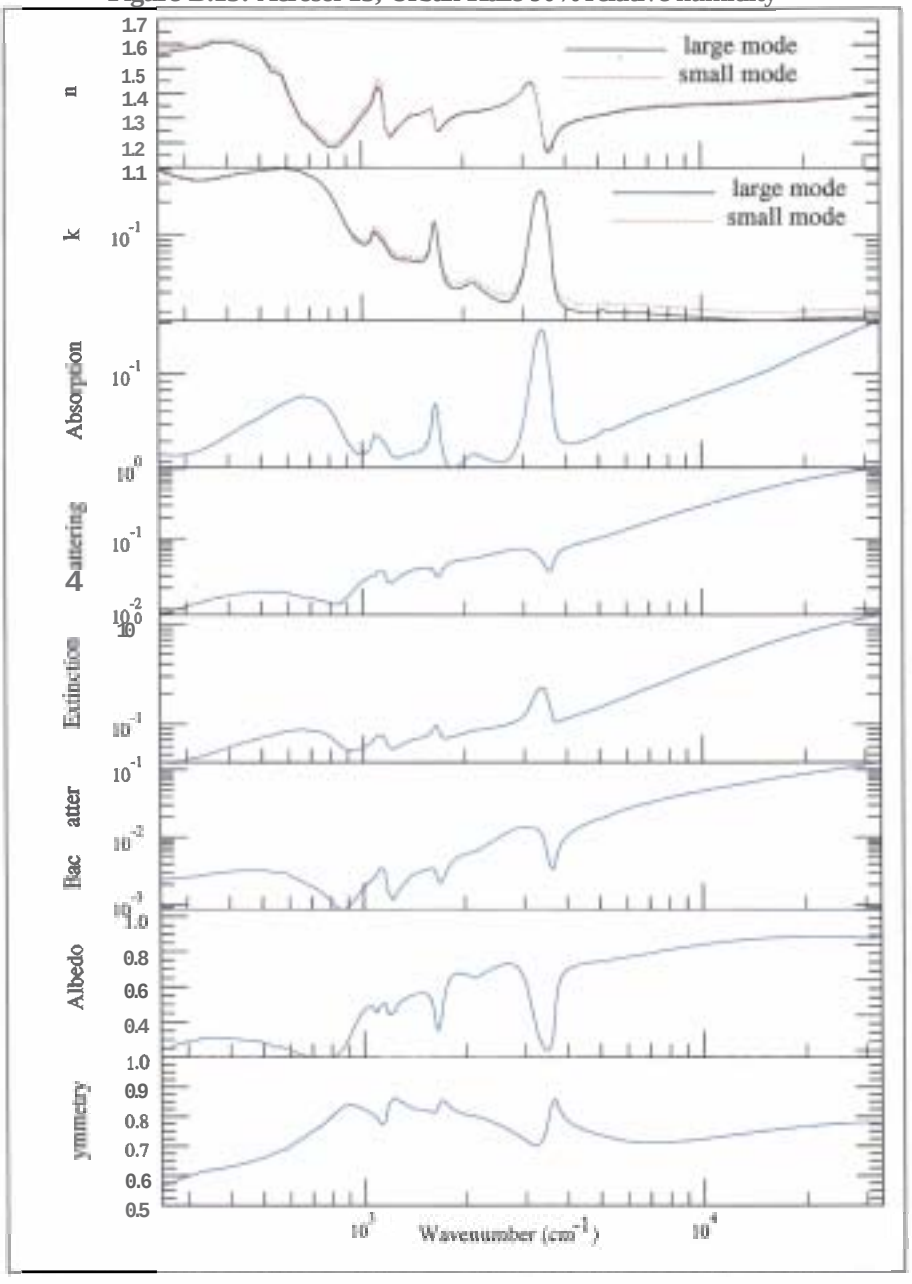

Figure B.14: Aerosol 14, Urban Haze 95% relative humidity

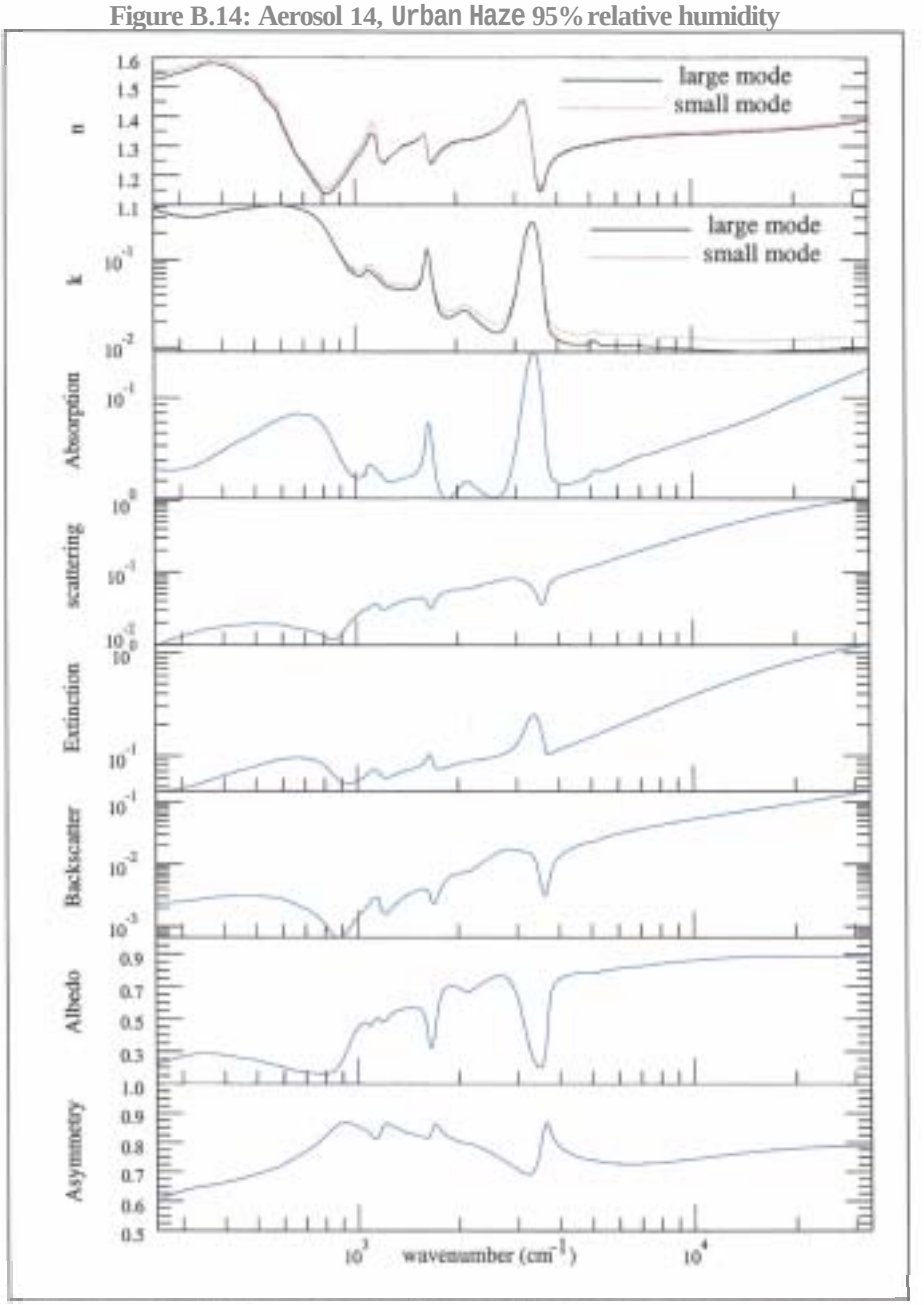

Figure B.15: Aerosol 15, Urban Haze 98% relative humidity

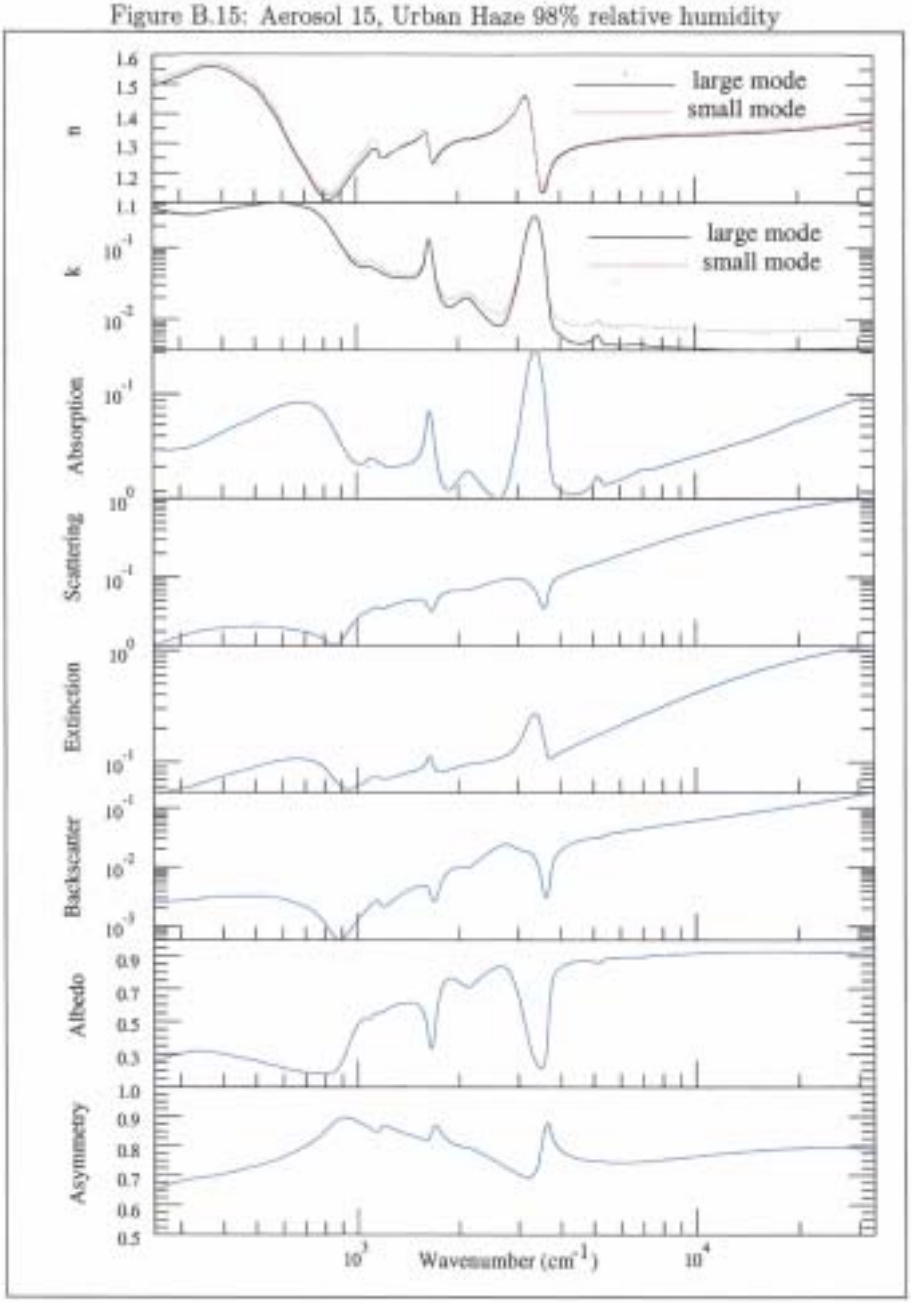

Figure B.16: Aerosol 16, Urban Haze 99% relative humidity

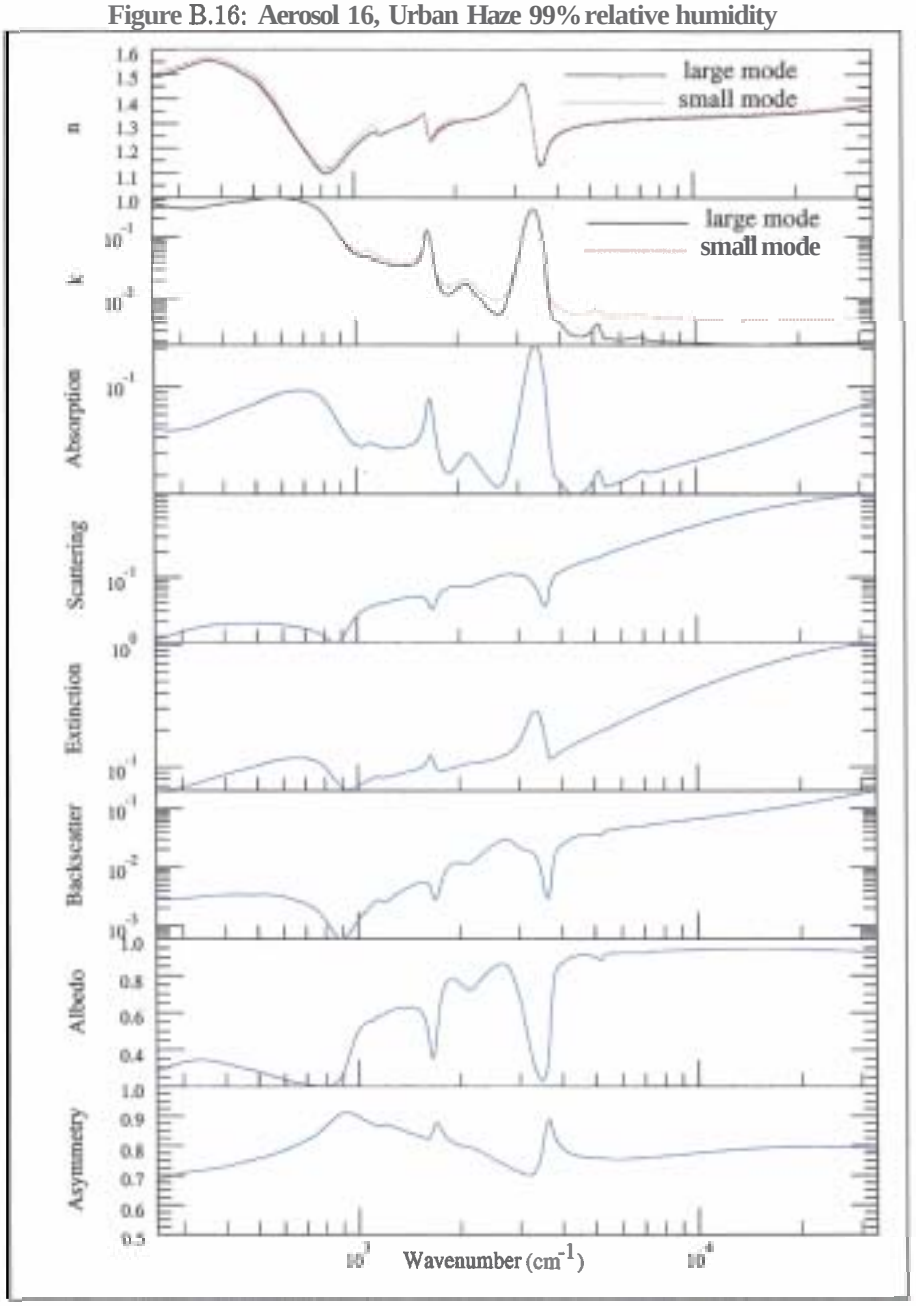

Figure B.17: Aerosol 17, Rural Haze 0% relative humidity

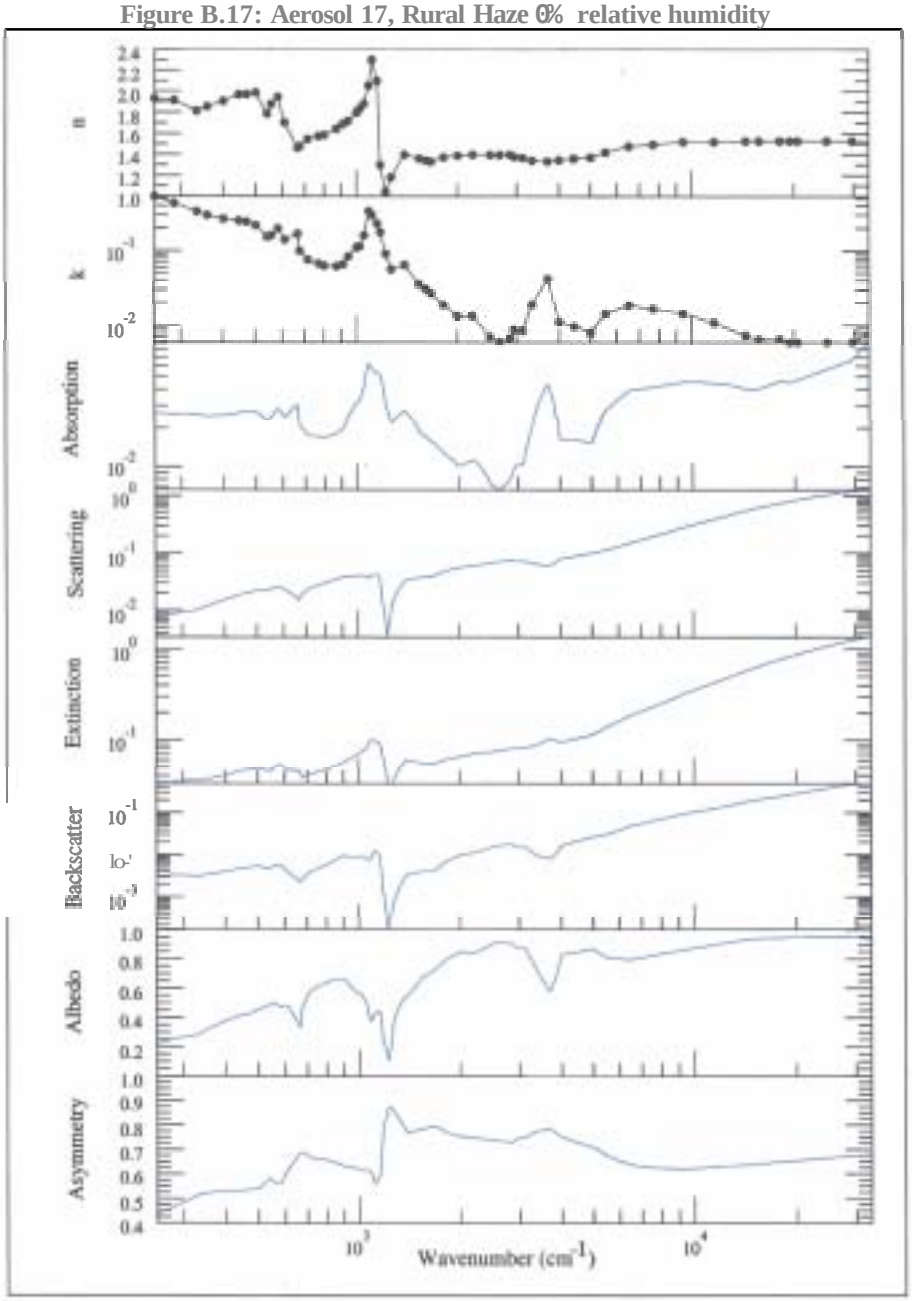

Figure B.18: Aerosol 18, Rural Haze 50% relative humidity

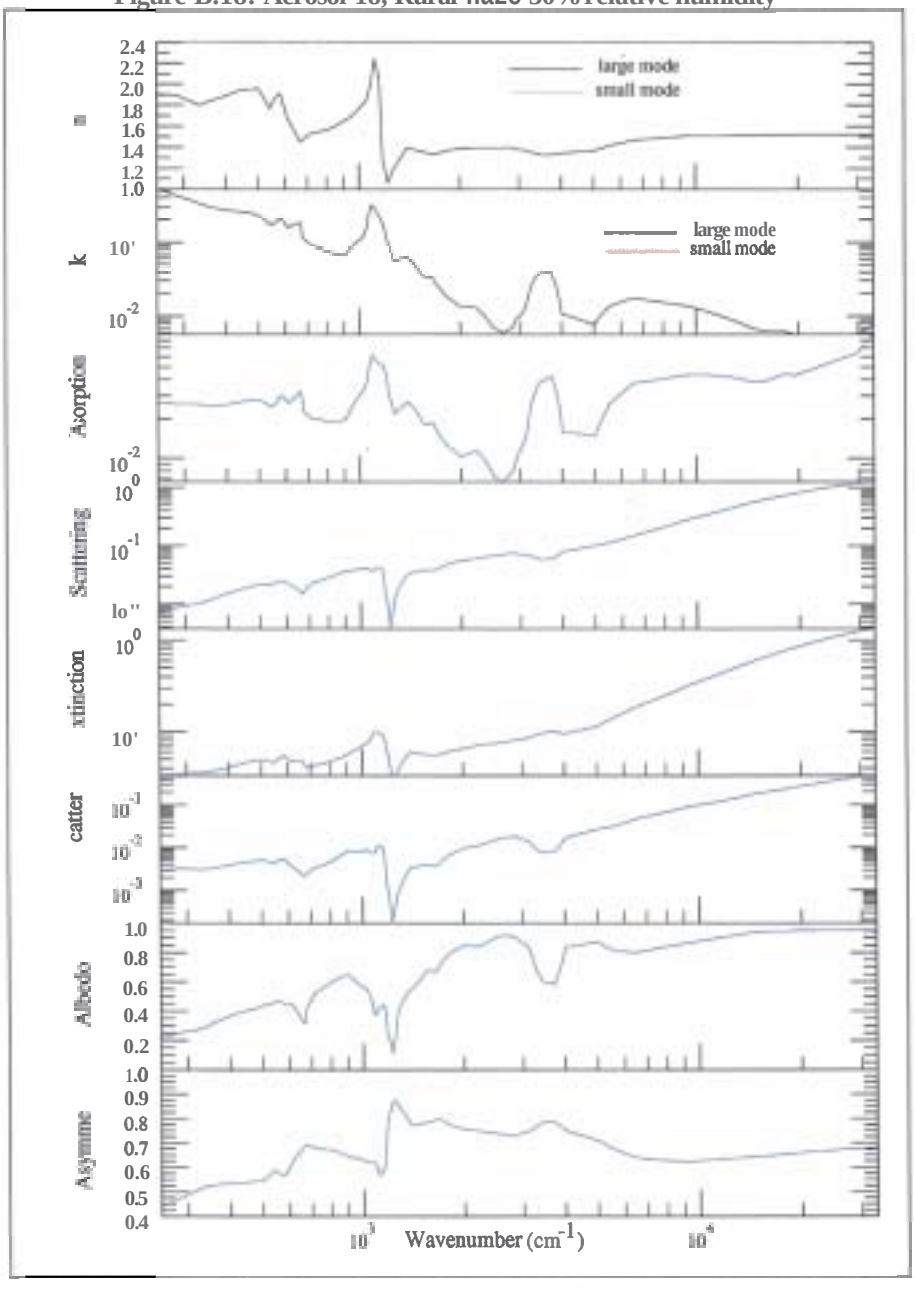

Figure B.19: Aerosol 19, Rural Haze 70% relative humidity

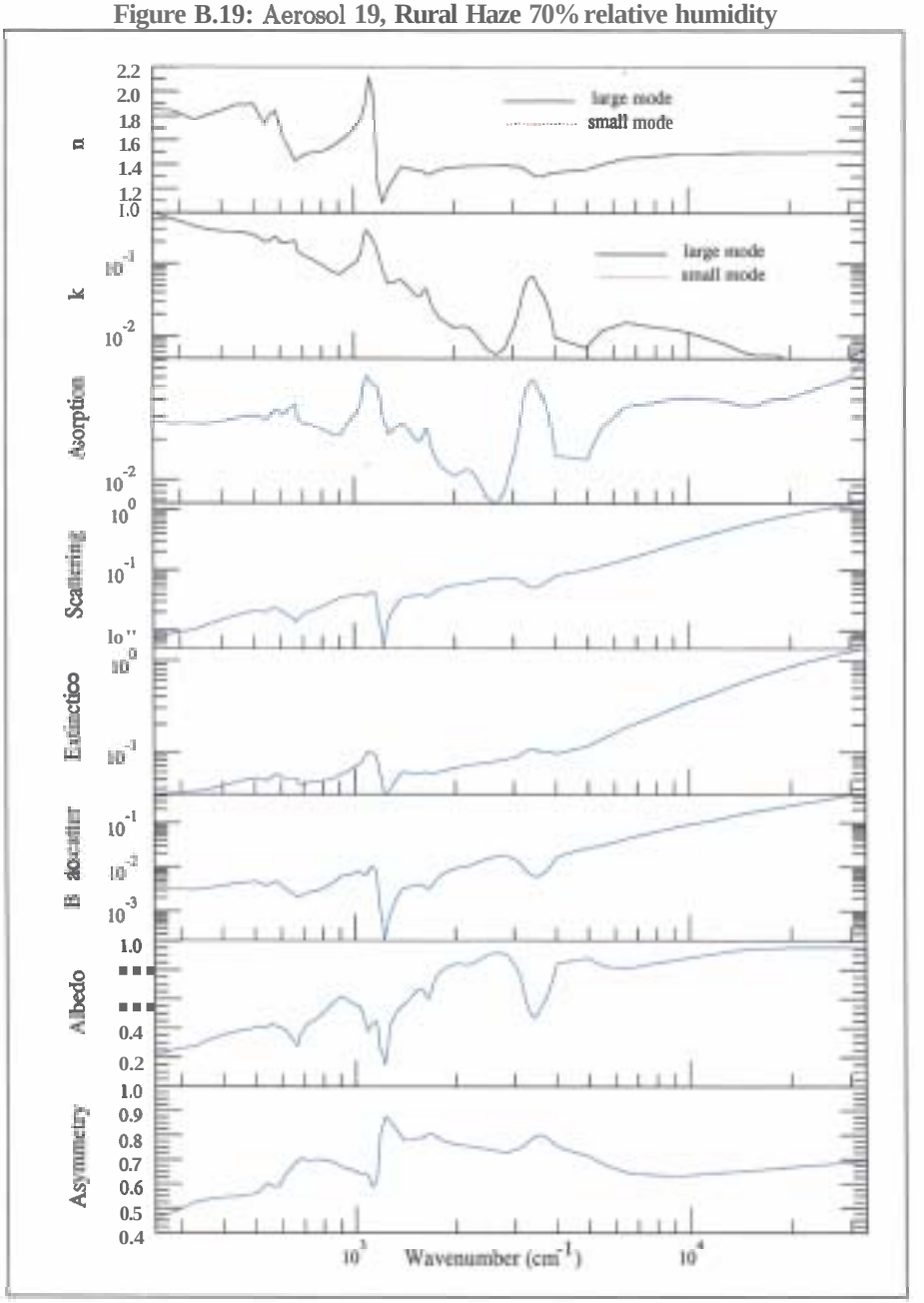

Figure B.20: Aerosol 20, Rural Haze 80% relative humidity

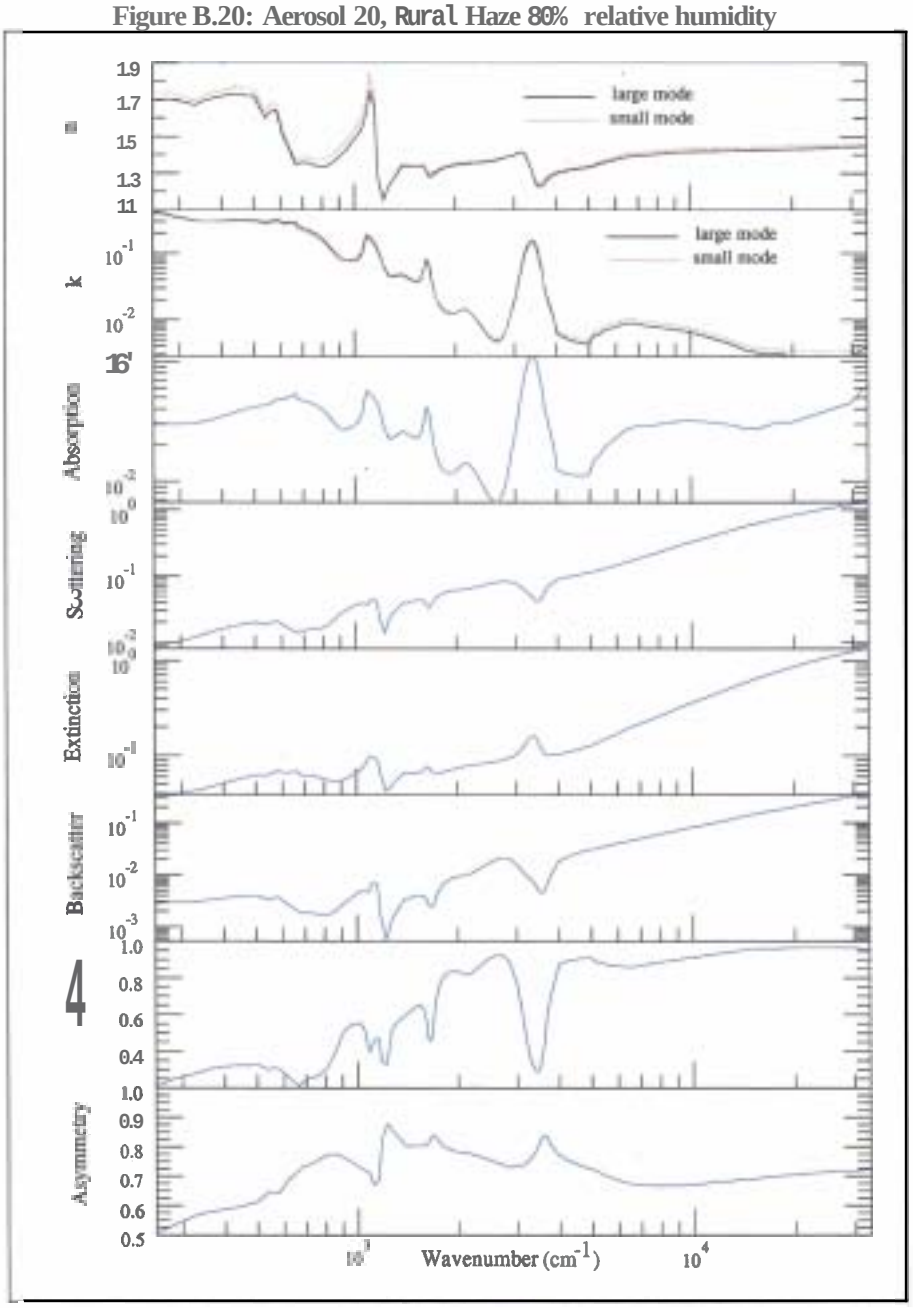

Figure B.21: Aerosol 21, Rural Haze 90% relative humidity

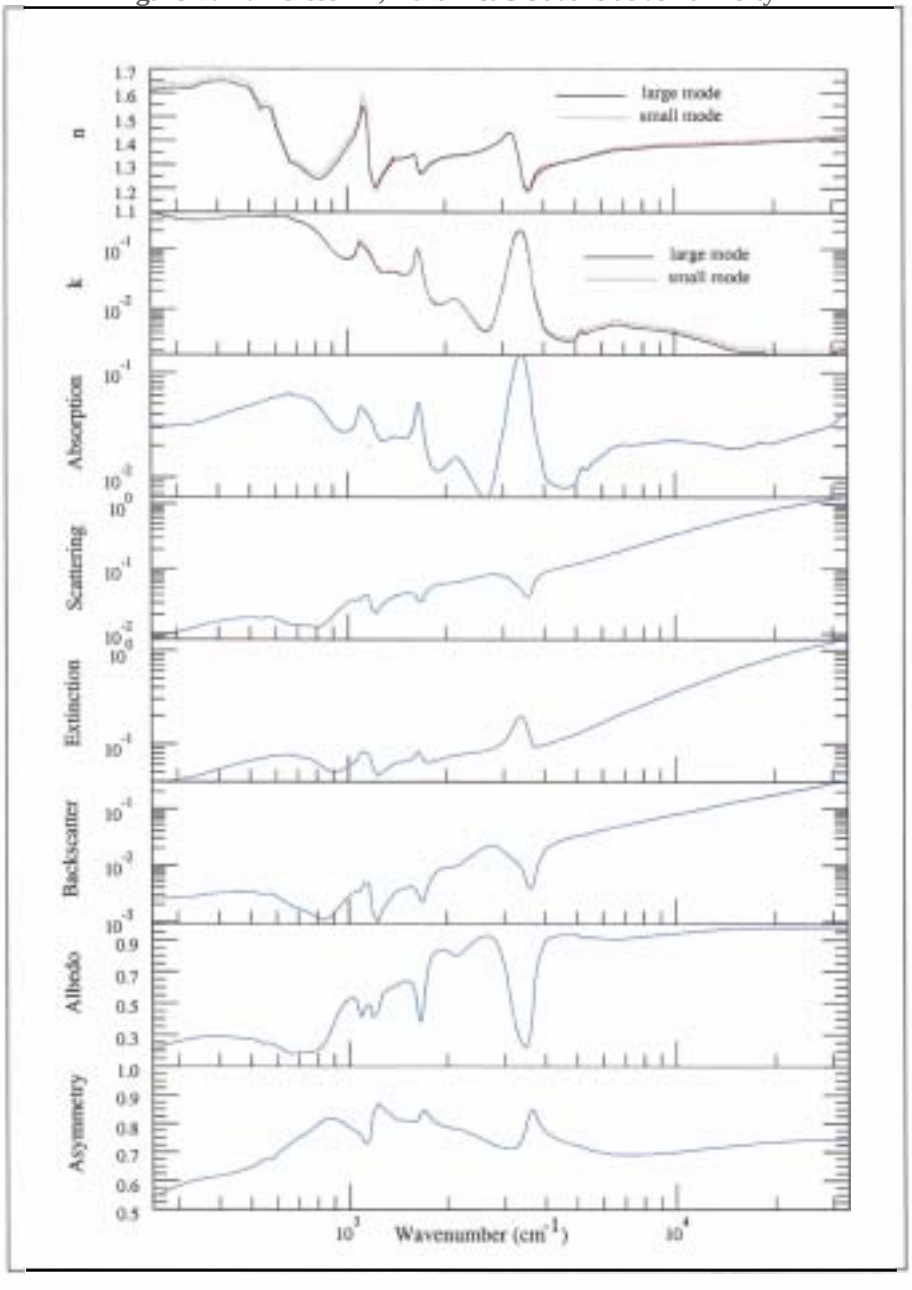

Figure B.22: Aerosol 22, Rural Haze 95% relative humidity

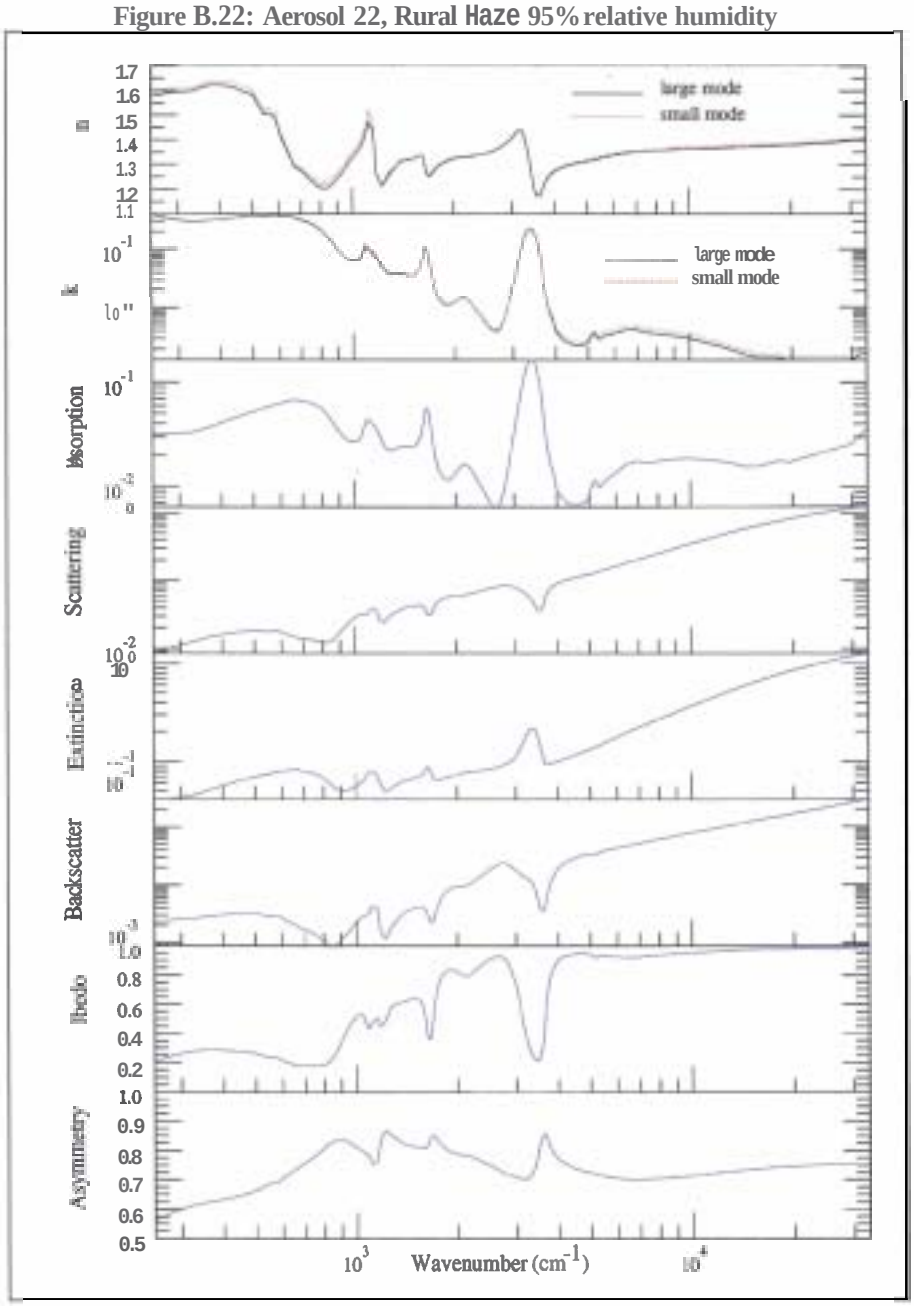

Figure B.23: Aerosol 23, Rural Haze 98% relative humidity

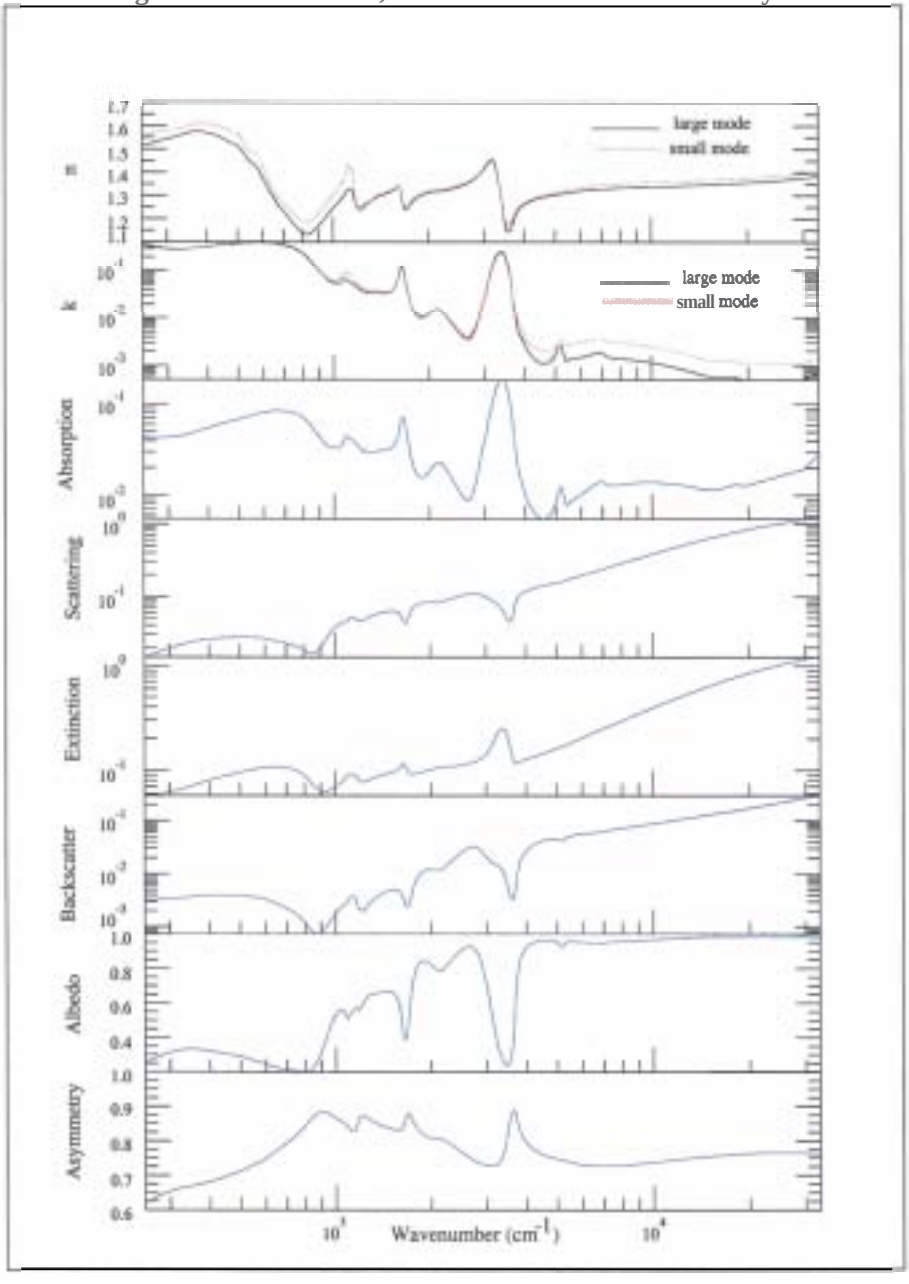

Figure B.24: Aerosol 24, Rural Haze 99% relative humidity

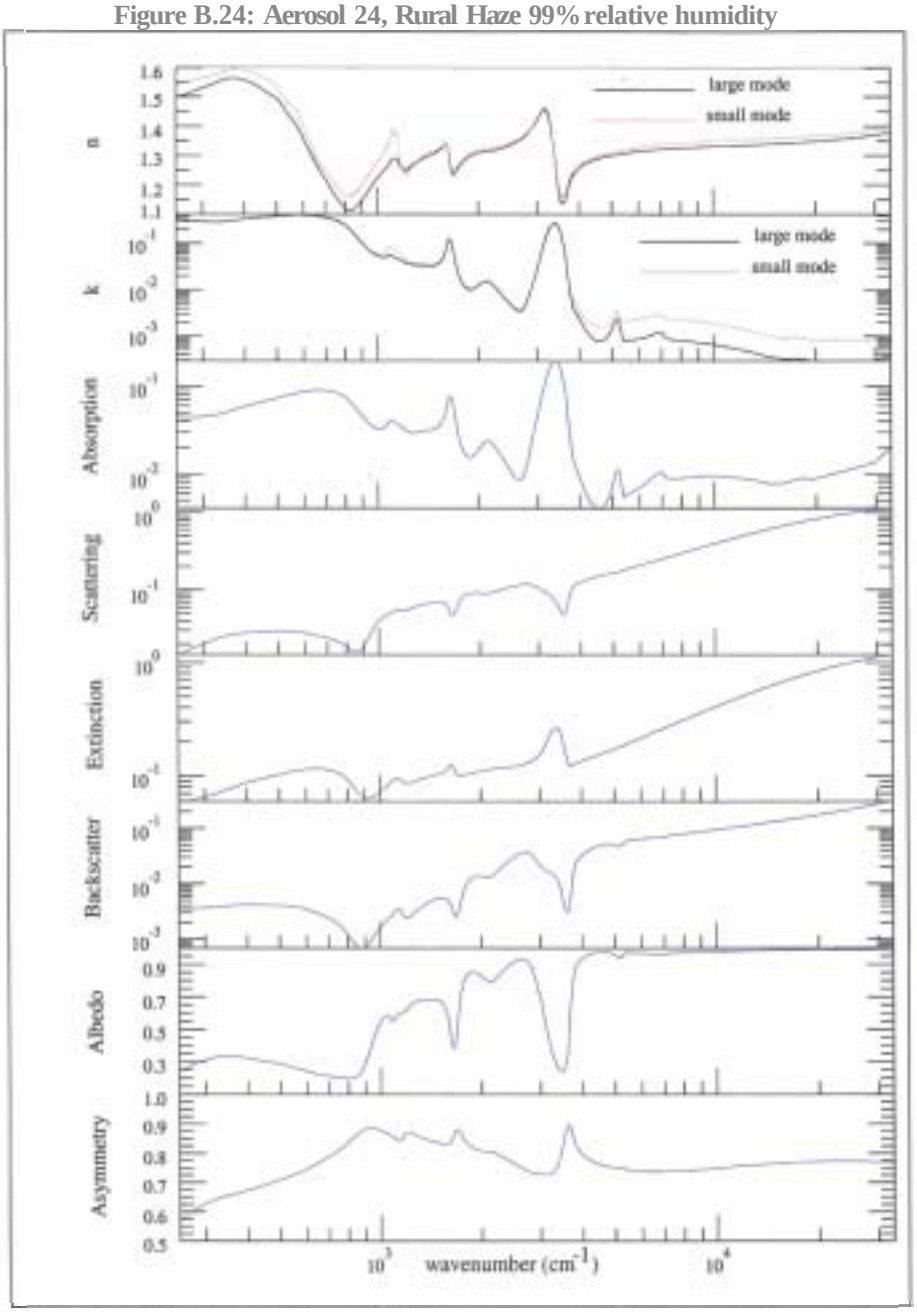

Figure B.25: Aerosol 25, Heavey Advection Fog

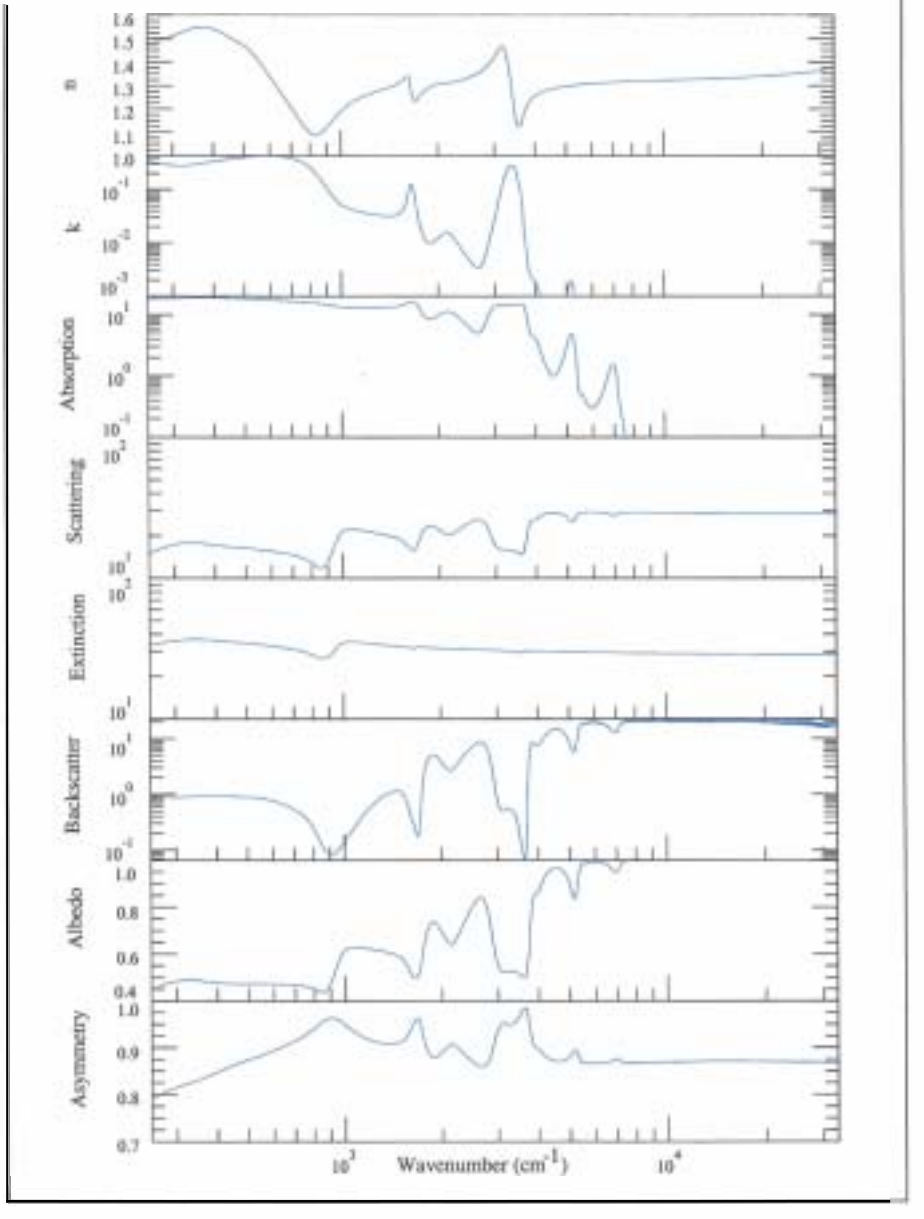

Figure B.26: Aerosol 26, Moderate Radiation Fog

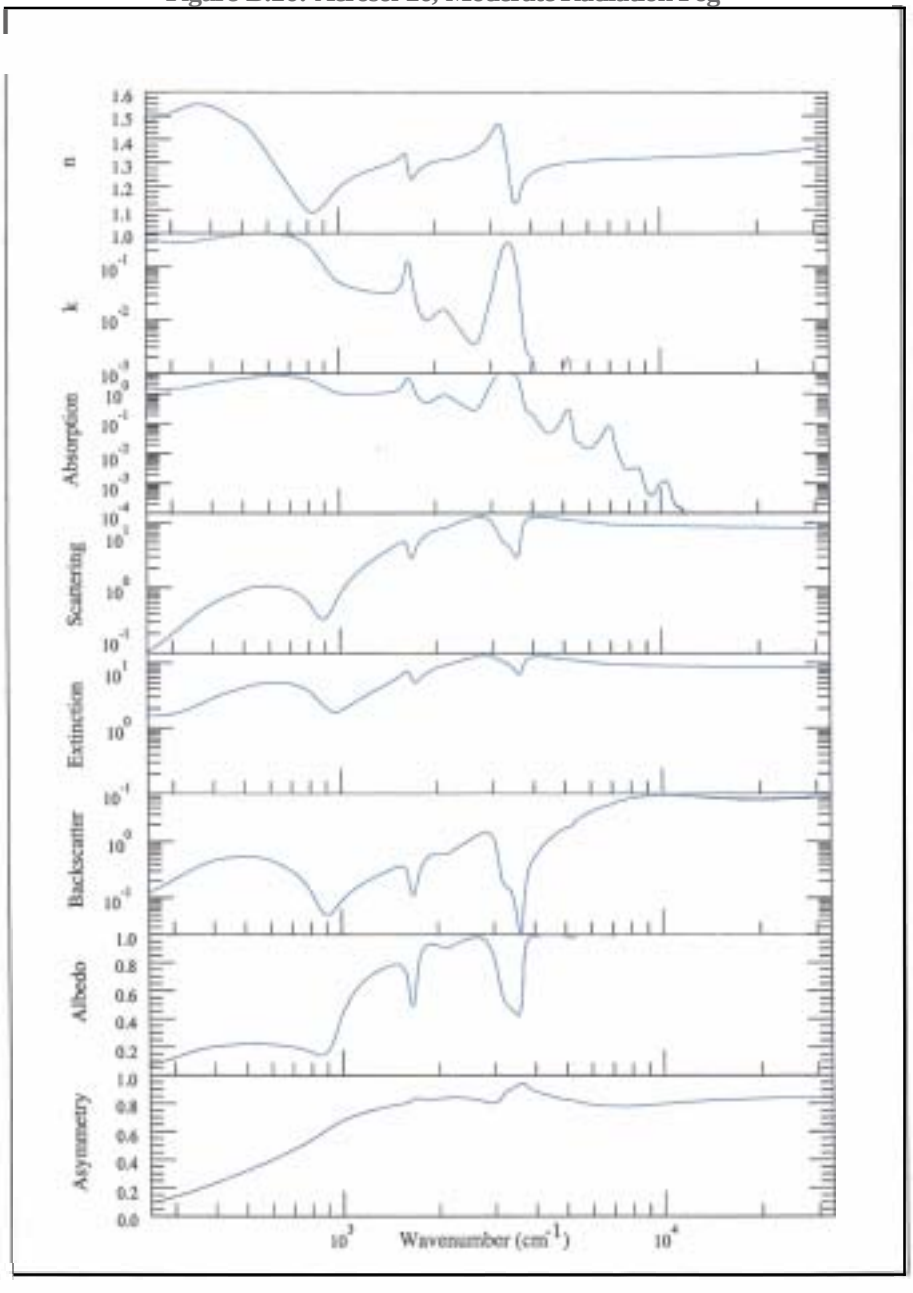

Figure B.27: Aerosol 56, Fog Oil

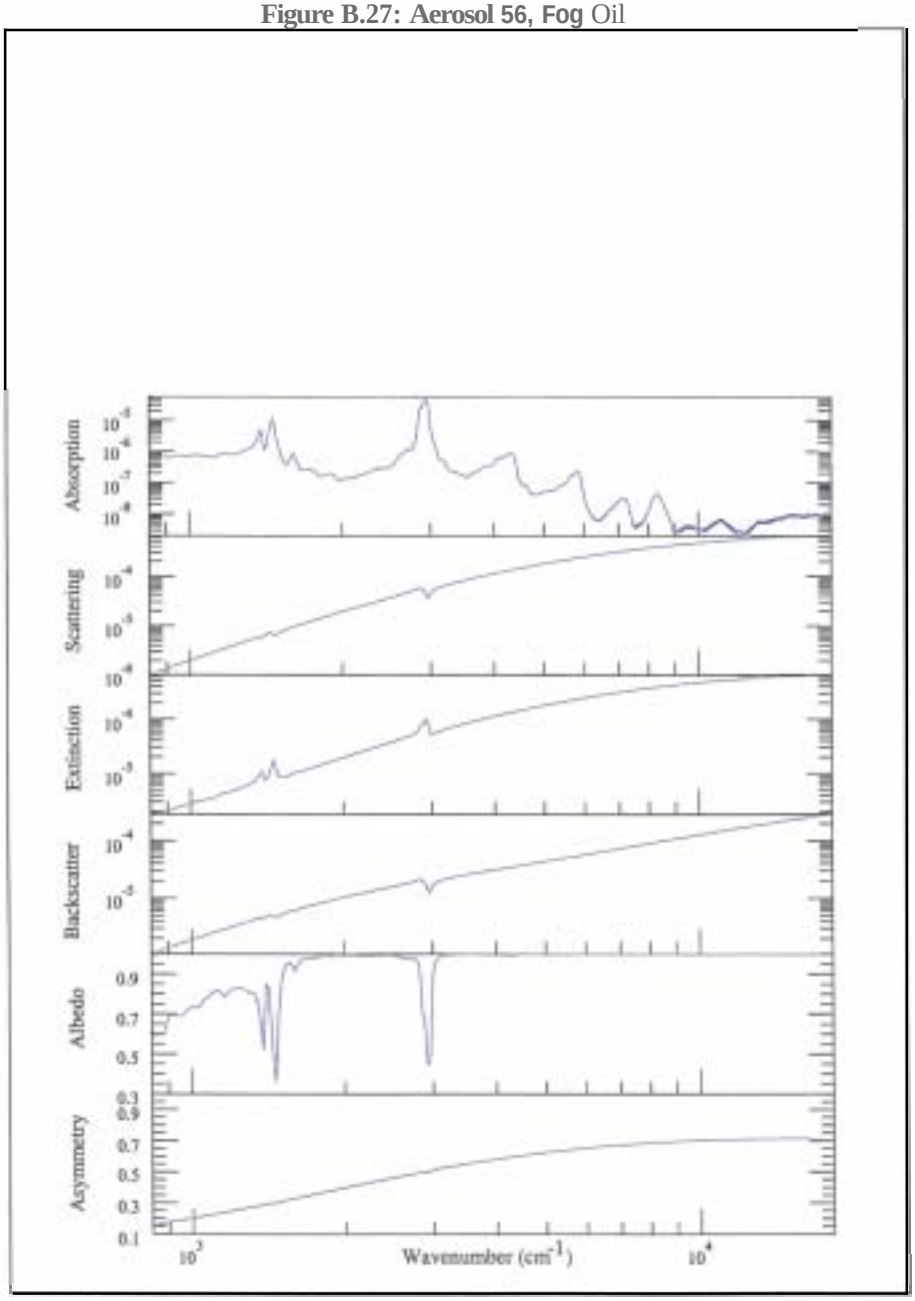

Bibliography

[1] Craig F. Bohren and Donald R. Huffman. Absorption and *Scattering* of *Light* by Small Particles. John Wiley and Sons, Inc., 1983. 1.1

[2] H.R. Carlon et al. Infrared extinction spectra of some cannon liquid aerosols. Appl Opt, 1b:1598–1605, 1977. 2.3

[3] L. D. Duncan. Eosael 82, transmission through battlefield aerosols. Technical Report ASL-TR-0122, U.S. Army Atmospheric Sciences Laboratory, White Sands Missile Range, NM 88002-5501, 1982. 1

[4] L. Elterman. Atmosphericattenuation model, 1964, in the ultraviolet, visible, and infrared regions for altitudes to 50 km. Technical Report AFCRL-64740, AFRL, 1964. 1

[5] L. Elterman. UV, visible, and IR attenuation for altitudes to 50km. Technical Report AFCRL–68-0153, AD 671933, AFRL, 1968. 1

[6] L. Elterman. Verticle attenuation model with eight surface meteorological ranges 2 to 13 kilometers. Technical Report AFCRL-70-0200, AD 707488, AFRL, 1970. 1

[7] Milton Kerker. The Scattering of Light and Other Electromagnetic Radiation, volume 16 of Physical Chemistry. Academic Press, 1969. 1.1

[8] F. X. Kneizys, E. P. Shettle, L. W. Abreu, G. P. Anderson, J. H. Chetwynd, W. O. Gallery, J. E. A. Selby, and S. A. Clough. Users guide to LOWTRAN 7. Technical Report AFGLTR-88-0177, Air Force Geophysics Laboratory, Hanscom Air Force Base, MA 01731, 1989. 1

[9] R.A. McClatchey, R.W. Fenn, J.E.A. Selby, F.E. Volz, and J.S. Garing. Optical properties of thje atmosphere. Technical Report AFCRL-70-0527, AD 715270, AFRL, 1970. 1

[10] R.A. McClatchey, R.W. Fenn, J.E.A. Selby, F.E. Volz, and J.S. Garing. Optical properties of the atmosphere (third edition). Technical Report AFCRL-72-0497, AD 754075, AFRL, 1972. 1

[11] P. Ray. Broadband complex refractive indices of ice and water. Appl. Opt, 11:1836–1844, 1972. 1.1.1, 2, 3, 4

[12] M. Seablom, A. Wetmore, D. Ligon, B. Van Aartsen, and P. Gillespie. Weather and atmospheric visualization effects for simulation (WAVES) toolkit and user's guide. Technical Report ARLTR-1721-6, Army Research Laboratory, Adelphi, MD, 1999. 1

[13] D. Segelstein. "the complex refractive index of water". Master's thesis, University of Missouri–Kansas City, 1981. 1.1.1

[14] E. P. Shettle and R. W. Fenn. Models for the aerosols of the lower atmosphere and the effects of humidity variations on their optical properties. Technical Report AFGL-TR-79-0214, ADA 085 951, U.S. Air Force Geophysics Laboratory, Hanscom AFB, Bedford, MA, 1979. 1, 1.1, 2.1, 2.2

[15] D. H. Tofsted, B. T. Davis, A. E. Wetmore, J. Fitzgerrel, R. C. Shirkey, and R. A. Sutherland. Eosael92 aerosol phase function data base pfndat. Technical Report ARLTR-273-9, Department of the Army, U.S. Army Research Laboratory, Battlefield Environment Directorate, White Sands Missile Range NM 88002-5501, June 1997. 1, 1, 2.3, 3.1

[16] D.M. Wieliczka, S. Weng, and M.R. Querry. Wedge shaped cell for highly absorbent liquids: Infrared optical constants of water. Appl. Opt., 28(9):1714–1719, 1989. 1.1.1

Distribution list

Admnstr
Defns Techl Info Ctr
ATTN DTIC-OCP (Electronic copy)
8725 John J Kingman Rd Ste 0944
FT Belvoir VA 22060-6218

DTRA/OSPTL
ATTN R Kvavilashvili
8725 John Kingman Rd
MSC 6201
Ft Belvoir VA 22060

DARPA
ATTN IXO S Welby
3701 N Fairfax Dr
Arlington VA 22203-1714

Ofc of the Secy of Defns
ATTN ODDRE (R&AT)
The Pentagon
Washington DC 20301-3080

ARL chemical Biology Nuc Effects Div
ATTN AMSRL-SL-CO
Aberdeen Proving Ground MD 21005-5423

US Army TRADOC
Battle Lab Integration & Techl Directrt
ATTN ATCD-B J A Klevecz
FT Monroe VA 23651-5850

Dept of the Army
Assist Secy of the Army
ATTN SAAL-TT L Stotts
2511 Jefferson Davis Hw Ste 9800
Arlington VA 22202-3911

Dir for MANPRINT Ofc of the
Deputy Chief of Staff for Prsnnl
ATTN J Hiller
The Pentagon Rm 2C733
Washington DC 20301-0300

US Army Corps of Engrs
Engr Topographics Lab
ATTN CETEC-TR-G P F Krause
7701 Telegraph Rd
Alexandria VA 22315-3864

Dir
ERDEC
ATTN SCBRD-TD
Aberdeen Proving Ground MD 21010-5423

SMC/GPA
2420 Vela Way Ste 1866
El Segundo CA 90245-4659

US Army Avn & Mis Crnnd
ATTN AMSMI-RD W C McCorkle
Redstone Arsenal AL 35898-5240

Director
US Army CECOM RDEC
FT Monrnouth NJ 07703-5201

US Army Field Artillery Schl
ATTN ATSF-TSM-TA
FT Sill OK 73503-5000

US Army Info Sys Engrg Cmnd
ATTN AMSEL-IE-TD F Jenia
FT Huachuca AZ 85613-5300

US Army Natick RDEC
Acting Techl Dir
ATTN SBCN-TP P Brandler
Kansas Street Bldg 78
Natick MA 01760-5056

US Army Topo Engrg Ctr
ATTN CETEC-ZC
FT Belvoir VA 22060-5546

US Army TRADOC
ATTN ATCD-FA
FT Monroe VA 23651-5170

Distribution list

US Army TRADOC
ATTN ATRC-WEC D Dixon
White Sands Missile Range NM 88002-5501

Nav Air War Ctr Wpn Div
ATTN CMD 420000D C0245 A Shlanta
1 Admin Cir
China Lake CA 93555-6001

Nav Surfc Weapons Ctr
ATTN Code G63
Dahlgren VA 22448-5000

AFSPC/DRFN
ATTN CAPT R Koon
150 Vandenberg Stret Ste 1105
Peterson AFB CO 80914-45900

Air Force Weather Techl Lib
151 Patton Ave Room 120
Asheville NC 28801-5002

ASC OL/YUH
ATTN JDAM-PIP LT V Jolley
102 W D Ave
Eglin AFB FL 32542

Phillips Lab
ATTN PL/LYP
Hanscom AFB MA 01731-5000

US Air Force
ATTN M Hoke
29 Randolph Rd
Hanscom AFB MA 01731

USAF Rome Lab Tech
ATTN Corridor W Ste 262 RL SUL
26 Electr Pkwy Bldg 106
Griffiss AFB NY 13441-4514

USAF Rsrch Lab Phillips Lab
Atmos Sci Div Geophysics Dirctrt
Hanscom AFB MA 01731-5000

NIST
ATTN MS 847.5 M Weiss
325 Broadway
Boulder CO 80303

D Robertson
4 Fourth Avenue
Burlington MA 01803-3304

J Schroeder
9 Village WAy
North Andover MA 01845-2000

R Davis
2107 Laurel Bush Rd Ste 209
Bel Air MD 21015

A K Goroch
7 Grace Hopper Ave
Monterey CA 93943

Natl Ctr for Atmos Rsrch
ATTN NCAR Library Serials
PO Box 3000
Boulder CO 80307-3000

NCAR ACD
ATTN S Massie
1850 Table Mesa Rd
Boulder CO 80305

Sci and Technology
101 Research Dr
Hampton VA 23666-1340

Distribution list

Director
US Army Rsrch Lab
4300 S Miami Blvd
Research Triangle Park NC 27709

Director
US Army Rsrch Lab
ATTN AMSRD-ARL-RO-EN W D Bach
PO Box 12211
Research Triangle Park NC 27709

US Army Rsrch Lab
ATTN AMSRD-CI-EI R Shirkey
White Sands Missile Range NM 88002

US Army Rsrch Lab
ATTN AMSRD-CI-EE D Hoock
Battlefield Envir Div
White Sands Missile Range NM 88002-5001

US Army Rsrch Lab
ATTN AMSRD-ARL-CI J D Gantt
ATTN AMSRD-ARL-CI-IS Mail & Records Mgmt
ATTN AMSRD-ARL-CI-OK-T Techl Pub (2 copies)
ATTN AMSRD-ARL-CI-OK-TL Techl Lib (2 copies)
ATTN AMSRD-CI-EE A Wetmore (10 copies)
ATTN AMSRD-CI-EE D Ligon (20 copies)
ATTN AMSRD-IS-E K Gurton (2 copies)